FOSSIL

DOE/PC/88850-T6
(DE92008470)

FUNDAMENTAL INVESTIGATION OF DUCT/ESP PHENOMENA

Final Report

By
Charles A. Brown
Michael D. Durham
William A. Sowa
Richard M. Himes
William A. Mahaffey

October 21, 1991

Work Performed Under Contract No. AC22-88PC88850

For
U.S. Department of Energy
Pittsburgh Energy Technology Center
Pittsburgh, Pennsylvania

By
Radian Corporation
Austin, Texas

and

ADA Technologies, Inc.
Englewood, Colorado

and

University of California at Irvine Combustion Laboratory
Irvine, California

and

Fossil Energy Research Corporation
Laguna Hills, California

and

CHAM of North America
Huntsville, Alabama

DISCLAIMER

Printed in the United States of America, Office of Scientific and Technical Information, Oak Ridge , Tennessee

DOE/PC/88850--T6

DE92 008470

Fundamental Investigation of Duct/ESP Phenomena
Final Report

Contract No. DE-AC22-88PC88850

Prepared for:
U.S. Department of Energy
Pittsburgh Energy Technology Center
Pittsburgh, PA 15236

Project Officer: Richard E. Tischer

Prepared by:

Charles A. Brown
Radian Corporation
Austin, Texas 78720-1088

Michael D. Durham
ADA Technologies, Inc.
Englewood, Colorado 80112

William A. Sowa
University of California at Irvine Combustion Laboratory
Irvine, California 92717

Richard M. Himes
Fossil Energy Research Corporation
Laguna Hills, California 92653

William A. Mahaffey
CHAM of North America
Huntsville, Alabama 35805

October 21, 1991

TABLE OF CONTENTS

LIST OF FIGURES

LIST OF FIGURES (Continued)

LIST OF FIGURES (Continued)

LIST OF TABLES

1.0 EXECUTIVE SUMMARY

1.1 Introduction

1.1.1 Background

The U.S. Department of Energy's Pittsburgh Energy Technology Center (DOE-PETC) is sponsoring a Flue Gas Cleanup (FGC) program to promote the use of coal in an environmentally and economically acceptable manner. One area of activity in the FGC program is the development of low-cost SO_2 emissions control technologies that can be installed on existing coal-fired power plants that were built before the 1971 New Source Performance Standards for SO_2 emission control.

A major effort under the FGC program is focused on developing duct injection of calcium-based reagent into the flue gas between the air heater and an existing electrostatic precipitator (ESP). This process is intended to be a low-capital-cost process which provides moderate levels of SO_2 control. Because it is targeted toward older plants with limited remaining life, relatively high reagent operating costs are acceptable when compared to operating costs for conventional wet scrubbers. The goal for duct injection technology is to be suitable for retrofit to existing boilers firing medium- to high-sulfur coal and be capable of a minimum of 50% SO_2 removal at a cost of less than \$500/ton of SO_2 removed.

Even though the duct injection process is an outwardly simple process, initial attempts at demonstrating the process showed that a number of technical problems need to be resolved. In particular, SO_2 removal performance needs to be improved and reagent utilization needs to be increased. Also, accumulation of deposits on the duct walls needs to be prevented, and increased particulate emissions from the existing ESP need to be avoided.

Several variations of the process of injecting calcium-based reagent into the duct downstream of an air heater have been investigated at the pilot scale under DOE funding in an earlier Flue Gas Cleanup program. Wall wetting and/or solids deposition was a common problem in most of these studies, although some problems were eventually resolved with multiple nozzles and two-stages of humidification with careful nozzle alignment. In the previous studies, lime reagent utilization generally was lower than desired. Also, few studies investigated the effects of the process on the particulate collection efficiency of the ESP.

In 1988, DOE-PETC put together a comprehensive program to further develop duct injection technology. The program consisted of five primary contracts to provide exploratory research and development, engineering development, system integration, and validation of the design basis. It involves the development of an engineering design base that will:

- Support the application of new technology to coal-fired utility boilers for the control of SO_2 emissions;
- Enable confident predictions of system performance at full-scale operation;
- Be applicable to a range of boiler sizes, flue gas compositions, and duct configurations; and
- Provide a foundation for further development of the technology.

At the end of the program, utilities will have sufficient information to evaluate duct injection as a competing technology for retrofitting SO_2 emission control to their power plant. Should this technology be best suited for their specific needs, a sound engineering design basis will allow them to complete detailed engineering for the system.

Radian Corporation was contracted to investigate duct injection and ESP phenomena in a 1.7 MW pilot plant constructed for this test program. This study was an

attempt to resolve problems found in previous studies and answer remaining questions for the technology using an approach which concentrates on the fundamental mechanisms of the process. The goal of the study was to obtain a better understanding of the basic physical and chemical phenomena that control: 1) the desulfurization of flue gas by calcium-based reagent, and 2) the coupling of an existing ESP particulate collection device to the duct injection process. Process economics are being studied by others.

1.1.2 Acknowledgements

This study was funded by DOE-PETC with additional funding provided by the Illinois Department of Energy and Natural Resources. Also, the Electric Power Research Institute (EPRI) loaned some equipment to the project, including the pilot ESP. Central Illinois Public Service Company provided the host site at their Meredosia Station.

1.2 1.7 MW Pilot Testing

Pilot testing of the duct injection process was performed at a 1.7 MW scale at the Meredosia Station of Central Illinois Public Service Company. The tests were aimed at determining how changes to various process parameters influenced the ability of the process to remove SO_2. Flue gas for the pilot plant was obtained from a slipstream of 6300 actual cubic feet per minute (acfm) withdrawn from Boiler #5. The boiler is a pulverized-coal, tangentially fired, 180 MW boiler which fires a medium-sulfur (3.2% S), low-chloride (<0.03% Cl) coal.

Powdered hydrated lime was metered using a weigh belt feeder, then injected into the test duct pneumatically either upstream or downstream of the water sprays. Particulate matter was removed from treated flue gas in a pilot ESP. The ESP

consisted of two 4-field ESPs connected in series with a full size transition union between them.

1.2.1 Wall Deposits

The formation of duct wall deposits was a difficult problem to overcome during most of the pilot plant operation. Several tests were ended prior to the desired 8 hours of data collection because the duct plugged with damp lime and fly ash deposits on the walls. Because the inside diameter of the duct was only 17.5 inches, it was easy to wet the duct walls with the water spray. It is unlikely that the severe difficulties with wall deposits encountered at the Meredosia pilot plant would exist at larger facilities, but it is not known if the difficulties can be avoided altogether.

Humidification with two nozzles staged in series was implemented after it became clear that wall wetting could not be avoided when used with a single nozzle. With this change, test durations were increased to up to 24 hours.

1.2.2 Baseline SO_2 Removal

The tests conducted at the Meredosia pilot plant were aimed at determining how changes to various process parameters influence the ability of the duct injection process to remove SO_2. Most tests were compared to a set of tests at the following baseline conditions:

- Lime upstream of humidification;
- 300° F inlet gas temperature;
- 1800 ppmv inlet SO_2 concentration;
- 2.0 reagent ratio;

- 30°F approach temperature; and
- No recycle.

Average baseline overall system SO_2 removal for four tests was 40%, with 27% removal in the duct and 13% in the ESP.

1.2.3 System Configuration

Injecting lime 4 feet downstream of humidification resulted in a significantly lower overall system SO_2 removal of 32%, with 24% removal in the duct and a contribution of 8 percentage points from the ESP. Injecting lime 20 to 24 feet downstream of humidification produced a similar overall system SO_2 removal of 30%, although the split between the contributions from the duct and the ESP were much different than in the 4-foot downstream case.

1.2.4 Reagent Ratio

As expected, increasing the reagent ratio increases SO_2 removal performance. However, the goal of 50% overall system SO_2 removal was not achieved by increasing only the reagent ratio from baseline conditions to 2.9 moles calcium per mole SO_2. Only 44% overall system SO_2 removal was obtained. Since the cost of fresh lime is one of the major operating costs for the duct injection process, it is desirable to maximize lime utilization and minimize the reagent ratio. A small incremental improvement in SO_2 removal efficiency does not warrant a large increase in lime consumption. Lime utilization decreased from 25% to 20% to 16% when increasing reagent ratio from 1.0 to 2.0 to 3.0, respectively.

1.2.5 Approach-to-Adiabatic-Saturation Temperature

Decreasing the approach-to-adiabatic-saturation temperature, or approach temperature, results in improved SO_2 removal performance. The goal for overall system SO_2 removal was achieved as reducing the approach temperature to 20° F while holding other conditions at baseline levels, produced 52% SO_2 removal.

Lowering the approach temperature does not significantly affect operating costs. However, using approach temperatures that are too low will result in significantly increased operations problems from buildup of duct wall deposits.

1.2.6 Recycle

The use of recycle solids produced significantly improved SO_2 removal performance when used with solids injected upstream of humidification. At baseline conditions but with recycle solids at a ratio of 2.0 pounds recycle solids per pound of fresh lime, 56% overall system SO_2 removal was achieved. 52% overall system SO_2 removal was achieved at a recycle ratio of 1.0 pounds recycle solids per pound of fresh lime. When solids were injected 20 to 24 feet downstream of humidification, the use of recycle produced no improvement in SO_2 removal performance.

1.2.7 Flue Gas Velocity

Reducing the gas flow by 25% had no observable effect on either deposits formation or SO_2 removal performance.

1.2.8 Inlet SO_2 Concentration

There was very little effect of inlet SO_2 concentration on SO_2 removal performance between SO_2 concentrations of 730 to 2990 ppm.

1.2.9 Inlet Flue Gas Temperature

Operation of the duct injection process at different inlet temperatures does have a noticeable effect on SO_2 removal. The effect is attributable to the amount of humidification water required at the different inlet temperatures. With other conditions at baseline levels, overall system SO_2 removal increased from 33% to 43% as the inlet temperature was raised from 260 to 340° F.

1.2.10 Chloride Addition

$CaCl_2$ was added to the humidification water during two tests to evaluate the effects of using a hygroscopic salt. Only a slight increase in SO_2 removal performance resulted from adding 0.9% $CaCl_2$ to the water when no recycle was used. However, when recycle was used and 3.4% $CaCl_2$ was added to the water, overall system SO_2 removal increased dramatically to 72 percent. Unfortunately, buildup of wall deposits also increased and the duct plugged repeatedly after only a very few hours of operation. Also, there were operation problems from damp deposits on the ESP distributor plate, one ESP penthouse, and the ESP hoppers.

Both the improved SO_2 removal performance and the increased operations problems with deposits are attributed to reduced droplet evaporation rate and increased moisture content of the solids due to the deliquescent nature of $CaCl_2$. While $CaCl_2$ could serve as a beneficial additive to improve SO_2 removal in the duct injection process, more study is required to determine a chloride addition rate that provides an improvement in SO_2 removal but does not cause operational difficulties.

1.2.11 ESP Residence Time

With the first two fields of the ESP turned off, the effect of increased residence time for gas/solid contact could be evaluated. The increase in overall system

SO_2 removal was only 2 to 3 percentage points, which is within experimental error. Therefore, increased residence time for gas/solid contact does not appear to have a major effect on SO_2 removal performance. The more important effect resulting from residence time in the duct may be more complete drying of wetted solids prior to impinging on the duct walls at the first bend in the ductwork.

1.2.12 NO Removal Performance

NO_x removal measurements were considered a low priority during this study. However, some NO removal measurements were made during some early tests. These data indicated that NO removal by the process was negligible, ranging from 0 to 6.5 percent.

1.2.13 Solid Waste Characteristics

Although investigation of solid waste characteristics was not an objective of this program, one solid waste sample was analyzed to obtain a landfill disposal permit. The results of the EP extraction analyses verified results from previous duct injection studies that the solid waste is non-hazardous.

1.3 ESP Test Results

1.3.1 Air Load ESP Tests

Air load and gas load tests were performed on the ESP prior to the start of the ESP evaluation to check out the ESP and to insure that the pilot unit was in proper working order. Any deficiencies that were discovered were corrected prior to the initiation of the test program.

The air load test included a characterization of the rapping system, measurement of the air flow distribution at the inlet to the ESP, and a check out of the electrical characteristics. This was followed by gas load tests to determine the air in-leakage and temperature gradients across the ESP, and velocity profiles at the sampling stations.

The air load and gas load testing on the pilot ESP demonstrated that it was in good mechanical condition. The electrical characteristics showed that all eight fields were properly aligned and the unit was capable of operating at high voltage levels and current densities that are typical of a well-working ESP.

1.3.2 Baseline Flyash ESP Tests

The baseline ESP performance test with flyash involved three different test conditions which allowed the measurement of ESP characteristics as a function of SCA and ESP velocity. In-spite of excellent electrical operating conditions, the collection efficiencies produced by the ESP were much lower than expected. This was especially true for the results obtained after two and three energized fields. Efficiencies below 70% were measured for an SCA on the order of 150 ft^2/kacfm. Particle size was not the cause of the low collection efficiency.

The most likely cause of the poor ESP performance is reentrainment due to the low resistivity of the particles. The coal burned at Meredosia produces a high iron flyash which results in higher than expected sulfur trioxide (SO_3) concentrations. In addition, the temperature of the flue gas at the pilot plant inlet was close to, or below, the acid dew point. This leads to very low particle resistivity. Repulsion, rather than scouring, is the most likely cause of reentrainment in the pilot ESP.

The baseline data were modeled using Version III of the SRI EPA ESP Model. It was determined that reentrainment of 44% of the particles collected in each section would be required to reduce the collection efficiency to the measured levels.

1.3.3 Duct Injection ESP Tests

Corona Quenching

During the sorbent injection tests, severe corona quenching occurred in the first field of the ESP, and significant corona suppression was measurable in the second and third field. The cause of the suppression was not due solely to the addition of the sorbent but also to effects of the humidification system. During sorbent injection, the increase in particles less than 0.4 μm was due primarily to the condensation of an acid aerosol produced by quenching the flue gas in the humidification system. However, the generation of the acid mist cannot fully account for all of the space charge effects that occur at sorbent injection conditions. It is probably the combination of the acid aerosol and the submicron sorbent particles that lead to severe quenching in the first field. When either of these two sources of particles are eliminated, the severe quenching does not occur.

Resistivity Measurements

Both laboratory and field extractive resistivity measurements indicate that the resistivity of the sorbent/flyash mixture was on the order of 10^{11} to 10^{12} ohm-cm. However, these resistivity levels were not consistent with the excellent electrical operating characteristics of the ESP at these conditions. With a resistivity of 10^{11} ohm-cm, sparking would be expected in the ESP. However, at these conditions the ESP was able to operate at voltages up to 60 kV and current densities greater than 100 nA/cm^2.

It is possible that the particles equilibrate with the moisture in the flue gas after the particles enter the ESP. There is only a one second residence time between the sorbent injection location and the port where the field extractive measurements were made. Since the particles reside on the collector plates from several minutes to hours, it is possible that the particle resistivity decreases as they begin to absorb water. However this effect should also occur in the laboratory resistivity cells where the samples are conditioned for several hours, but this effect was not seen in the laboratory tests.

ESP Performance

The efficiency of the ESP was measured at four different values of specific collection area. The most significant effect of duct sorbent injection was an increase in mass loading at the ESP inlet from 1.5 gr/dscf at baseline conditions to 7.3 gr/dscf for lime only injection and 11.3 gr/dscf for lime with recycle.

Based upon the resistivity measurements, electrical characteristics, particle size distribution, and flue gas conditions, it was expected that the ESP performance at duct injection conditions would be much better than at baseline conditions. However, the measured collection efficiencies measured were very similar to the baseline efficiencies.

These data were modeled in a similar manner as the baseline results. The value determined for reentrainment for the duct injection conditions was 0.44, which is identical to the value used for the baseline tests. This indicates that the material was very easy to reentrain.

Effect of Recycle

The addition of recycle produced a significant increase in the inlet mass loading to the ESP. However, because the mass was primarily associated with particles

greater than 1μm, there was minimal effect on the corona suppression in the first three ESP fields. The recycle also had minimal effect on the resistivity measurements. Since the recycle did not affect the primary parameters that control ESP performance, no change in collection efficiency from the lime only test would be expected. The performance data measured during the recycle test confirmed that this was true.

1.3.4 Testing of ESP Upgrades

The final phase of ESP test were designed to evaluate the effectiveness of ESP upgrades to increase the collection efficiency at duct injection conditions. Three strategies were investigated including the use of: 1) high current density electrodes in the first field of the ESP, 2) higher voltage power supplies, and 3) calcium chloride as an additive to increase cohesion of particles collected on the ESP plates.

Barbed wires were installed as emitter electrodes in the first section of the ESP. However, these high current electrodes did not overcome the corona suppression caused by duct injection.

The high voltage tests were run with the controllers set up to operate in a spark rate mode or at the 50 mA current limit of the supplies. The primary improvement in operating conditions occurred in the first three fields which operated at increased currents and voltage levels greater than 60kV. At the increased voltage, the first section had an increase in current to above 5 mA which provided a current density on the order of 15 nA/cm^2. However, this did not improve the performance of the ESP.

This is not surprising for a situation that appears to be dominated by low-resistivity reentrainment. The increased operating voltage would lead to higher electric fields for charging and collecting. However, for low-resistivity particles, the repulsion force on the collected particles is proportional to the electric field and therefore, the increase in operating voltage has both a positive and a negative effect on collection

efficiency as it increases the collection force but it also increases the repulsion force. Therefore, increasing the capacity of the power supplies is not an effective ESP upgrade to overcome the impact of duct sorbent injection on emissions.

One of the means to reduce reentrainment is to improve the cohesive characteristics of the dust. The use of chloride as an additive for sorbent injection brought about dramatic improvement in the removal of sulfur dioxide as efficiencies as high was 70% were obtained. Although the chloride addition also produced a large reduction in the resistivity of the particles, there appeared to be no significant effect on the performance of the ESP. However, the chloride addition tests represented only about 24 hours of operation. These tests may not have been run for sufficient time for improvements due to a more cohesive dust to take place.

1.3.5 Full-Scale Test at Edgewater

The evaluation of the full-scale ESP operating at the demonstration of the Coolside process at the Ohio Edison Edgewater Station provided some data to compare with the pilot plant results. The data from this test program were analyzed using the SRI ESP computer model. It appears that the full-scale unit also suffered from low-resistivity reentrainment but not to as great an extent as the pilot ESP. The results indicated that the reentrainment in the ESP was 26% which is much lower than the reentrainment at the pilot plants. The difference may be due to increased particle cohesion at a lower approach temperature at Edgewater, or due to differences in the coal, sorbent, and process conditions.

1.4 Droplet Size Characterization

The University of California at Irvine Combustion Laboratory (UCI) was subcontracted to provide water droplet size and velocity measurements for several humidification nozzles that potentially could be used at the Meredosia pilot plant. Such

two-fluid nozzles characteristically produce dense sprays featuring very narrow dispersion angles and high droplet velocities. The objective of this work was to characterize sprays produced by nozzles to: 1) better understand the atomization process, 2) provide a data base for computational fluid dynamics (CFD) modeling of the process, and 3) provide data to support nozzle selection.

Data were generated from measurements of the water spray using an Aerometrics Phase Doppler Particle Analyzer (PDPA), at a distance of 3 feet from the tip of the nozzle. General observations regarding the results include the following five points:

- Droplet size decreases when inlet air pressure increasesr for a given water flow rate;
- Droplet size decreases as the water flow rate decreases for a given air pressure;
- Spatially resolved profiles of SMD become relatively flatter when there is relatively more atomizer air and less water;
- Mean axial velocity increases as inlet nozzle air pressure increases; and
- Mean axial velocity is almost unaffected by variations of water flow rate for a given inlet water pressure (with the exception of the small Lechler nozzle 170.641.17).

The PDPA measures droplet size and velocity within a small volume, essentially at a point within the spray pattern. A laser diffraction instrument, such as the Malvern, measures a line-of-sight. Laser diffraction instruments are commonly used to report droplet size distributions for atomizers. To compare results obtained by the PDPA and a laser diffraction (Malvern) instrument, the spray from one atomizer was measured using both instruments. The composite SMD from laser diffraction size measurements are about 30% lower than from the phase Doppler. One factor that can affect laser diffraction measurements is obscuration, or the attenuation of the laser beam

as the light travels from the transmitter to the receiver. However, corrections for obscuration did not resolve the difference in measurements between the two instruments.

1.5 Hot-Flow, Physical Model

To facilitate observation of the humidification process in a 17.5 inch diameter duct, a full-scale glass model of the Meredosia pilot plant duct was constructed by Fossil Energy Research Corporation. Air was heated to 300° F, then sprayed with water using two-fluid atomizers. Thus, the pilot plant humidification process was simulated and visualized. Wetting of duct walls due to impingement of water droplets could be observed. Atomizers and atomizer configurations were screened in this facility prior to installation at the pilot plant.

Atomizers were tested in several configurations including: 1) single nozzle centered in the duct, 2) single nozzle centered in the duct at reduced gas temperature and water flow to simulate the second stage of a two-stage series configuration, 3) two-stage series, and 4) two nozzles in parallel. None of these configurations produced complete evaporation in the glass duct facility while operating at conditions typical of the Meredosia pilot plant. However, the two-stage series configuration was demonstrated to produce more complete evaporation than either a single nozzle or a parallel configuration.

Results indicate that, at a flow rate of 1.5 gpm, a tradeoff existed within the 18-inch duct geometry. In order to approach an acceptable drop size distribution, and minimize droplet evaporation times, the air/liquid ratio needed to be increased to maximum achievable levels. Increases in the air/liquid ratio within a confined flow, however, enhanced the recirculating flow out toward the duct wall, thereby reducing time available for droplet evaporation.

1.6 Duct Injection Model

The First Generation duct injection model is a two- and three-dimensional, multiphase reacting flow analyzer using computational fluid dynamics methods. The model is called DIAN3D, an acronym for Duct Injection Analyzer--3 dimensional. The gaseous phase is solved in an Eulerian frame while the droplets of particles are traced in a Lagrangian frame. The model includes aerodynamics, heat transfer, sorbent particle interception by water droplets, and SO_2 reactions with $Ca(OH)_2$.

The First Generation Model has been successfully validated for a number of single-phase flows such as laminar, turbulent and swirling pipe flows, and turbulent flow in a backward facing stope. Two-phase flow and heat/mass transfer simulations produced plausible results.

However, the SO_2 removal submodel is very sensitive to the prevailing ambient conditions in the duct and will often diverge during the calculation of the liquid calcium and sulfur profiles. Either a different solution approach for convergence of the SO_2 removal submodel or use of a simpler submodel is recommended.

1.7 ESP Performance Model

A personal-computer-based model to characterize the performance of electrostatic precipitators (ESPs) operating downstream of duct injection scrubbing systems was developed by ADA Technologies, Inc. The model is applicable for the high mass loadings and low resistivities experienced during duct injection. In addition to the non-ideal effects of sneakage, gas velocity distribution and rapping reentrainment, non-rapping reentrainment and particle charge limitations were considered.

Particle charge limitations are caused by space charge induced corona quenching and the build-up of high potentials along the center lines of the ESP gas

passages. Non-rapping reentrainment is experienced in all ESPs but has been found to be especially important in ESPs handling low resistivity materials. The model addresses the problem by the addition of a non-rapping reentrainment factor as a non-ideal effect. Model self-consistency was obtained by explicitly calculating the ion distribution, voltage distribution including particle space charge, particle charges, and current density using an iterative technique until mathematical convergence was achieved for each length increment within the ESP. In addition to improving the accuracy of the model calculations, making the model easier to use was also a prime objective. The model provides a full-screen, menu-driven interface that isolates the user from the complexity of the ESP model input formats, validates input data, and performs unit conversions.

The model is fully operational and has been extensively compared to the existing ESP models which are available to the public. Additional testing to enlarge the data base relating to particle charge, rapping reentrainment, and non-rapping reentrainment in duct sorbent injection ESPs needs to be conducted. This is necessary for further validation of the model, since data were available for only a limited number of pilot-scale duct sorbent injection cases and empirical data were gathered from a single full-scale source.

2.0 INTRODUCTION

The U.S. Department of Energy's Pittsburgh Energy Technology Center (DOE-PETC) is sponsoring a Flue Gas Cleanup (FGC) program to promote the use of coal in an environmentally and economically acceptable manner. One area of activity in the FGC program is the development of low-cost SO_2 emissions control technologies that can be installed on existing coal-fired power plants that were built before the 1971 New Source Performance Standards for SO_2 emission control. Many of these power plants burn medium- to high-sulfur coals and their combined emissions are a principal source of SO_2 emissions in the United States. Nationwide, only about 10% of the utility boilers are equipped with flue gas desulfurization (FGD) systems to control the emission of sulfur dioxide (1). The older, uncontrolled plants, which are located mainly in the eastern part of the country, represent approximately 200,000 MW of generating capacity (2).

One major effort under the FGC program is focused on developing duct injection of calcium-based reagent into the flue gas between the air heater and an existing electrostatic precipitator (ESP). This process is intended to be a low-capital-cost process which provides moderate levels of SO_2 control. Because it is targeted toward older plants with limited remaining life, relatively high reagent operating costs are acceptable when compared to operating costs for conventional wet scrubbers. The goal for duct injection technology is to be suitable for retrofit to existing boilers firing medium- to high-sulfur coal and be capable of a minimum of 50% SO_2 removal at a cost of less than $500/ton of SO_2 removed.

Even though the duct injection process is an outwardly simple process, initial attempts at demonstrating the process showed that a number of technical problems need to be resolved. In particular, SO_2 removal performance needs to be improved and reagent utilization needs to be increased. Also, accumulation of deposits

on the duct walls needs to be prevented, and increased particulate emissions from the existing ESP need to be avoided.

2.1 Background

Several variations of the process of injecting calcium-based reagent into the duct downstream of an air heater have been investigated at the pilot scale under DOE funding in an earlier Flue Gas Cleanup program. General Electric Environmental Systems studied injection of slaked lime slurry into the ductwork upstream of an ESP using a rotary atomizer for slurry atomization in a 12 MW pilot plant (3). The Bechtel Confined Zone Dispersion (CZD) process was studied at pilot (7 MW) and small commercial (70 MW) scales with an ESP as the particulate collection device (4). The CZD process utilized two-fluid nozzles to inject slaked lime slurry into the flue gas. Dravo Lime Company studied the HALT (Hydrate Addition at Low Temperature) process at a 5 MW pilot plant utilizing an ESP and a fabric filter for particulate collection (5). Hydrated lime was injected upstream of two-fluid nozzles which were used to produce water droplets and humidify the flue gas.

Additional studies of variations of the process have been carried out by others. The Consolidated Coal Company (Consol) has tested calcium hydroxide injection upstream of humidification at a 1 MW pilot plant which used an ESP for particulate control (6), and a full scale 105 MW demonstration is being made at Ohio Edison's Edgewater Power Station (7). In one adaptation of their "Coolside" process, humidification water contains a small amount of sodium hydroxide to enhance SO_2 removal. Also, EPRI sponsored studies of dry calcium hydrate injection both upstream and downstream of humidification, with either an ESP or a fabric filter, at the Arapahoe Test Facility (8, 9) and short-term studies of in-duct spray drying upstream of an ESP (10).

Wall wetting and/or solids deposition was a common problem in most of these studies, although Dravo reported eventually resolving the problem with multiple nozzles and two-stages of humidification (5) and Consol reported resolving deposits problems with careful nozzle alignment (6). In the previous studies, lime reagent utilization generally was lower than desired. Also, few studies investigated the effects of the process on the particulate collection efficiency of the ESP. Based on experience with the effects of spray dryer technology on ESP performance in medium- and high-sulfur-coal applications, which also produces calcium-based particulate in a humid, low-temperature environment, there was reason to believe that particulate emissions from a duct injection application retrofit to an ESP may be higher than desired (10).

In 1988, DOE-PETC put together a comprehensive program to further develop duct injection technology. The program consisted of five primary contracts to provide exploratory research and development, engineering development, system integration, and validation of the design basis. It involves the development of an engineering design base that will:

- Support the application of new technology to coal-fired utility boilers for the control of SO_2 emissions;
- Enable confident predictions of system performance at full-scale operation;
- Be applicable to a range of boiler sizes, flue gas compositions, and duct configurations; and
- Provide a foundation for further development of the technology.

At the end of the program, utilities will have sufficient information to evaluate duct injection as a competing technology for retrofitting SO_2 emission control to their power plant. Should this technology be best suited for their specific needs, a sound engineering design basis will allow them to complete detailed engineering for the system.

The five primary contracts for the duct injection technology development program include:

- Basic research of mass transfer effects on a theoretical basis (Acurex and University of Texas);
- Investigation of mass transfer effects at the bench scale combined with a preliminary computer model (Energy and Environmental Research Corporation);
- Fundamental investigation of duct injection and ESP phenomena at a 1.7 MW pilot scale and development of first generation computer models for fluid dynamics combined with SO_2 removal and ESP particulate removal performance (Radian Corporation, ADA Technologies, CHAM of North America, Fossil Energy Research Corp., University of California at Irvine, and Stone & Webster);
- Scale-up tests and supporting research at a 12 MW pilot scale (Gilbert-Commonwealth and Southern Research Institute); and
- Coordination of the duct injection technology prototype development program culminating in a second generation computer model and a design handbook (United Engineers and Babcock & Wilcox).

2.2 Objective

Radian Corporation was contracted to investigate duct injection and ESP phenomena in a 1.7 MW pilot plant constructed for this test program. This study was an attempt to resolve problems found in previous studies and answer remaining questions for the technology using an approach which concentrates on the fundamental mechanisms of the process. The goal of the study was to obtain a better understanding of the basic physical and chemical phenomena that control: 1) the desulfurization of flue gas by calcium-based reagent, and 2) the coupling of an existing ESP particulate collection device to the duct injection process. Process economics are being studied by others (11).

2.3 Acknowledgement

This study was funded by DOE-PETC with additional funding for the project provided by the Illinois Department of Energy and Natural Resources. Also, the Electric Power Research Institute (EPRI) loaned some equipment to the project, including the pilot ESP. Central Illinois Public Service Company provided the host site at their Meredosia Station.

2.4 Report Organization

This Final Report provides summarized descriptions of each major portion of the contract for Fundamental Investigation of Duct/ESP Phenomena. An Executive Summary was provided in Section 1. A description of the pilot plant at Meredosia, IL, and a discussion of SO_2 removal performance test results are provided in Section 3. ESP test results are discussed in Section 4.0. The nozzle performance characterization tests are discussed in Section 5.0. Section 6.0 provides a summary of the hot-flow, glass duct physical model testing of the duct at the Meredosia pilot plant. A discussion of the computational fluid dynamics first generation model of the duct injection process is provided in Section 7.0. A computational model for particulate removal performance in the ESP is discussed in Section 8.0.

Further details of results from this test program may be found in the following topical reports:

- Topical Report No. 2--1.7 MW pilot plant results for dry injection SO_2 removal performance, and operating experience with humidification and wall deposits (12);
- Topical Report No. 3, Volume 1--Details of nozzle characterization test results in support of pilot plant nozzle selection (13);
- Topical Report No. 3, Volume 2--Flow Visualization test results from a hot-flow glass model of the pilot plant duct (14);

- Topical Report No. 4 and 5--ESP performance results (15);
- Topical Report No. 6--First Generation Duct Injection Model, which is a 3-dimensional mathematical model of the fluid dynamic, heat transfer, and SO_2 removal processes of duct injection (16); and
- Topical Report No. 7--Mathematical model of ESP performance (17).

2.5 References

1. Melia, M. T., R. S. McKibben, and F. M. Jones. "Trends in Commercial Applications of FGD." Proceedings of the Tenth Symposium on Flue Gas Desulfurization, Atlanta, GA, November 18-21, 1986. U.S. Environmental Protection Agency. U.S. Government Printing Office, Washington, D.C., 1986. EPA-600/9-87-004a.

2. Drummond, C. J., Editor; M. Babu, A. Demian, D. S. Henzel, D. A. Kanary, D. Kerivan, K. Lee, K. R. Murphy, J. T. Newman, E. A. Samuel, R. M. Statnick, and M. R. Stouffer. "Duct Injection Technologies for SO_2 Control." Presented at the EPA/EPRI First Combined FGD and Dry SO_2 Control Symposium, St. Louis, MO, October 25-28, 1988.

3. Samuel, E. A., K. R. Murphy, and A. Demian. A 12-MW-Scale Pilot Study of In-Duct Scrubbing (IDS) Using a Rotary Atomizer. U.S. DOE Contract DE-AC22-85PC81010, November, 1989.

4. Bechtel National, Inc. Desulfurization of Flue Gas by the Confined Zone Dispersion Process. DOE/PC/81009-T33, NTIS 1821148, October 1989.

5. Babu, M., J. College, R. Forsythe, R. Herbert, D. Kanary, D. Kerivan, and K. Lee. 5-MW Toronto HALT Pilot Plant Test Results. DOE/PC/81012-T1-PT.I-A, NTIS 1415924, December 1988.

6. Yoon, H., M. R. Stouffer, W. A. Rosenhoover, J. A. Withum, and F. P. Burke. "Pilot Process Variable Study of Coolside Desulfurization." Environmental Progress, vol. 7, no. 2, May 1989, pp. 104-111.

7. Stouffer, M. R., W. A. Rosenhoover, and H. Yoon. "Pilot Plant Process and Sorbent Evaluation Studies for 105 MWe Coolside Desulfurization Process Demonstration." Third International Conference on Processing and Utilization of High-Sulfur Coals, Ames, Iowa, November 14-16, 1989.

8. Blythe, G. M., V. Bland, C. Martin, M. McElroy, and R. Rhudy. "Pilot-Scale Studies of SO_2 Removal by Calcium Injection Upstream of a Particulate Control Device." Proceedings of the Tenth Symposium on Flue Gas Desulfurization, Atlanta, GA, November 18-21, 1986. U.S. Environmental Protection Agency, U.S. Government Printing Office, Washington, D.C., 1986. EPA-600/9-87-004a.

9. Blythe, G. M., R. A. Smith, L. J. Muzio, C. A. Martin, and V. V. Bland. Calcium Injection Upstream of an Electrostatic Precipitator and a Fabric Filter for Simultaneous SO_2 and Particulate Removal: Pilot and Bench-Scale Results-Draft Final Report. Prepared for Electric Power Research Institute, Research Project 2784-1, June 1989.

10. Durham, M. D., D. E. Rugg, R. G. Rhudy, and E. J. Puschaver. "Low-resistivity Related ESP Performance Problems in Dry Scrubbing Applications," Journal of the Air and Waste Management Association. Vol. 40, No. 1, January 1990, pp. 112-124.

11. Ireland, P. A., and C. E. Martin. "Duct Injection Technology Engineering Design and Scale-up Criteria." Proceedings of the Sixth Annual Coal Preparation, Utilization, and Environmental Control Contractors Conference, Pittsburgh, Pennsylvania, August 6-9, 1990, pp. 352-358.

12. McGuire, L. M., and C. A. Brown. Fundamental Investigation of Duct/ESP Phenomena: 1.7 MW Pilot Parametric Testing Results. U.S. DOE Contract No. DE-AC22-88PC88850, Topical Report No. 2, February 11, 1991.

13. Brown, C. T., W. A. Sowa, and G. S. Samuelsen. Fundamental Investigation of Duct/ESP Phenomena: Flow Visualization--Drop size and Velocity Measurements of Duct Humidification Atomizers. U.S. DOE Contract No. DE-AC22-88PC88850, Topical Report No. 3, Volume 1, November, 1990.

14. Himes, R. M. Fundamental Investigation of Duct/ESP Phenomena: Flow Visualization--Duct Humidification Atomizer Performance Evaluation In a Hot Flow Physical Model. U.S. DOE Contract No. DE-AC22-88PC88850, Topical Report No. 3, Volume 2, January 1991.

15. Durham, M. D., T. G. Ebner, and D. B. Holstein. Fundamental Investigation of Duct/ESP Phenomena: 1.7 MW Pilot ESP Testing, Results, and Upgrade Strategies. U.S. DOE Contract No. DE-AC22-88PC88850, Topical Reports No. 4 and 5, January, 1991.

16. Vlachos, N. S., W. A. Mahaffey and P. L. Daley. Fundamental Investigation of Duct/ESP Phenomena: First Generation Duct Injection

Model. U.S. DOE Contract No. DE-AC22-88PC88850, Topical Report No. 6, December 1990.

17. Holstein, D. B., D. E. Rugg, and M. D. Durham. Fundamental Investigation of Duct/ESP Phenomena: Mathematical Modeling of ESP Performance. U.S. DOE Contract No. DE-AC22-88PC88850, Topical Report No. 7, February 25, 1991.

3.0 1.7 MW PILOT TESTING

3.1 Introduction

Pilot testing of the duct injection process was performed at a 1.7 MW scale at the Meredosia Station of Central Illinois Public Service Company. The tests were aimed at determining how changes to various process parameters influenced the ability of the process to remove SO_2. A description of the pilot plant, a discussion of operating experience, and a summary of SO_2 removal performance results are discussed in the following sections.

3.2 Pilot Plant Description

A simplified process flow schematic of the 1.7 MW pilot plant is provided in Figure 3-1. Flue gas for the pilot plant was obtained from a slipstream of 6300 actual cubic feet per minute (acfm) withdrawn from Central Illinois Public Service Company's Meredosia Station Boiler #5. The boiler is a pulverized-coal, tangentially fired, 180 MW boiler which fires a medium-sulfur (3.2% S), low-chloride (<0.03% Cl) coal. The flue gas SO_2 concentration typically was between 1500 and 2000 parts per million by volume (ppmv), but was controlled to target levels of either 1500 ppmv or 1800 ppmv for most tests. SO_2 concentration was controlled by dilution with air or by spiking with SO_2 gas as needed to meet the specified target concentration for a test.

The temperature of the flue gas at the inlet of the pilot plant also was controlled to the specified target level for a test. The temperature could be raised using an electric resistance heater or lowered using an air-to-gas heat exchanger.

Flue gas was treated using the duct injection process in a horizontal test duct 17.5 inches in diameter. In early tests, water was injected into the duct using a single two-fluid, air-atomizing nozzle. To avoid problems in later tests with wet duct

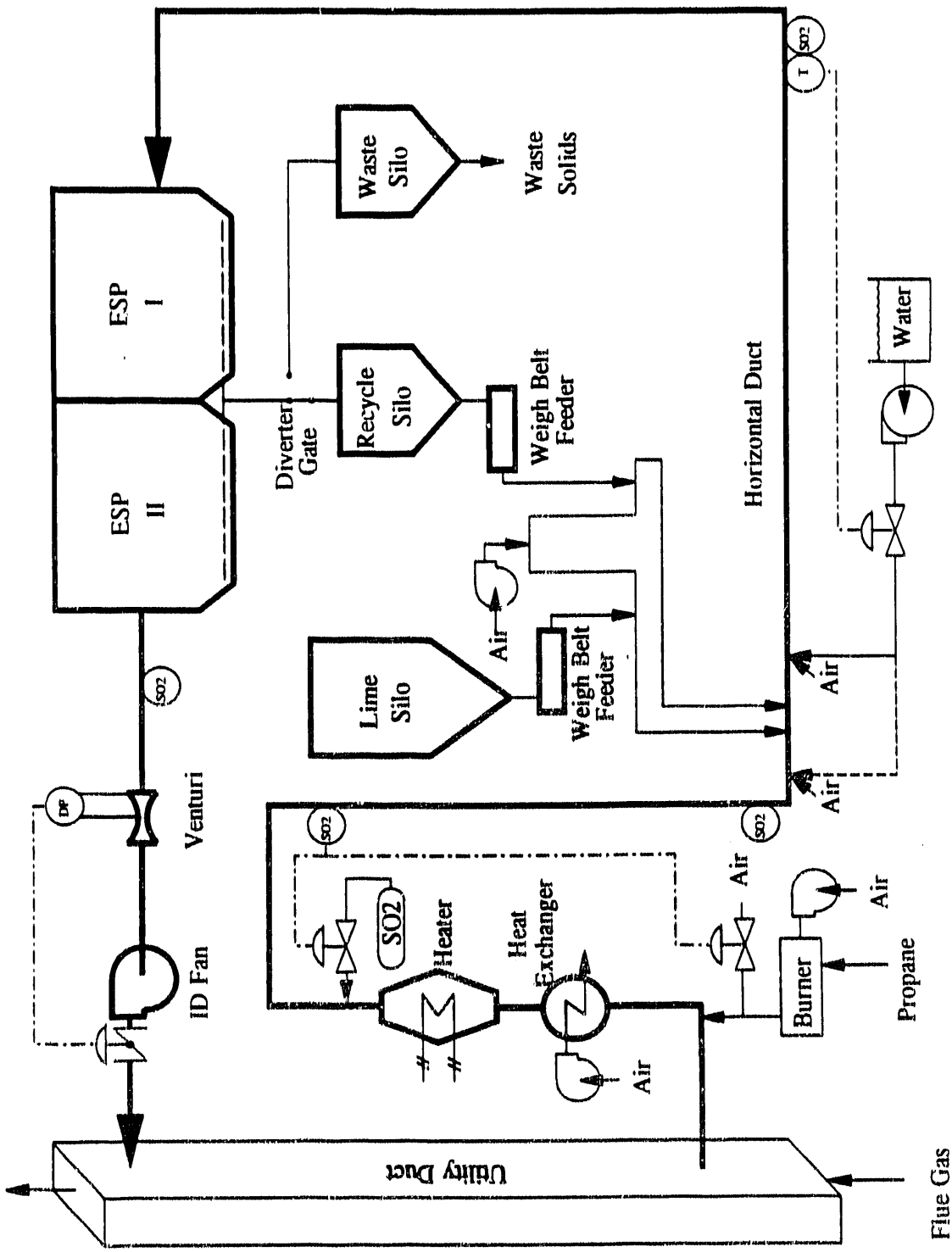

Figure 3-1. Simplified Process Flow Diagram for the Meredosia Pilot Plant

walls and buildup of solids deposits, water was injected through two nozzles staged in series. Powdered hydrated lime was metered using a weigh belt feeder, then injected into the test duct pneumatically either upstream or downstream of the water sprays.

Particulate matter was removed from treated flue gas in a pilot ESP. The ESP consisted of two 4-field ESPs connected in series with a full size transition union between them. With eight fields in operation at design flue gas flow rate of 6300 acfm, the total specific plate collection area was 533 square feet per thousand acfm. The ESP is described in further detail in Section 4.2.

Collected solids could be either wasted and shipped to an off-site landfill, or recycled to the inlet of the horizontal test duct. Recycle solids, when used, were metered using a weigh belt feeder, then pneumatically injected into the duct.

SO_2 removal performance was measured using two sets of continuous SO_2 and O_2 analyzers. One set of analyzers continuously monitored the inlet flue gas composition. A second set of analyzers was switched periodically between the outlet of the horizontal test section and the outlet of the ESP. In this manner, the overall system SO_2 removal and the contributions to overall removal by the duct and by the ESP could be determined.

3.3 Duct Wall Deposits

The formation of duct wall deposits was a difficult problem to overcome during most of the pilot plant operation. Several tests were ended prior to the desired 8 hours of data collection because the duct plugged with damp lime and fly ash deposits on the walls.

Because the inside diameter of the duct was only 17.5 inches, it was easy to wet the duct walls with the water spray. Nozzles were centered axially in the duct,

leaving a maximum of only 8.75 inches between the nozzle tip and the duct wall. Unlike larger scale facilities, there was no flexibility at Meredosia for pointing a nozzle away from the wall or for increasing the spacing between nozzles and the wall. Larger facilities are likely to utilize a manifold of several nozzles in parallel for humidification, allowing the outside set of nozzles to be canted inward or to be placed well away from the wall. It is unlikely that the severe difficulties with wall deposits encountered at the Meredosia pilot plant would exist at larger facilities, but it is not known if the difficulties can be avoided altogether.

Wall wetting was detectable by monitoring skin thermocouples installed around the outside wall of the duct as shown in Figure 3-2. Using wall temperatures, nozzles could be aligned accurately to produce uniform high temperatures around the duct wall. Also, by monitoring wall temperatures, it was determined that wall wetting did not cause a gradual accumulation of solids deposits over the course of a test. Instead, skin temperatures often would drop quickly after several hours of testing, indicating that the deposits formed as a result of an incident or change that had occurred. An typical example of a sudden drop in duct skin temperature is illustrated in Figure 3-3. The following incidents were attributed to be sources of sudden changes which could produce wall wetting:

- Growth of deposits on the tip of the nozzle which eventually affected the water spray pattern;
- Accumulation of large agglomerates of deposits on the floor of the duct caused by large air-foil shaped buildup which formed and grew on the back of nozzle and its air and water tubing until it fell to the floor of the duct;
- Changes in humidification water flow rate when steam sootblowing started or stopped;

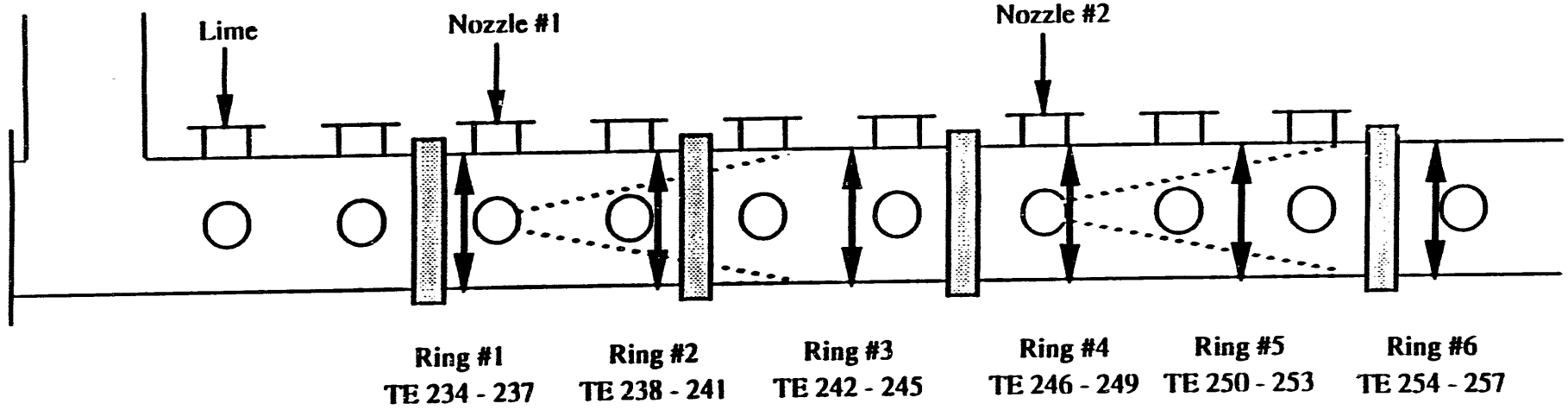

Figure 3-2. Location of Skin Temperature Thermocouples

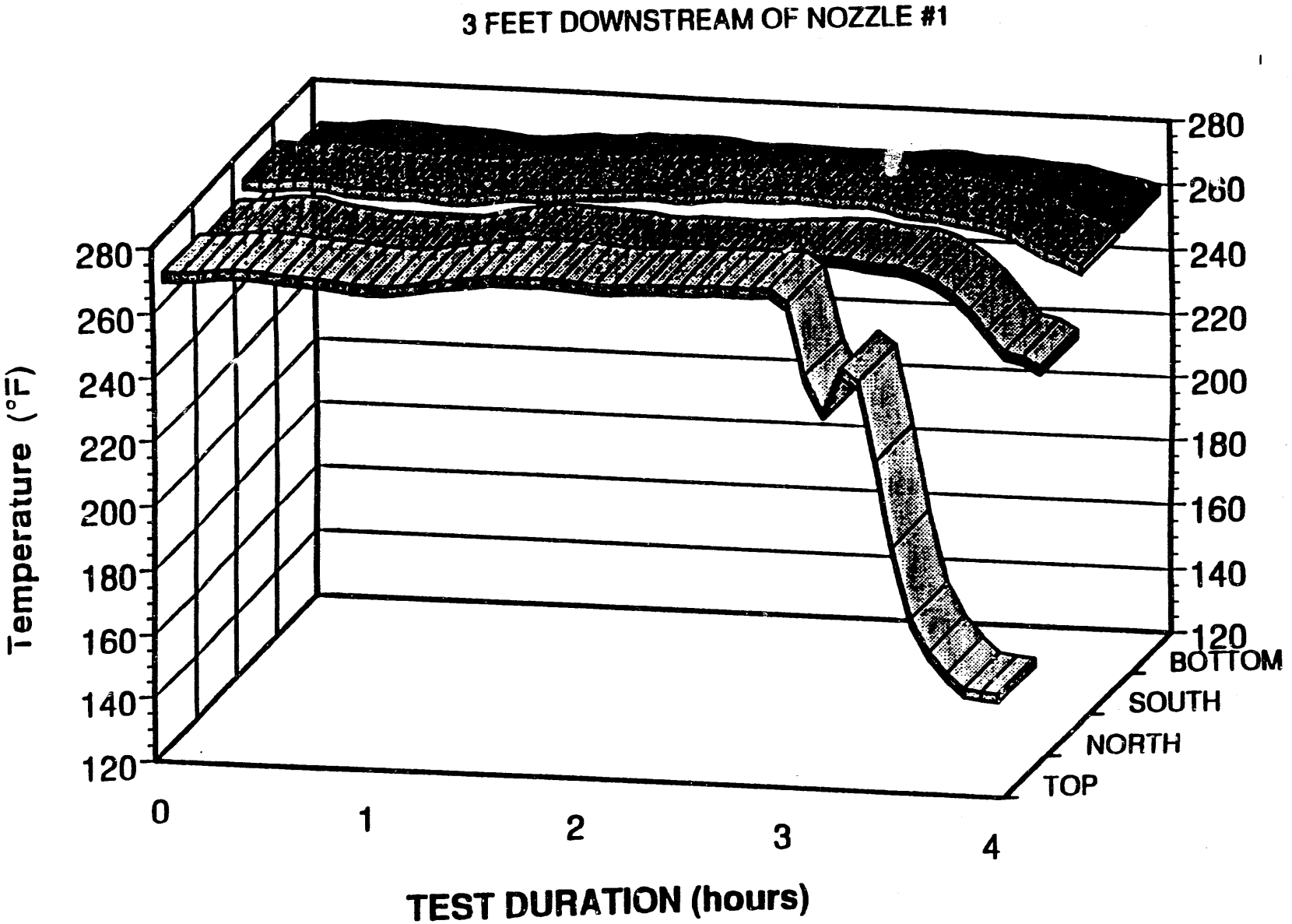

Figure 3-3. Detection of Wall Wetting Using Skin Temperature Thermocouples

- Fluctuations in humidification water flow rate upon system startup or when the water filter plugged; and
- Opening the port at the inlet of the test section to take wet-bulb temperature measurements.

Initially, tests were performed using one nozzle positioned in the center of the duct and with lime injected either upstream or downstream of the single nozzle. When lime was injected upstream of the single nozzle, operation was possible for only 1 to 6 hours. Lime injection was moved 4 feet downstream of the humidification nozzle, but wall deposits plugged the duct quickly in those tests also. When lime was injected 20 to 24 feet downstream of humidification, operation was extended to 22 hours. Although extended operation could be achieved with lime injected well downstream of humidification, SO_2 removal efficiency in this configuration was low.

Humidification with two nozzles staged in series was implemented after it became clear that wall wetting could not be avoided when used with a single nozzle. One option for utilizing multiple small nozzles would be to arrange them in a parallel configuration. However, hot-flow physical modeling and computational fluid dynamics modeling indicated that two nozzles staged in series would produce less wall wetting than two nozzles in a parallel configuration in the round duct. Use of the two-stage series configuration was fairly successful and allowed testing with lime injected upstream of humidification to continue, although problems with wall wetting and deposits buildup were not eliminated completely. The durations for tests using various nozzle and system configurations are plotted in Figure 3-4.

Several different models of two-fluid nozzles were tried at Meredosia. Prior to using nozzles in the pilot plant, they were screened by measuring droplet size and velocities on a spray test stand at the University of California at Irvine, and by measuring unevaporated water flows in a hot-flow physical glass model. Nozzles which produced the smallest droplet size distributions, and produced a higher degree of evaporation in the glass model, were chosen for use in the pilot plant. Nozzles used in

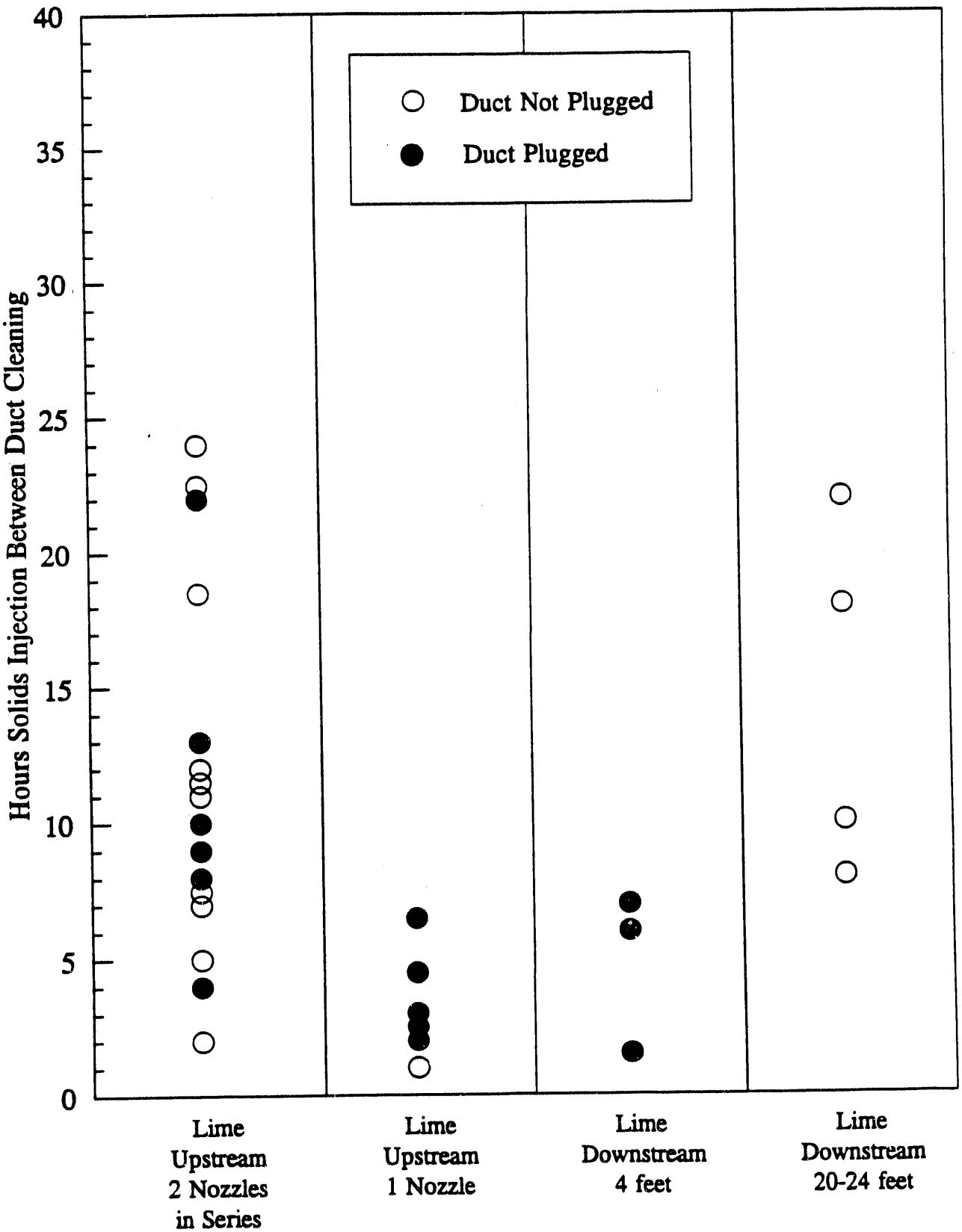

Figure 3-4. Test Duration for Various System Configurations

pilot plant testing are listed in Table 3-1. In general, the nozzles that consumed more air produced the smaller droplets. Although air consumption rates were very high and may be uneconomical in full-scale facilities, the objective for this study was to humidify the flue gas without wetting the walls of the small diameter duct to produce test results for SO_2 removal performance. Therefore, the high air consumption rates were accepted for this pilot study. The effort required to solve and optimize humidification in the small duct probably would not be useful for large-scale facilities.

Although there were some differences in spray patterns produced by the different nozzles, none of the nozzles could prevent wall wetting and deposits accumulation in the single-stage configuration, and no significant differences in performance between the Lechler and Delavan nozzles were observed in the two-stage configuration. Given a well-designed, properly sized two-fluid nozzle, other factors leading to wall-wetting, such as those described above, appeared to be more important than the make and model of the nozzle.

Two tests demonstrated the use of calcium chloride as an additive in the humidification water to investigate enhancement of SO_2 removal performance. $CaCl_2$ is a deliquescent salt which absorbs moisture then dissolves in the absorbed moisture. During the chloride spiking test with recycle, duct wall deposits formed rapidly. The deposits were more moist and heavier than found in previous tests. Also, buildup of deposits on the ESP distributor plate, in one of the ESP penthouse compartments, and in the ESP hopper caused operating problems during this test. Although SO_2 removal was high during this test, deposits problems were severe. Future studies would be needed to investigate addition of chloride at lower levels to determine if a moderate amount of chloride addition could improve SO_2 removal, yet avoid duct deposits in a full-scale system.

Table 3-1

Nozzle Types and Configurations Used in Pilot Plant Testing

Nozzle #1	Nozzle #2*
Parker-Hannifin 6890764M2	--
Delavan Airo 30616-17	--
Bete Fog SA 12H-14N-283	--
Lechler 170.641.17	--
Lechler 170.641.17	Bete Fog SA 12H-14N-283
Lechler 170.641.17	Lechler 170.641.17
Lechler 170.641.17	Delavan Airo 30616-17
Lechler 170.641.17	Delavan Airo 30616-11
Delavan Airo 30616-11	Lechler 170.641.17
Delavan Airo 30615-46	Lechler 170.641.17
Delavan Airo 30616-17	Lechler 170.641.17

* Where only one nozzle is listed, single-nozzle humidifications tests were being conducted. Where two nozzles are listed, the two nozzles were operated in series, with Nozzle #1 upstream of Nozzle #2.

3.4 SO_2 Removal Performance

3.4.1 Baseline Tests

The tests conducted at the Meredosia pilot plant were aimed at determining how changes to various process parameters influence the ability of the duct injection process to remove SO_2. Most tests were compared to a set of tests at the following baseline conditions:

- Lime upstream of humidification;
- 300° F inlet gas temperature;
- 1800 ppmv inlet SO_2 concentration;
- 2.0 reagent ratio;
- 30° F approach temperature; and
- No recycle.

Average baseline overall system SO_2 removal for four tests was 40%, with 27% removal in the duct and 13% in the ESP. Baseline test results are plotted in Figure 3-5. Repeatability of results for the baseline tests was very good; the 95% confidence interval for overall SO_2 removal for an individual baseline test was ± 3 percentage points.

3.4.2 System Configuration

The effect of system configuration on SO_2 removal performance is illustrated by the results plotted in Figure 3-6. Injecting lime 4 feet downstream of humidification resulted in a significantly lower overall system SO_2 removal of 32%, with 24% removal in the duct and a contribution of 8 percentage points from the ESP. Injecting lime 20 to 24 feet downstream of humidification produced a similar overall system SO_2 removal of 30%, although the split between the contributions from the duct

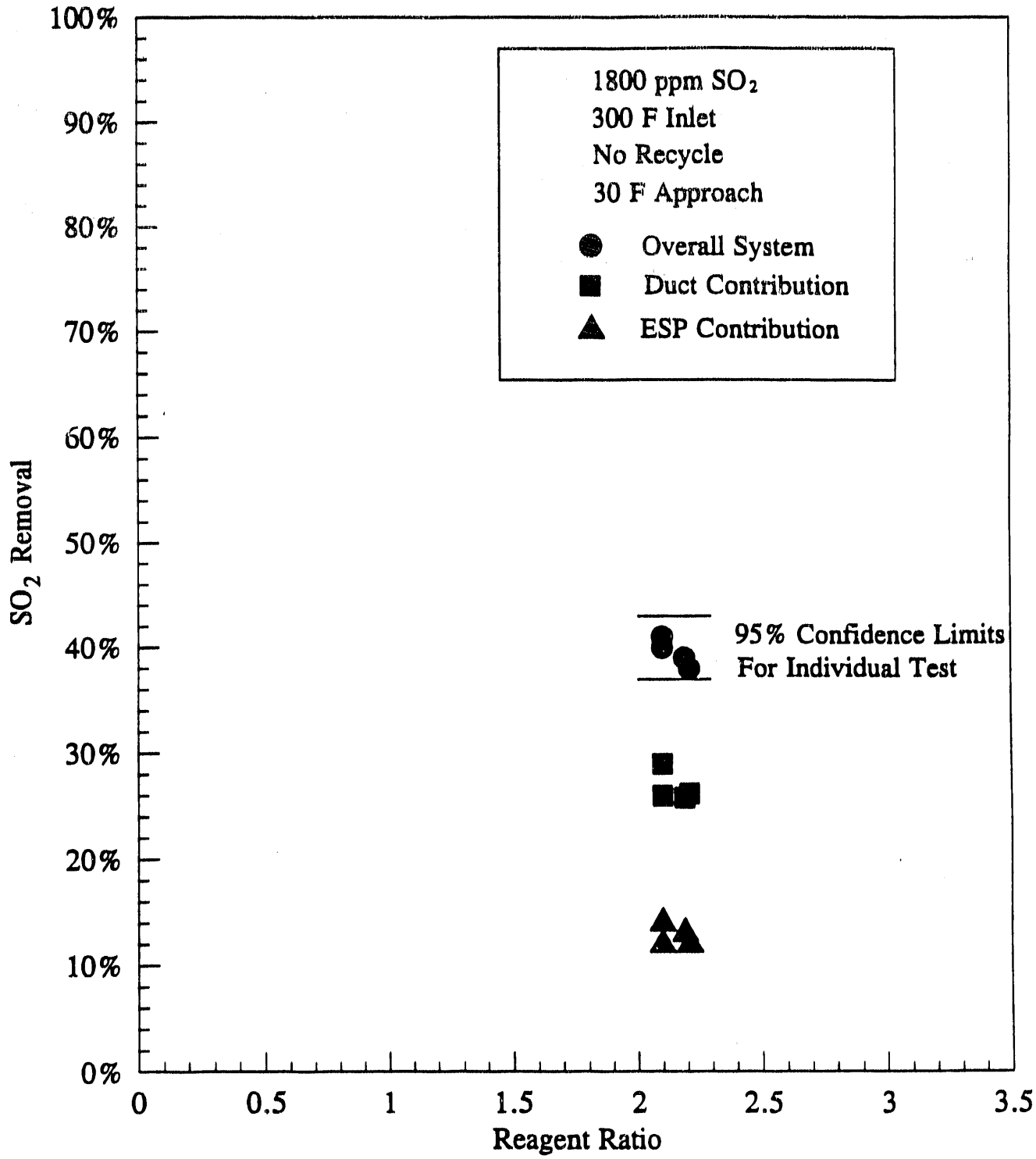

Figure 3-5. Baseline Test SO_2 Removal Performance

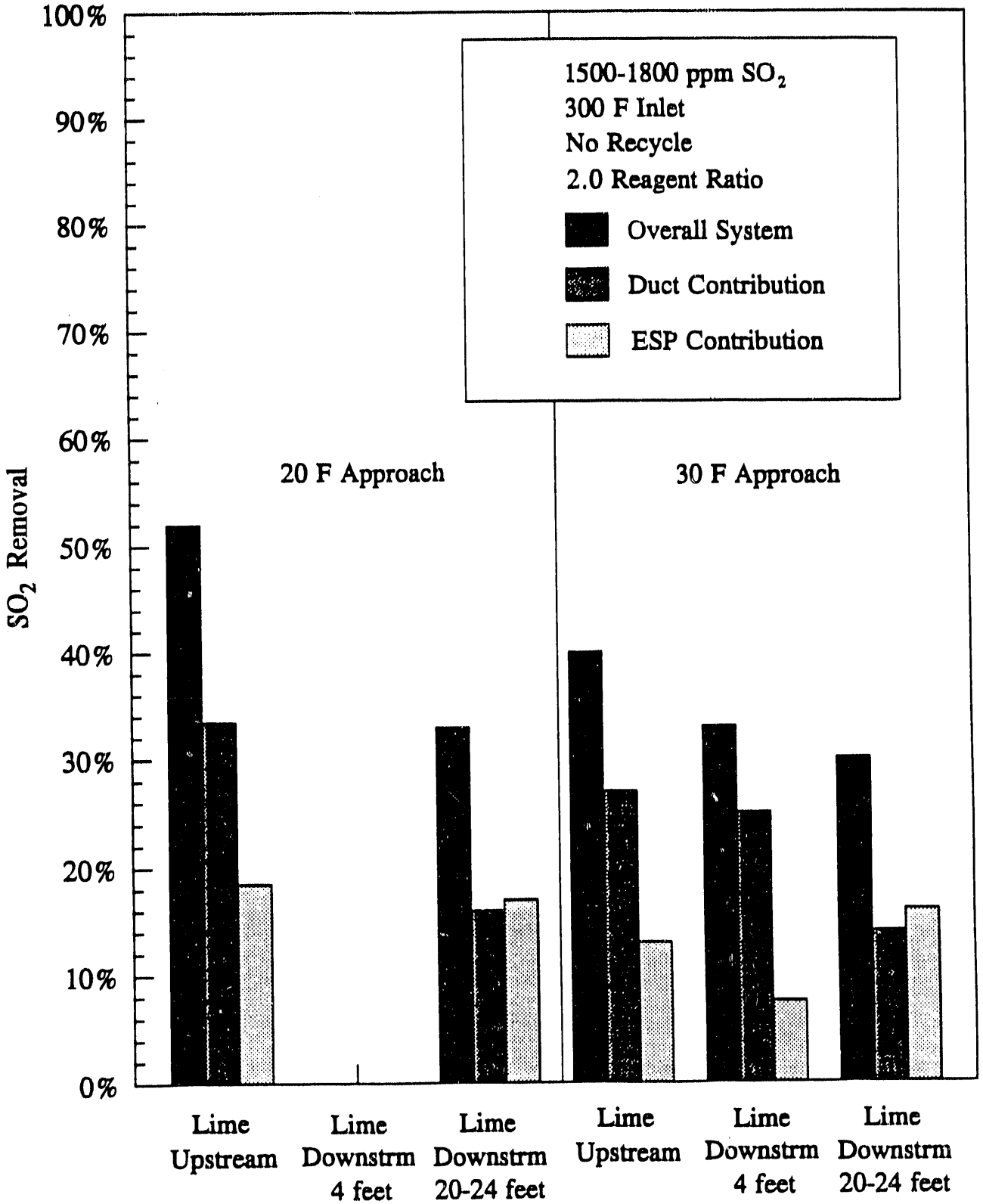

Figure 3-6. Effect of System Configuration on SO_2 Removal Performance

and the ESP (14% and 16%, respectively) were much different than in the 4-foot downstream case. The lower overall system SO_2 removal results with lime injected downstream is attributed to decreased interception and impaction, or "scavenging", of lime particles by water droplets. The high velocities of water droplets exiting a two-fluid nozzle are calculated to decrease rapidly, within a few feet, decreasing the velocity differential between droplets and lime particles.

3.4.3 Reagent Ratio

As expected, the data plotted in Figure 3-7 show that increasing the reagent ratio increases SO_2 removal performance. However, the goal of 50% overall system SO_2 removal was not achieved by increasing only the reagent ratio from baseline conditions to 2.9 moles calcium per mole SO_2. Only 44% overall system SO_2 removal was obtained. At a reagent ratio of 1.0 with other conditions at baseline values, overall system SO_2 removal was 25 percent. Thus, incremental improvement in SO_2 removal performance was much greater when increasing the reagent ratio from 1.0 to 2.0 than when increasing the reagent ratio from 2.0 to 2.9. Meanwhile, lime utilization decreased from 25% to 20% to 16%, when increasing reagent ratio from 1.0 to 2.0 to 3.0, respectively. The cost of fresh lime reagent is one of the major operating costs for the duct injection process. Therefore, it is desirable to maximize lime utilization and minimize the reagent ratio.

3.4.4 Approach-to-Adiabatic-Saturation Temperature

The data plotted in Figure 3-8 show that decreasing the approach-to-adiabatic-saturation temperature, or approach temperature, results in improved SO_2 removal performance. The goal for overall system SO_2 removal was achieved as reducing the approach temperature to 20° F while holding other conditions at baseline levels, produced 52% SO_2 removal.

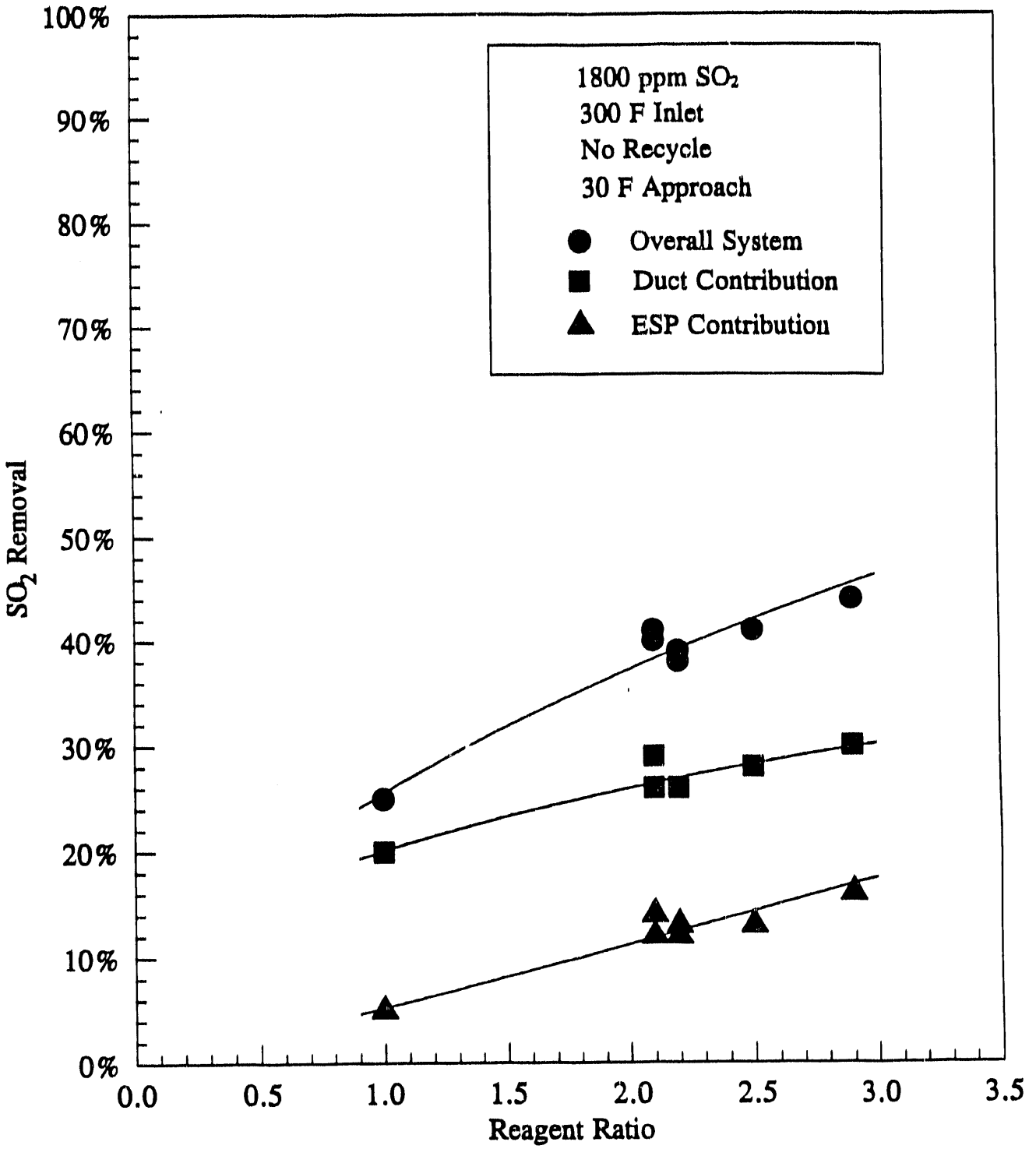

Figure 3-7. Effect of Reagent Ratio on SO_2 Removal Performance

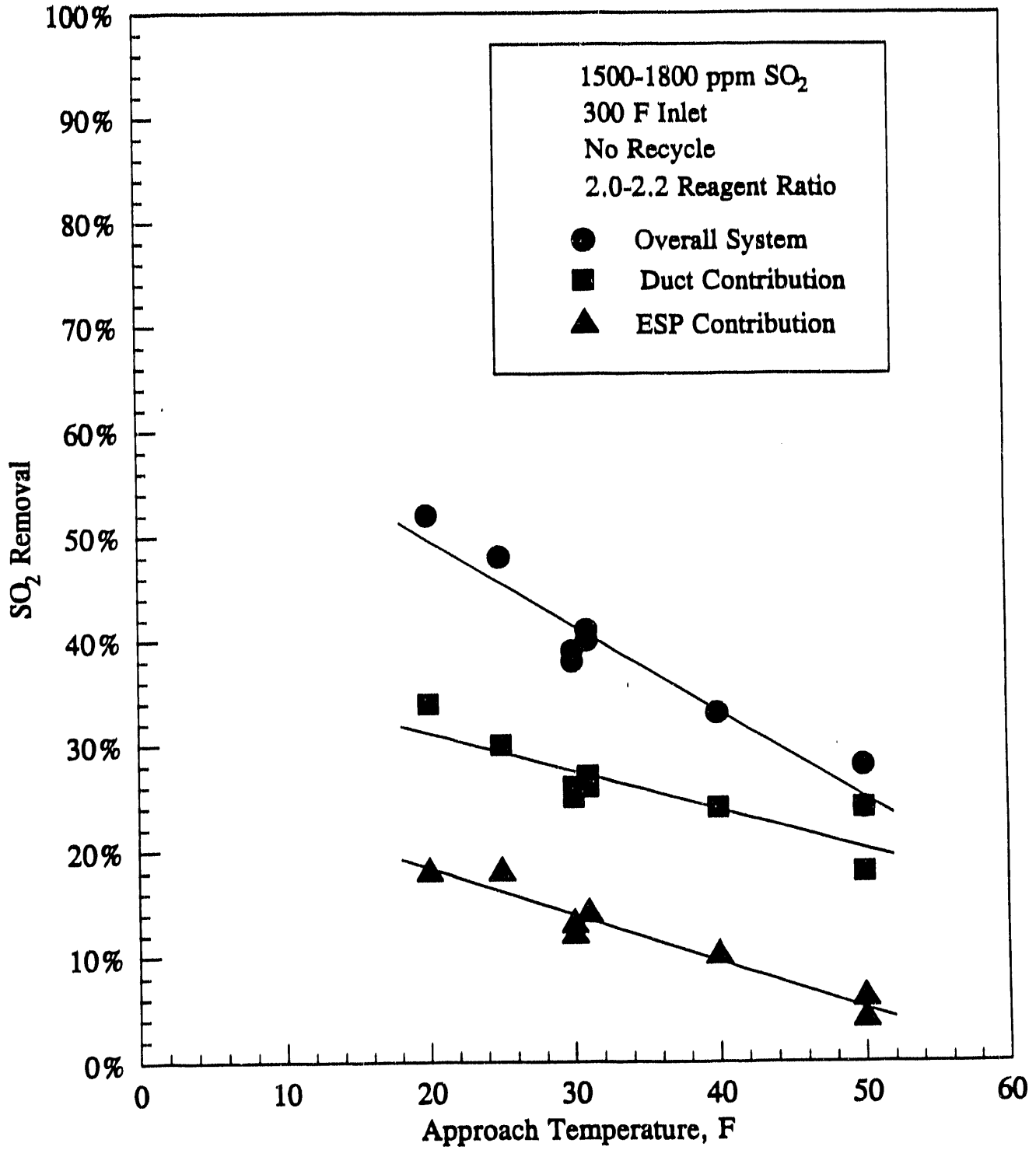

Figure 3-8. Effect of Approach Temperature on SO_2 Removal Performance

Lowering the approach temperature to improve SO_2 removal performance does not significantly affect the operating costs for the process, although lime consumption could be lowered to achieve the same level of SO_2 removal at a low approach temperature as at a higher approach temperature. However, using approach temperatures that are too low will result in significantly increased operations problems from buildup of duct wall deposits.

3.4.5 Recycle

Because lime utilization usually is low with the duct injection process,the solids collected in the ESP contain a high fraction of unreacted $Ca(OH)_2$. A portion of these collected solids can be recycled back to the duct to provide another opportunity for the $Ca(OH)_2$ to react with SO_2. Recycling these solids increases the total $Ca(OH)_2$ content in the system without increasing the addition rate of fresh lime. Therefore, any increase in SO_2 removal can be achieved without increasing the operating cost of fresh reagent. However, an additional solids handling system is required and the solids loading at the inlet of the ESP is increased. Thus, the ESP particulate removal efficiency must be increased to maintain the same particulate emission rate as before the retrofit of a duct injectioin FGD system.

The use of recycle solids produced significantly improved SO_2 removal performance when used with solids injected upstream of humidification. The data plotted in Figure 3-9 show that, at baseline conditions but with recycle solids at a ratio of 2.0 pounds recycle solids per pound of fresh lime, 56% overall system SO_2 removal was achieved. 52% overall system SO_2 removal was achieved at a recycle ratio of 1.0 pounds recycle solids per pound of fresh lime.

The beneficial effect of recycle was affected by the configuration of the system. As illustrated in Figure 3-10, when solids were injected 20 to 24 feet downstream of humidification, the use of recycle produced no improvement in SO_2

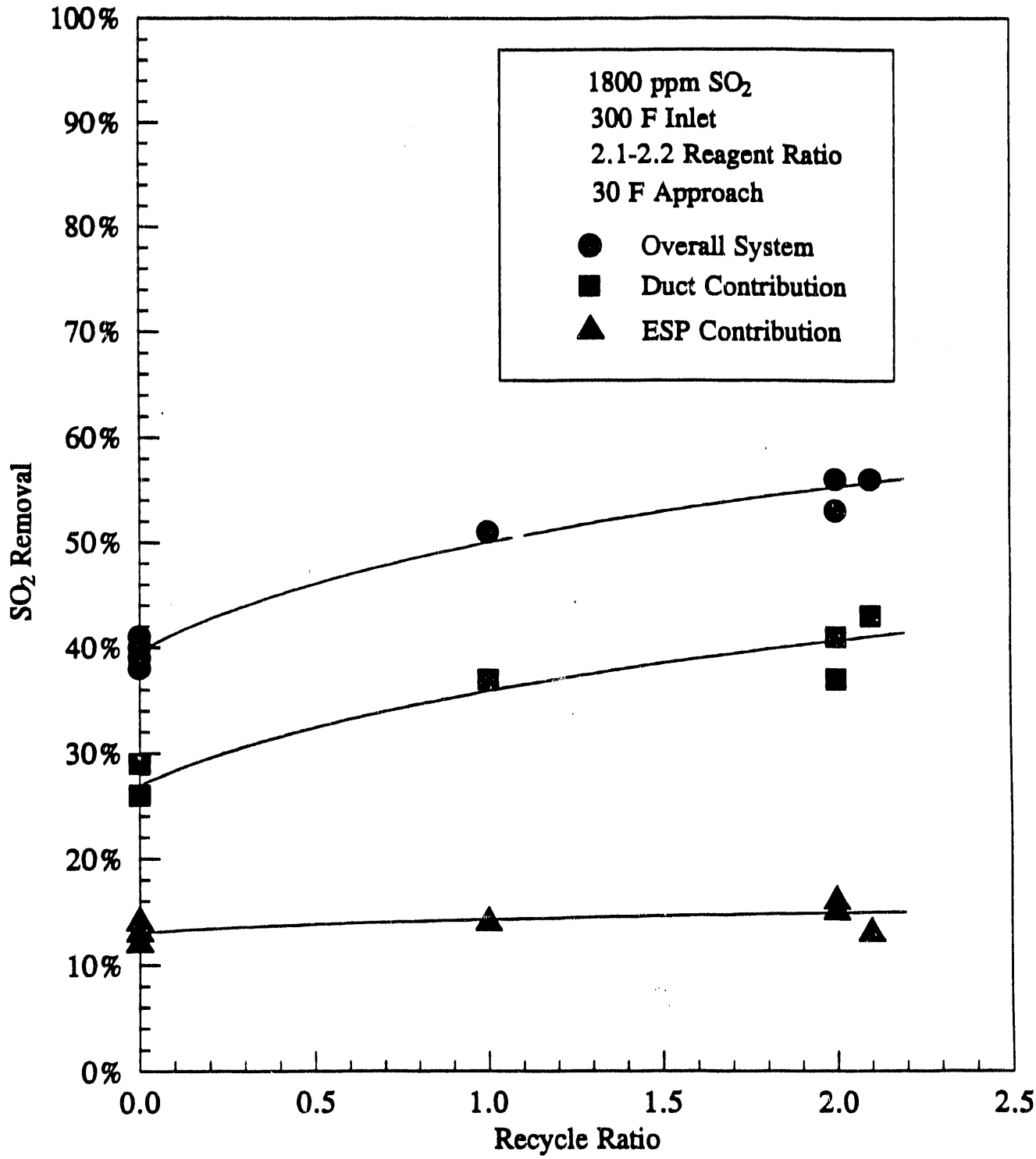

Figure 3-9. Effect of Recycle Ratio on SO_2 Removal Performance

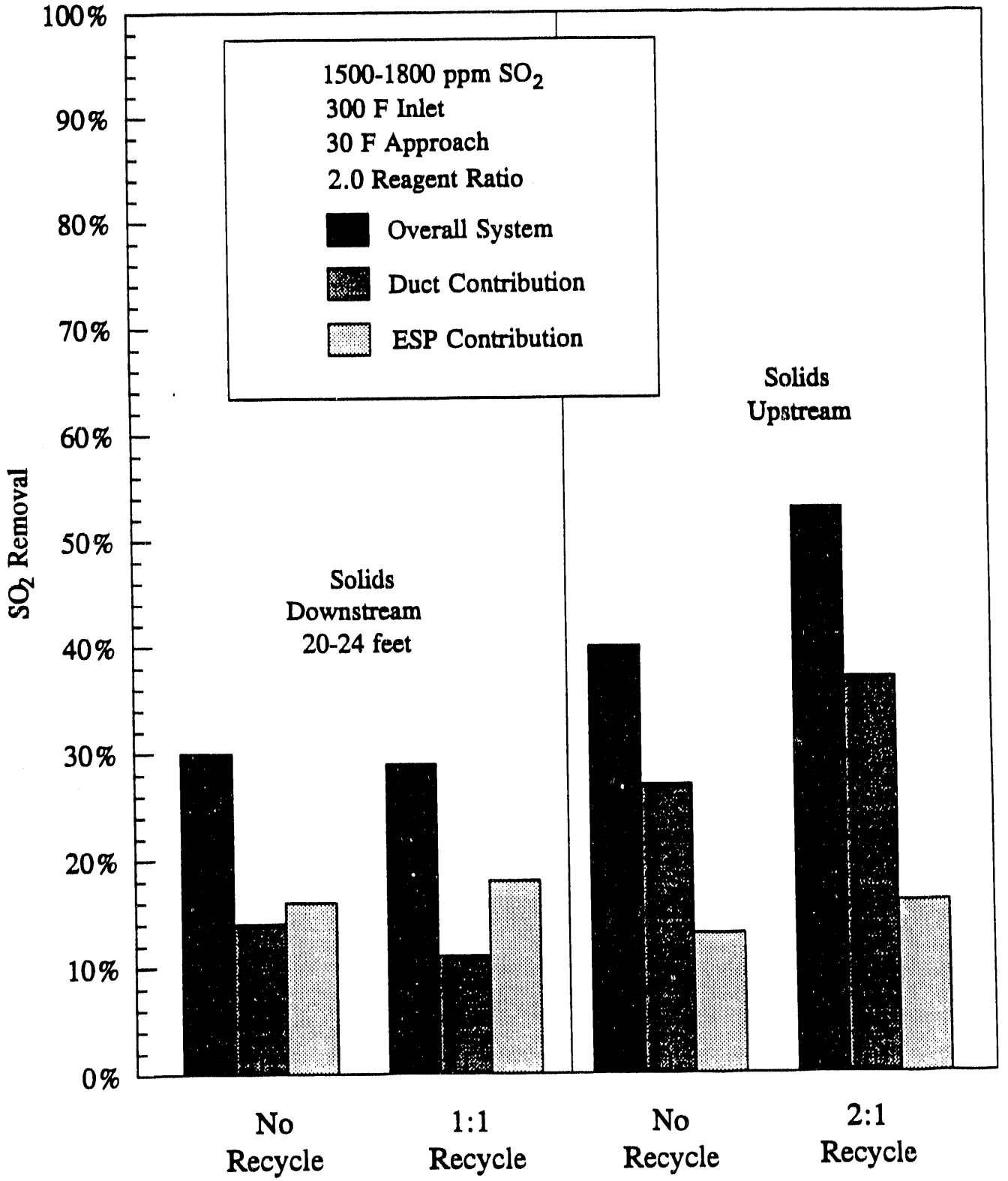

Figure 3-10. Effect of Humidification Configuration on Effectiveness of Recycle to Enhance SO_2 Removal

removal performance. This observation may be explained by the hypothesis that accumulation of calcium sulfite around a shrinking core of lime prevents further reaction of the unused lime when the material is recycled. It appears that wetting of recycle solids by scavenging with water droplets releases the unused lime in the recycle solids.

The data presented in Figure 3-11 illustrate that the incremental improvement in SO_2 removal performance obtained by adding a fixed amount of recycle solids was greater at a higher reagent ratio of 2.1 (11 percentage points improvement) than at a reagent ratio of 1.1 (5 percentage points improvement). At a lower reagent ratio, more of the fresh lime is utilized in the first pass through the duct leaving less unreacted lime in the recycle material.

Also, as illustrated in Figure 3-12, there was less incremental improvement in SO_2 removal performance when recycle solids at a ratio of 2.0 pounds recycle per pound of fresh lime were used at an approach temperature of 20° F (11 percentage points) than at an approach temperature of 30° F (15 percentage points). Again, the explanation for this is that at lower approach temperatures, more fresh lime is utilized in the first pass leaving less unreacted lime in the recycle material.

3.4.6 Flue Gas Velocity

One test was run with the flue gas flow rate reduced by 25% to reduce the humidification water flow rate. This was done in an attempt to reduce buildup of wall deposits. However, reducing the gas flow had no observable effect on either deposits formation or, as illustrated in Figure 3-13, SO_2 removal performance.

3.4.7 Inlet SO_2 Concentration

The literature contains conflicting information regarding the effect of inlet SO_2 concentration on SO_2 removal performance in duct injection systems using separate

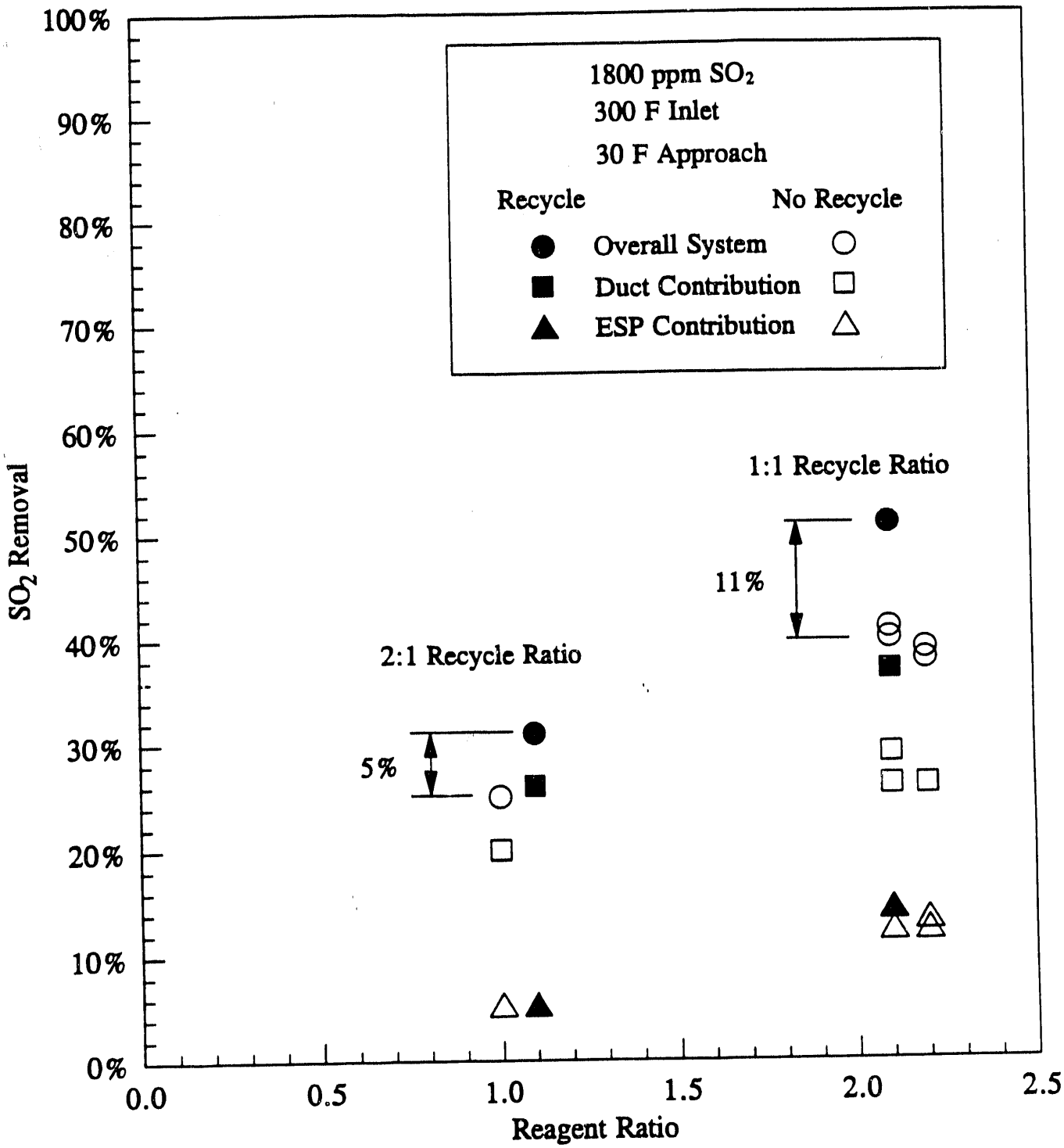

Figure 3-11. Effect of Reagent Ratio on Effectiveness of Recycle to Enhance SO_2 Removal Performance

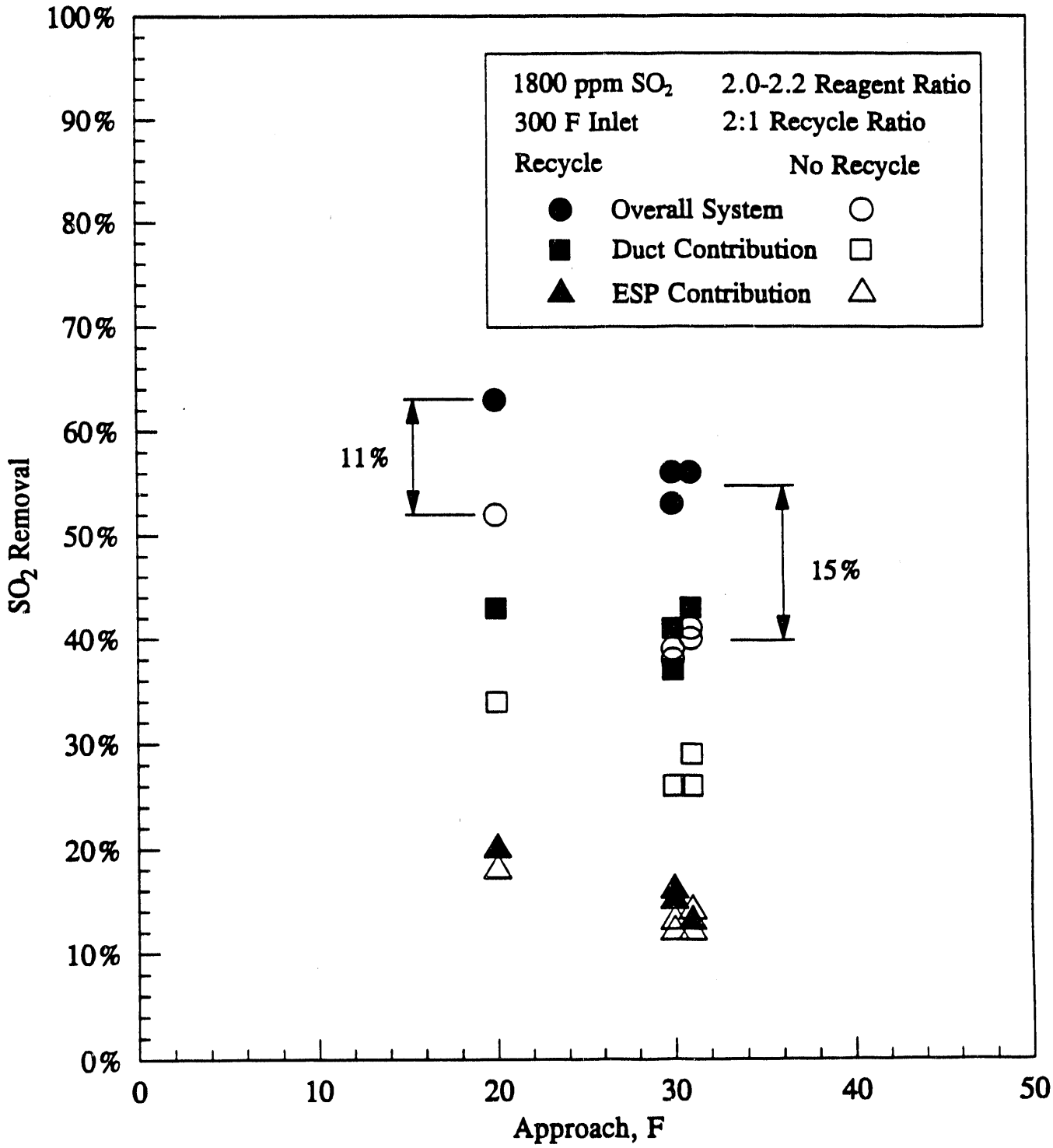

Figure 3-12. Effect of Approach Temperature on the Ability of Recycle to Enhance SO_2 Removal

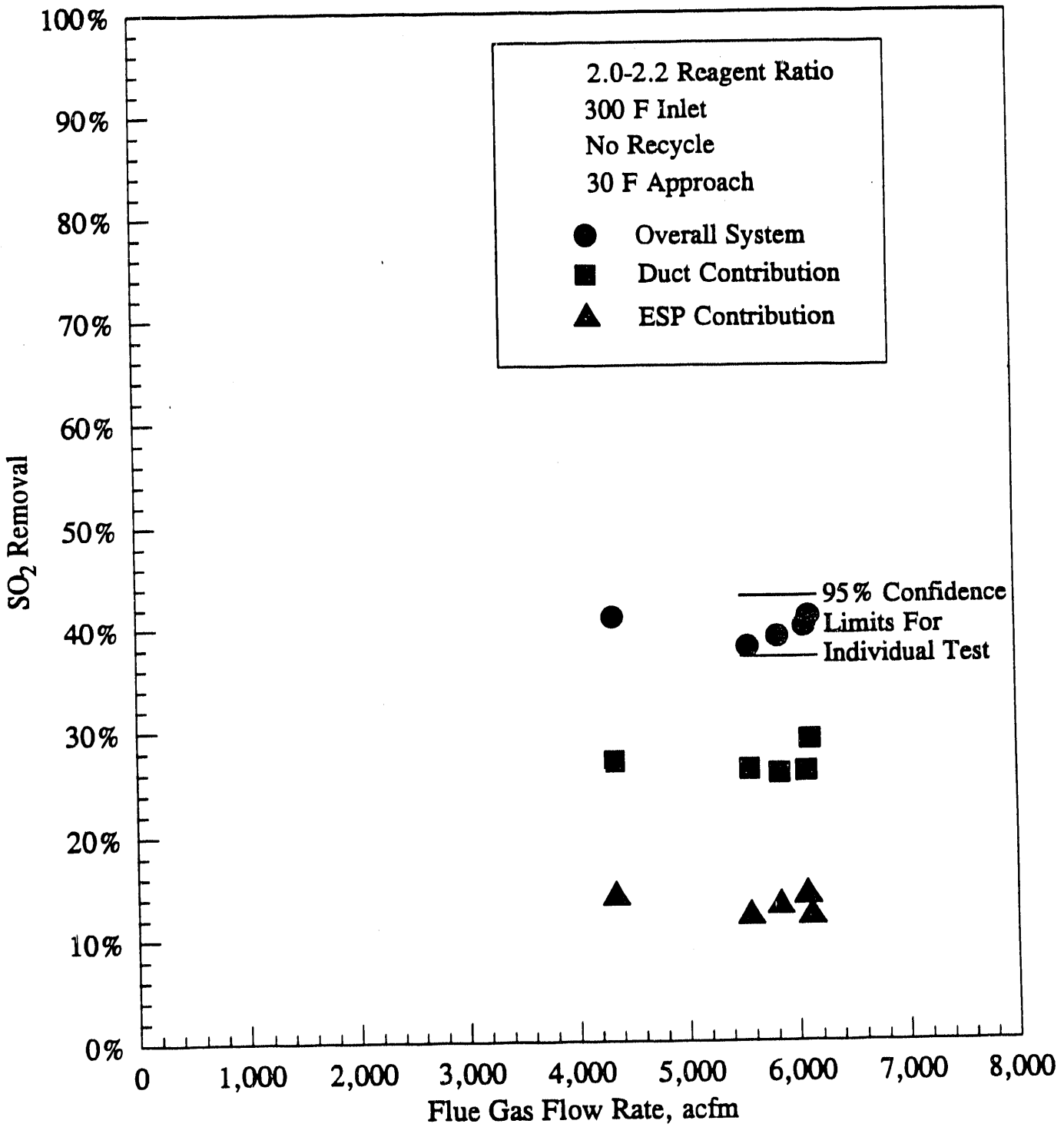

Figure 3-13. Effect of Reduced Flue Gas Flow Rate on SO_2 Removal

humidification and lime injection (1 and 2). A possible explanation for this discrepancy is that the effect is related to the details of the process design and configuration, although data interpretation also may be contributing to the observed difference.

The trend of decreasing SO_2 removal efficiency with increasing inlet SO_2 concentration from similar processes, such as spray drying and duct slurry injection (3, 4, and 5), may not apply to dry injection because of the inherent difference in the mechanism of contacting lime and water. With slurry injection, all of the lime particles are contained in water droplets and are wetted. As the inlet SO_2 concentration increases, more SO_2 must be transferred across nearly the same droplet surface area. The droplet surface area does not change appreciably because the amount of water required to cool the flue gas does not increase significantly with SO_2 concentration. However, with the dry injection process, lime particles must be scavenged by water droplets to become reactive. As the inlet SO_2 concentration increases, more lime is injected to maintain a fixed reagent ratio, and the increased lime particle concentration in the duct results in more lime being scavenged by the water droplets.

In this study, two tests were run at markedly different inlet SO_2 levels. A high concentration of 2990 ppm was produced by spiking with pure SO_2, and a low inlet SO_2 concentration of 730 ppm was produced by diluting flue gas with ambient air heated to 300° F. Since dilution with air also lowered the humidity and the measured wet-bulb temperature of the flue gas during the low-inlet-SO_2 test, the inlet flue gas temperature was dropped by 10° F so that the rate of humidification water addition would be the same as for baseline tests. This eliminated water addition rate as a variable that could influence SO_2 removal performance through scavenging. The data plotted in Figure 3-14 show that little effect on SO_2 removal performance was observed between inlet SO_2 concentrations of 730 to 2990 ppm.

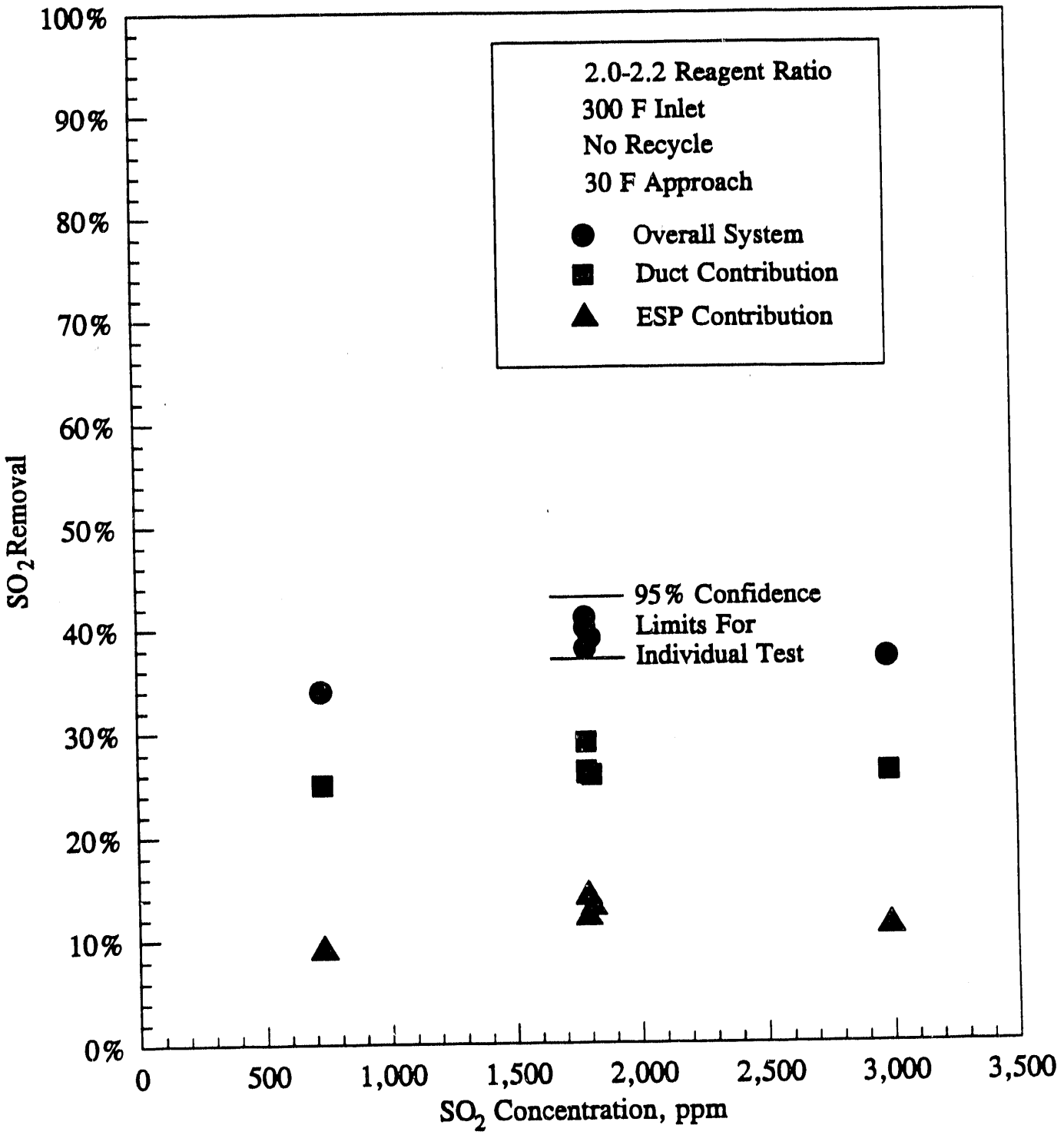

Figure 3-14. Effect of Inlet SO_2 Concentration on SO_2 Removal Performance

3.4.8 Inlet Flue Gas Temperature

Operation of the duct injection process at different inlet temperatures does have a noticeable effect on SO_2 removal, as illustrated by the data plotted in Figure 3-15. The effect is attributable to the amount of humidification water required at the different inlet temperatures. With other conditions at baseline levels, overall system SO_2 removal increased from 33% to 43% as the inlet temperature was raised from 260 to 340° F.

3.4.9 Chloride Addition

$CaCl_2$ was added to the humidification water during two tests to evaluate the effects of using a hygroscopic salt. The results are plotted in Figure 3-16. Only a slight increase in SO_2 removal performance resulted from adding 0.9% $CaCl_2$ to the water when no recycle was used. However, when recycle was used and 3.4% $CaCl_2$ was added to the water, overall system SO_2 removal increased dramatically to 72 percent. Unfortunately, buildup of wall deposits also increased and the duct plugged repeatedly after only a very few hours of operation. Also, there were operation problems from damp deposits on the ESP distributor plate, one ESP penthouse, and the ESP hoppers. Both the improved SO_2 removal performance and the increased operations problems with deposits are attributed to reduced droplet evaporation rate and increased moisture content of the solids due to the deliquescent nature of $CaCl_2$. While $CaCl_2$ could serve as a beneficial additive to improve SO_2 removal in the duct injection process, more study is required to determine a chloride addition rate that provides an improvement in SO_2 removal but does not cause operational difficulties.

3.4.10 ESP Residence Time

Two tests were made at baseline conditions, but with the first two fields of the ESP turned off. Thus, the effect of increased residence time for gas/solid contact could be evaluated. The data plotted in Figure 3-17 show that the increase in overall

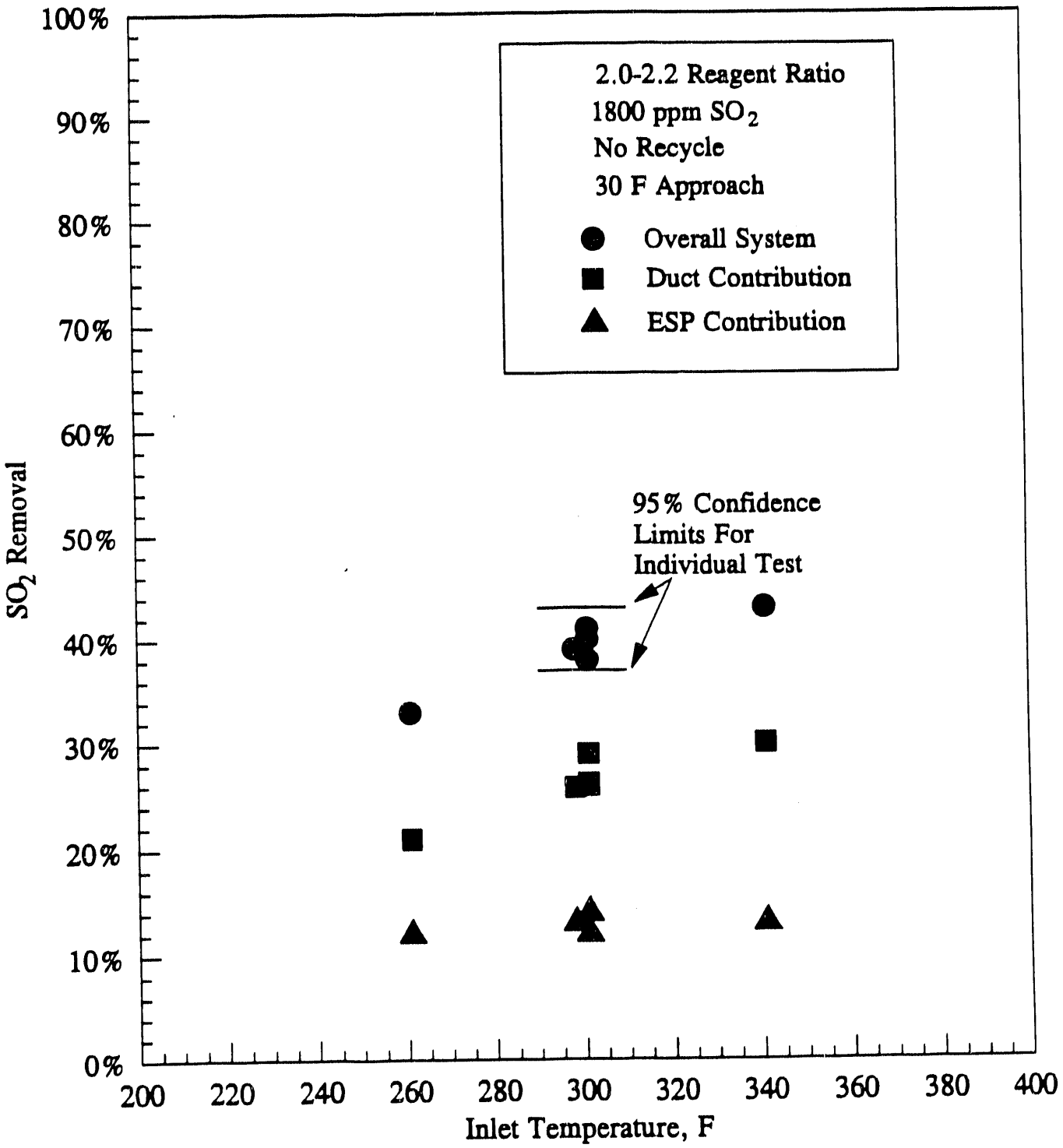

Figure 3-15. Effect of Flue Gas Inlet Temperature on SO_2 Removal Performance

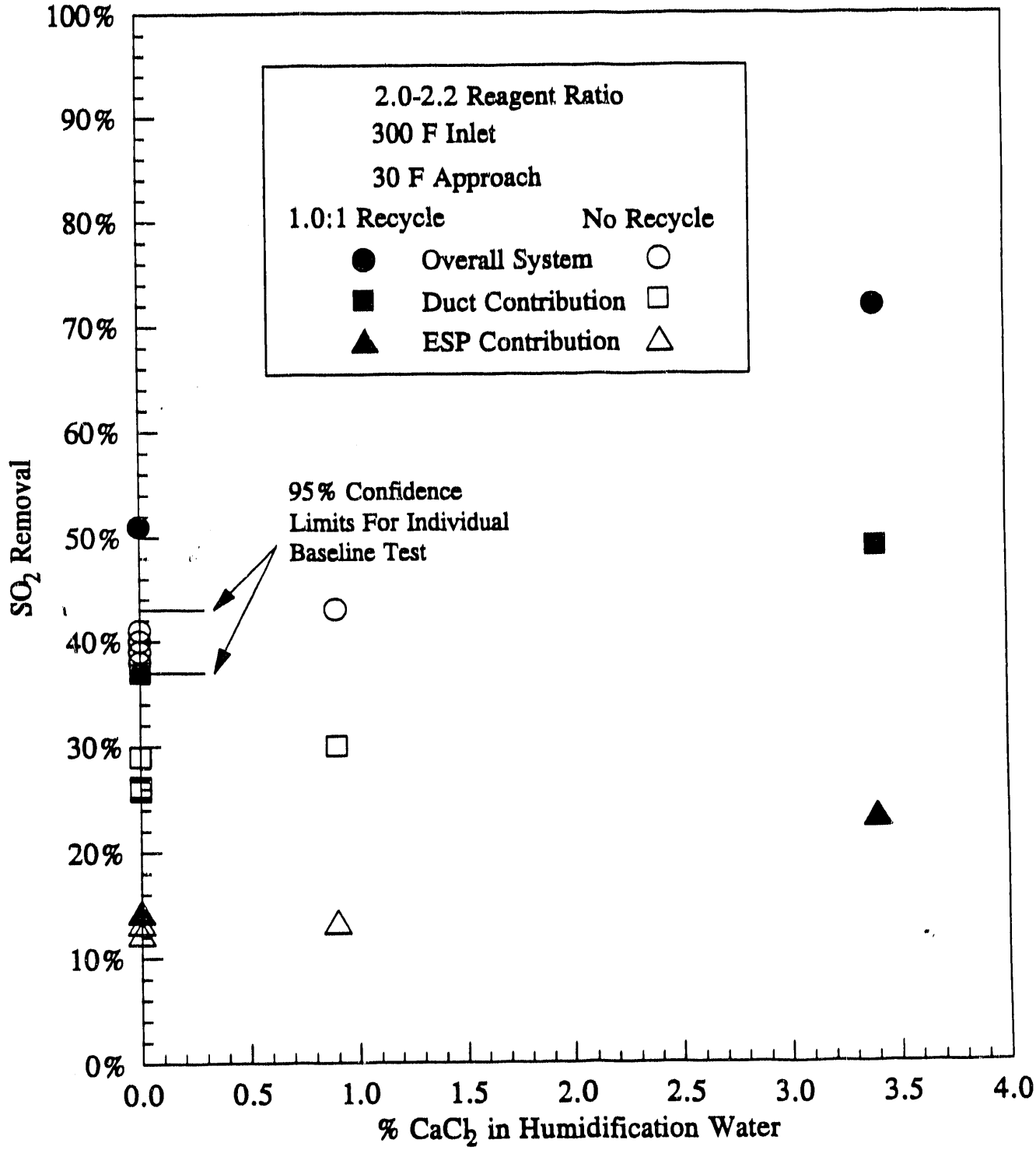

Figure 3-16. Effect of Chloride Addition on SO_2 Removal Performance

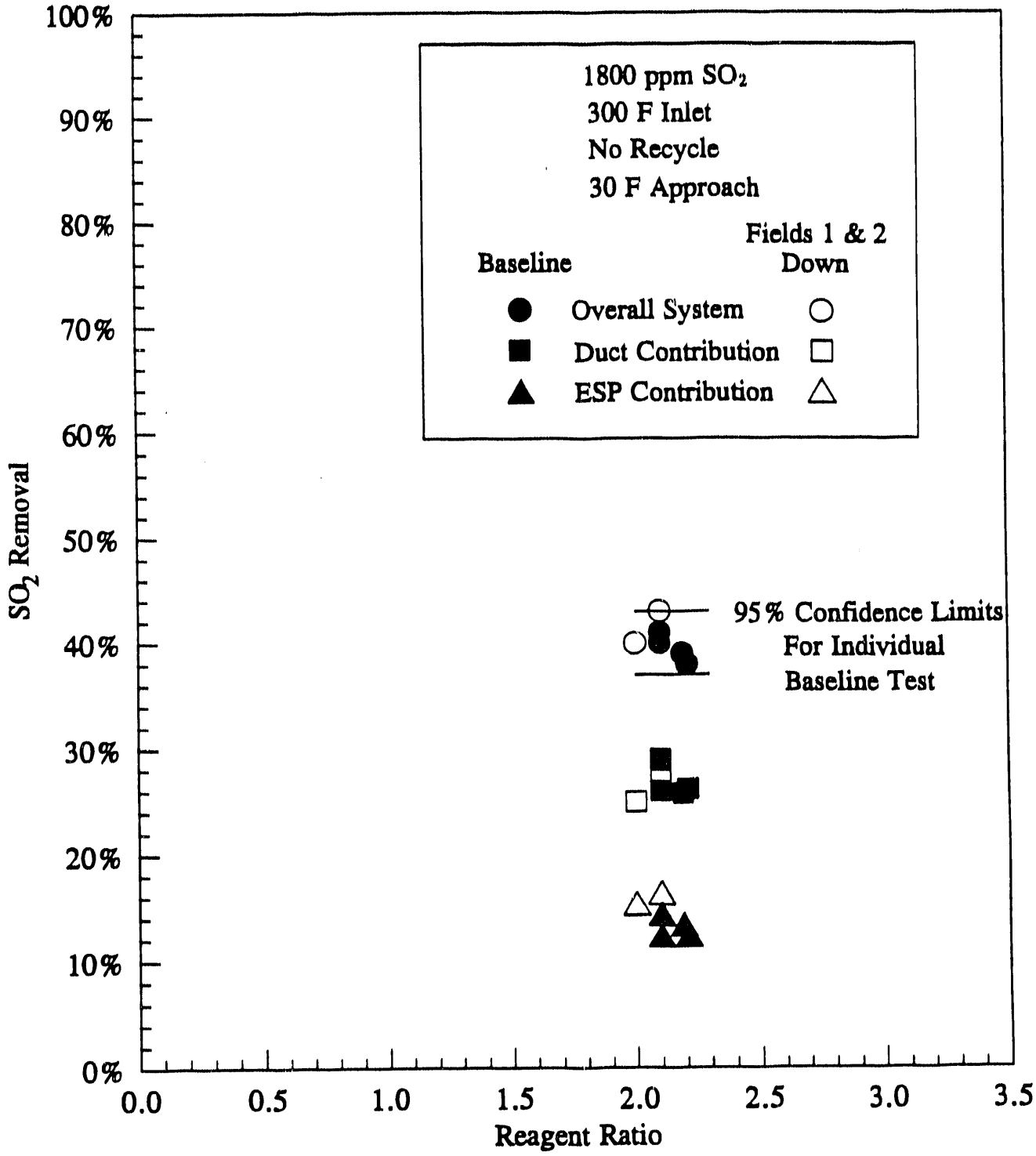

Figure 3-17. Effect of Increased Residence Time in ESP Due to Fields Being Out of Service

system SO_2 removal was only 2 to 3 percentage points, which is within experimental error. Therefore, increased residence time for gas/solid contact does not appear to have a major effect on SO_2 removal performance. The more important effect resulting from residence time in the duct may be more complete drying of wetted solids prior to impinging on the duct walls at the first bend in the ductwork.

3.5 NO Removal Performance

NO_x removal measurements were considered a low priority during this study. However, some NO removal measurements were made during some early tests. These data indicated that NO removal by the process was negligible, ranging from 0 to 6.5 percent.

3.6 Solid Waste Characteristics

Although investigation of solid waste characteristics was not an objective of this program, one solid waste sample was analyzed to obtain a landfill disposal permit. The results of the EP extraction analyses verified results from previous duct injection studies that the solid waste is non-hazardous.

3.7 Conclusions

The following conclusions are drawn from the duct injection pilot testing at Meredosia:

- 40% overall system SO_2 removal can be achieved at baseline operating conditions of 30° F approach temperature, 2.0 reagent ratio, 300° F inlet temperature, with lime injected upstream of humidification, and without using recycle.
- The ESP provides a significant contribution to overall system SO_2 removal. The contribution is 13 percentage points at baseline operating conditions.

- Overall system SO_2 removal performance is reduced to about 32% when lime is injected downstream of humidification at baseline conditions.

- Humidification using either a single nozzle or two nozzles in series does not have a significant effect on measured SO_2 removal performance.

- Increasing reagent ratio from 2.0 at baseline conditions to 2.9 produces a small increase in overall system SO_2 removal efficiency to 44 percent. Therefore, increasing reagent ratio alone does not appear to be a practical means to achieve the goal of 50% SO_2 removal. Decreasing the reagent ratio to 1.0 produces a large reduction in overall system SO_2 removal efficiency to 25 percent.

- Decreasing the approach temperature from 30° F at baseline conditions to 20° F produces a significant increase in overall system SO_2 to 52 percent. Although there is increased potential for buildup of damp wall deposits when using low approach temperatures, no significant increase in the amount of wall deposits was observed during the 20° F approach temperature test at the Meredosia pilot plant. However, the length of the water spray plume did increase to wet a thermocouple located at a residence time of 1.3 seconds downstream of the nozzle. This may be an important limiting factor in systems with short available residence time.

- Recycle significantly enhances SO_2 removal when added upstream of humidification. At baseline conditions with 2.0 pounds recycle solids per pound fresh lime, 55% SO_2 removal was achieved. When recycle and lime are added downstream of humidification, recycle does not significantly enhance SO_2 removal performance.

- Enhancement of SO_2 removal performance with the addition of recycle is reduced at low reagent ratios and low approach temperatures. Lime utilization during the first pass is higher under these conditions, leaving less unreacted lime available in recycle solids.

- Reducing the flue gas flow rate by 25% has a negligible effect on either SO_2 removal efficiency or on reducing duct wall deposits formation.

- Changing inlet SO_2 concentration between 750 and 3000 ppm does not significantly affect SO_2 removal performance.

- Increasing inlet flue gas temperature from 260° F to 340° F increased overall system SO_2 removal from 33% to 43% with other conditions at baseline levels. This is attributed to the increased humidification water flow rate which increases wetting of lime particles.

- Addition of moderate amounts of calcium chloride to the humidification water (0.9% $CaCl_2$ in the water) does not significantly enhance SO_2 removal efficiency when recycle is not used.

- Addition of large amounts of calcium chloride to the humidification water (3.4% $CaCl_2$ in the water) significantly increases overall system SO_2 removal to 72% when recycle is used with other conditions at baseline levels.

- Adding a large amount of gas/solid contact time by turning off inlet fields of the ESP does not significantly affect SO_2 removal efficiency.

- NO removal is negligible.

3.8 References

1. Babu, M., J. College, R. Forsythe, R. Herbert, D. Kanary, D. Kerivan, and K. Lee. 5-MW Toronto HALT Pilot Plant Test Results. DOE/PC/81012-T1-PT.I-A, NTIS 1415924, December 1988.

2. Blythe, G. M., R. A. Smith, L. J. Muzio, C. A. Martin, and V. V. Bland. Calcium Injection Upstream of an Electrostatic Precipitator and a Fabric Filter for Simultaneous SO_2 and Particulate Removal: Pilot and Bench-Scale Results-Draft Final Report. Prepared for Electric Power Research Institute, Research Project 2784-1, June 1989.

3. Tennessee Valley Authority, Ontario Hydro, Electric Power Research Institute, Kentucky Energy Cabinet Laboratory. 10-MW Spray Dryer/ESP Pilot Plant Test Program High-Sulfur Coal Test Phase (Phase III) Final Report. TVA/OP/ED&T-88/35, July 1988.

4. Blythe, G. M., J. M. Burke, and R. L. Glover. Evaluation of a 2.5-MW Spray Dryer/Fabric Filter SO_2 Removal System. Electric Power Research Institute, Report CS-3953, Palo Alto, CA May 1985.

5. Hovis, L. S., R. E. Valentine, B. J. Jankura, P. Chu, and J. C. S. Chang. "E-SO_x Pilot Evaluation." presented at the EPA/EPRI First Combined FGD and Dry SO_2 Control Symposium, St. Louis, MO, October 1988.

4.0 ESP TEST RESULTS

4.1 Introduction

Pilot plant tests to characterize the performance of an ESP operating downstream of an in-duct scrubbing system were conducted by ADA Technologies, Inc., acting as a subcontractor to the Radian Corporation. The performance of an ESP downstream of a duct sorbent injection systems is critical to the success of duct injection technology. The interest in dry scrubbing is primarily directed at retrofit applications for existing utility and industrial boilers burning medium- and high-sulfur coal. The 1990 Clean Air Act requires that many older facilities provide control of sulfur dioxide. For dry scrubbing technologies to be cost effective as a retrofit flue gas desulfurization process, it is important that the existing particulate control equipment perform well. Since the large majority of older boilers use ESPs for particulate control, it is important that the ESP be capable of collecting the injected sorbent in addition to the flyash.

4.2 Pilot ESP Description

Two identical four-field ESPs were installed in series with a straight transition section connecting the two units. Details of the physical geometry and electrical specifications of the ESP are given in Table 4-1.

The transition section was 4 feet long and had the same cross sectional area as the active sections of the ESP so that the gas flow distribution was not disturbed. This resulted in an ESP with eight electrical fields and a nominal SCA of 533 ft^2/kacfm. The transition section provided a sampling section between the two ESPs so that it was possible to test the system simultaneously at two SCA levels.

The ESPs used a rigid frame corona elctrode design. Eight NWL transformer-rectifier (T/R) sets were used to energize the eight electrical sections of the

Table 4-1

ESP Description

Specification	
Plate Height	7 feet
Plate Spacing	9 inches
Number of Gas Passages	4
Plate Length	7.5 feet
Number of Electrical Sections	8
Nominal Flow Rate	6300 acfm
Nominal Velocity	5 ft/sec
SCA per section at 5 ft/sec	67 ft^2/kacfm
Total SCA at 5 ft/sec	533 ft^2/kacfm
Secondary Voltage	75 kV
Secondary Current	50 mA
Electric Field Strength	6.6 kV/cm
Current Density	128 nA/cm^2

ESP. The ESP unit used two different types of rappers. A hammer and anvil design was used to clean the collecting plates, and an electric solenoid design was used to clean the high voltage frames.

4.3 Air and Gas Load Testing

Air load and gas load tests were performed on the ESP prior to the start of the ESP evaluation. These test were performed to check out the ESP and to insure that the pilot unit was in proper working order. Any deficiencies that were discovered were corrected prior to the initiation of the test program. These included the addition of a second perforated gas distribution plate at the inlet of the ESP, adjustments to the high voltage frame alignment and wire tension, and replacement of missing wires.

The air load test included a characterization of the rapping system, measurement of the air flow distribution at the inlet to the ESP, and a check out of the electrical characteristics. This was followed by gas load tests to determine the air in-leakage and temperature gradients across the ESP, and velocity profiles at the sampling stations.

The air load and gas load testing on the pilot ESP demonstrated that it was in good mechanical condition. The electrical characteristics showed that all eight fields were properly aligned and the unit was capable of operating at high voltage levels and current densities that are typical of a well working ESP. Electrical conditions for the first four fields of the ESP under air load conditions are plotted as voltage/current (VI) curves in Figure 4-1.

4.4 Baseline Flyash Tests

The baseline ESP performance test with flyash involved three different test conditions which allowed the measurement of ESP characteristics as a function of SCA

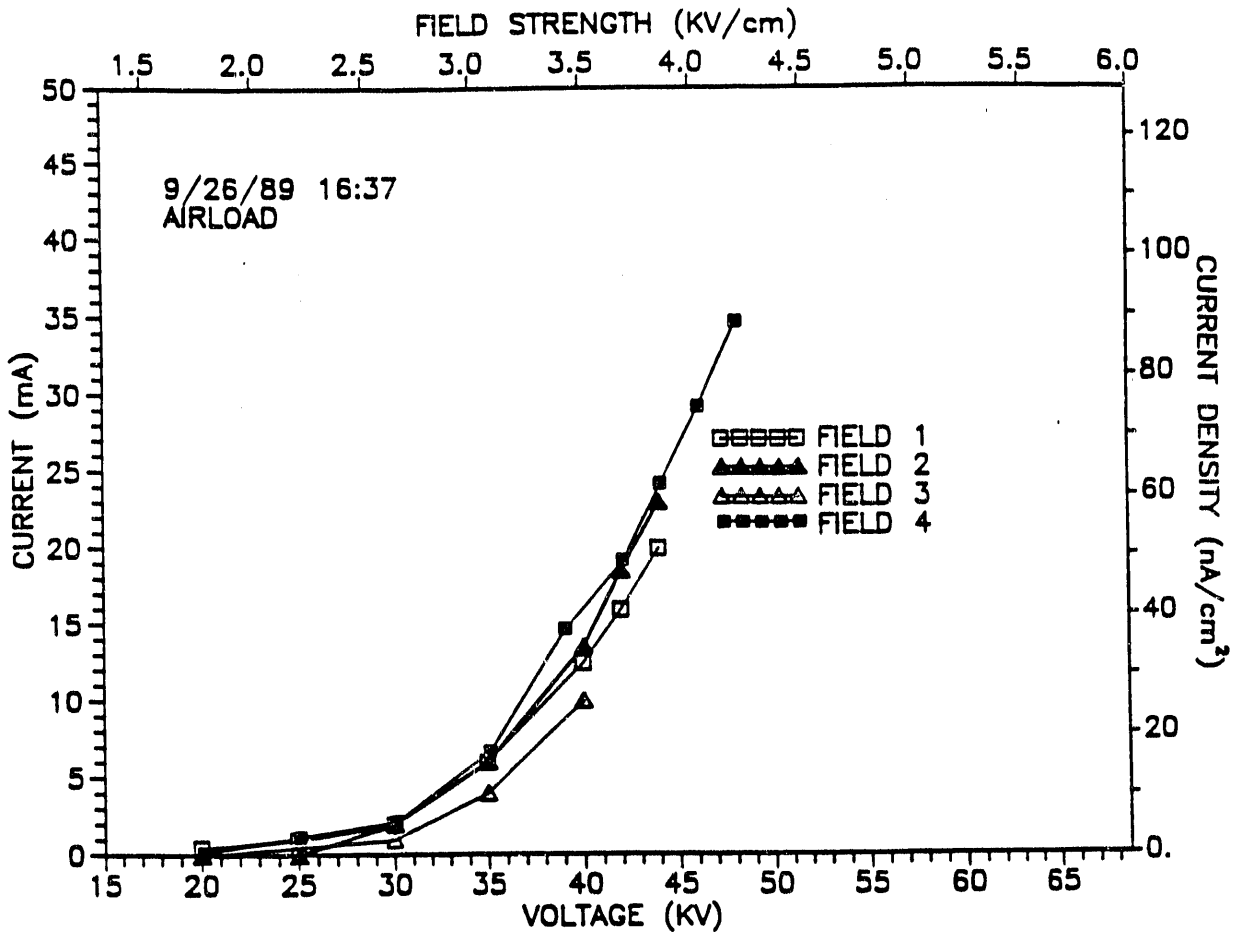

Figure 4-1. Air Load Electrical Conditions for the First Four Fields of ESP

and ESP velocity. A summary of the measurement results for baseline flyash tests is presented in Table 4-2, and the data are plotted in Figure 4-2. Typical VI curves for baseline flyash tests are illustrated in Figure 4-3.

In-spite of excellent electrical operating conditions, the collection efficiencies produced by the ESP were much lower than expected. This was especially true for the results obtained after two and three energized fields. Efficiencies below 70% were measured for an SCA on the order of 150 ft^2/kacfm. The particle size distributions showed that the flyash was not extremely fine as 70% of the particles were captured in the precutter. Therefore, particle size was not the cause of the low collection efficiency.

The most likely cause of the poor ESP performance is reentrainment due to the low resistivity of the particles. The coal burned at Meredosia produces a high iron flyash which results in higher than expected sulfur trioxide (SO_3) concentrations. In addition, the temperature of the flue gas at the pilot plant inlet was close to, or below, the acid dew point. This leads to very low particle resistivity. Measurements made at the ESP inlet at 300° F showed that the resistivity was in the low 10^9 ohm-cm range. This is not surprising because at the SO_3 levels that were measured, 9-18 ppm, an acid dew point of 280° F would be expected. The temperature data show that when the flue gas is 300° F at the inlet of the ESP, it drops to as low as 258° F at the outlet of the ESP. This means that the flue gas temperature decreases below the acid dew point in the ESP. It is likely that the particle resistivity values would fall to the 10^7 to 10^8 ohm-cm range in the ESP. This range has been associated with reentrainment of collected particles by electrostatic repulsion of particles (1). Repulsion, rather than scouring, is the most likely cause of reentrainment in the pilot ESP as the data indicated that the ESP efficiency did not decrease at an increased gas velocity. If particles were reentrained by a scouring of the plates by the gas flow, reentrainment would increase at high velocity.

Table 4-2

Meredosia Pilot ESP Baseline (Flyash Only) Particulate Sampling Results June, 1990

Collection Efficiency Does Not Include Final Rap

ESP Fields	SCA (ft^2/kacfm)	Face Velocity (ft/s)	Inlet Loading (gr/dscf)	Outlet Loading (gr/dscf)	Collection Efficiency (%)	Emission Rate (lb/MBTU)
8	590	4.5	1.567	0.00208	99.87	0.0047
4	295	4.5	1.567	0.0730	95.34	0.164
6	409	4.5	1.198	0.00473	99.70	0.0108
2	136	4.5	1.198	0.529	66.90	1.184
7	384	6.1	1.443	0.00735	99.49	0.01671
3	164	6.1	1.443	0.611	57.67	1.368

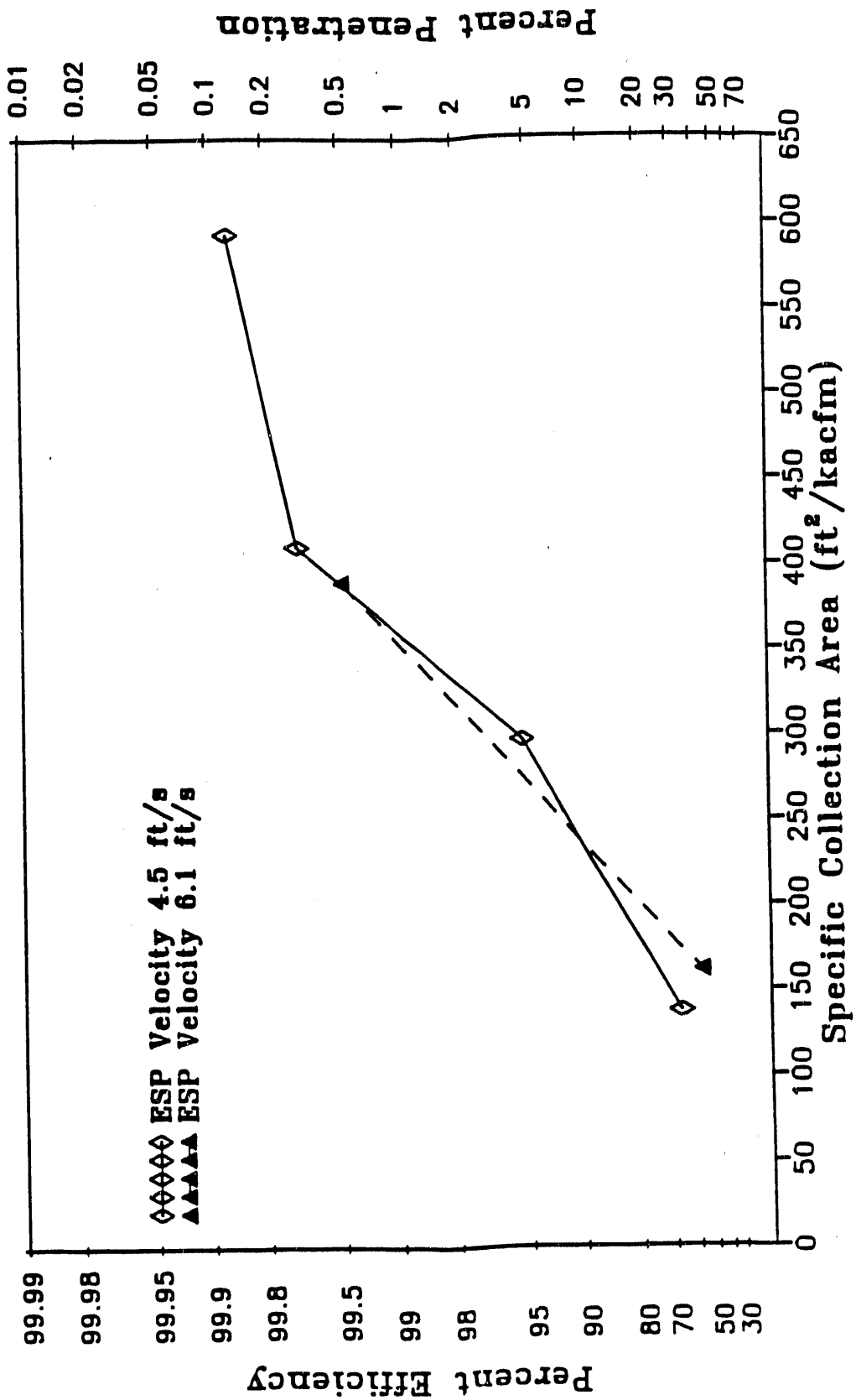

Figure 4-2. ESP Performance as a Function of Specific Collection Area - Baseline Flyash Conditions at the Meredosia Pilot ESP

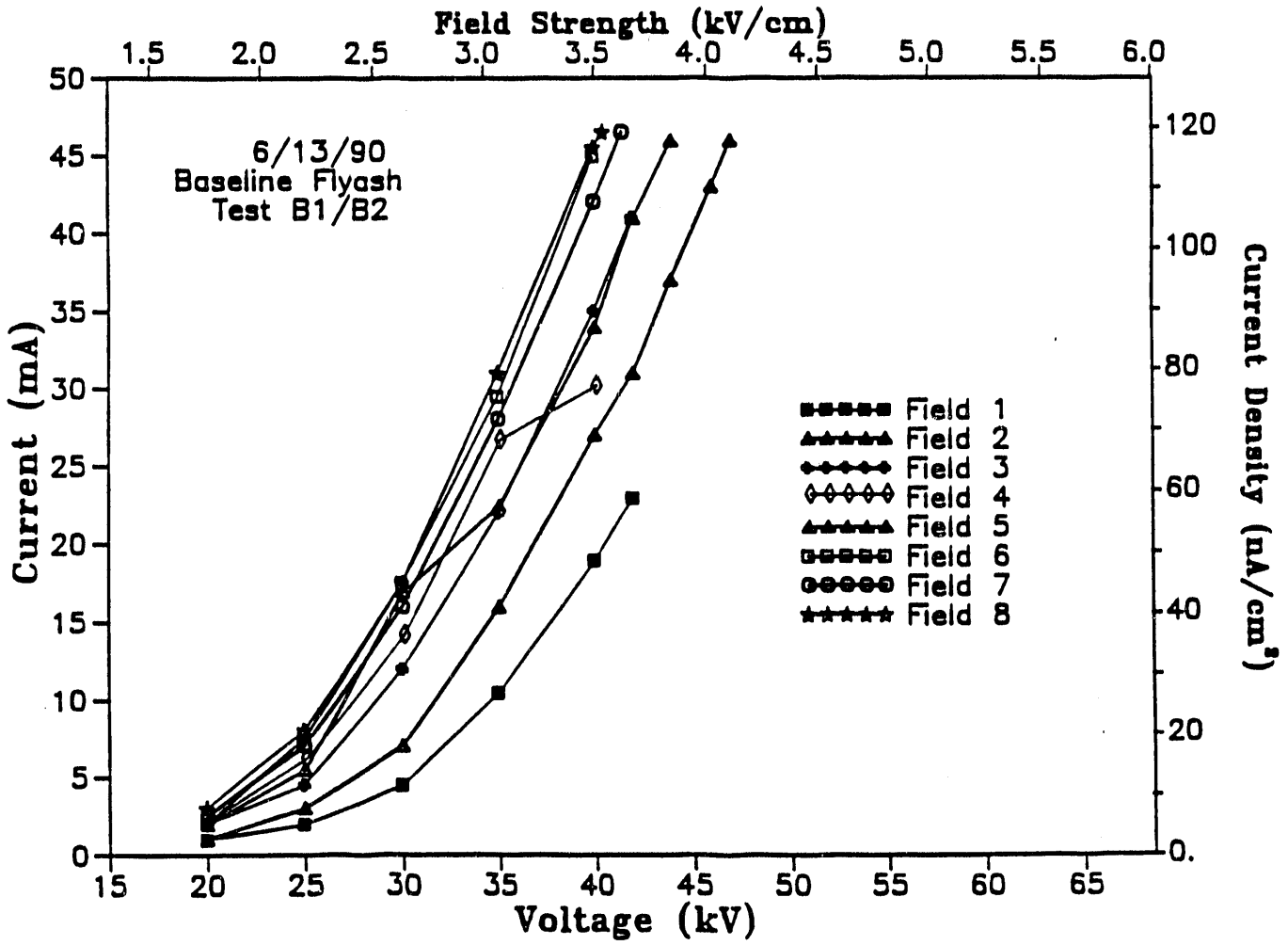

Figure 4-3. Typical Electrical Characteristics During Baseline Flyash Conditions

The baseline data were modeled using Version III of the SRI EPA ESP Model. The geometry of the pilot ESP as well as the operating voltages and currents and flue gas conditions measured during the baseline tests were input into the model. Based upon the results of the gas flow distribution tests, the parameter for the standard deviation of the gas flow was set at 0.25 for all cases. The model was then run for each case and the parameter for sneakage and reentrainment was adjusted until the calculated efficiency matched the measured data. It was determined that reentrainment of 44% of the particles collected in each section would be required to reduce the collection efficiency to the levels shown in Table 4-2.

4.5 Duct Injection Tests

4.5.1 Corona Quenching

During the sorbent injection tests with sorbent injection downstream of humidification, severe corona quenching occurred in the first field of the ESP, and significant corona suppression was measurable in the second and third field. This can be seen in Figure 4-4. VI curves for the first four active fields with sorbent injected upstream of humidification are plotted in Figure 4-5. From the differences in VI curves for the first active field, it was apparent that the cause of the suppression was not due solely to the addition of the sorbent but also to effects of the humidification system.

Particle size distribution measurements were made downstream of the spray nozzle to quantify the effect of humidification on the generation of fine particles. It was determined that the humidification of the flue gas produced a sulfate aerosol that had a concentration of 30 mg/dscm for particles less than 0.4 μm. This relates to a conversion of approximately 7 ppm of SO_3 to H_2SO_4. During the baseline measurements, the concentration of all particles less than 0.4 μm was determined to be 27.5 mg/dscm. This concentration increased to 57.4 mg/dscm during the lime-only (no recycle) duct injections test based upon impactor measurements. Therefore, there was an increase of

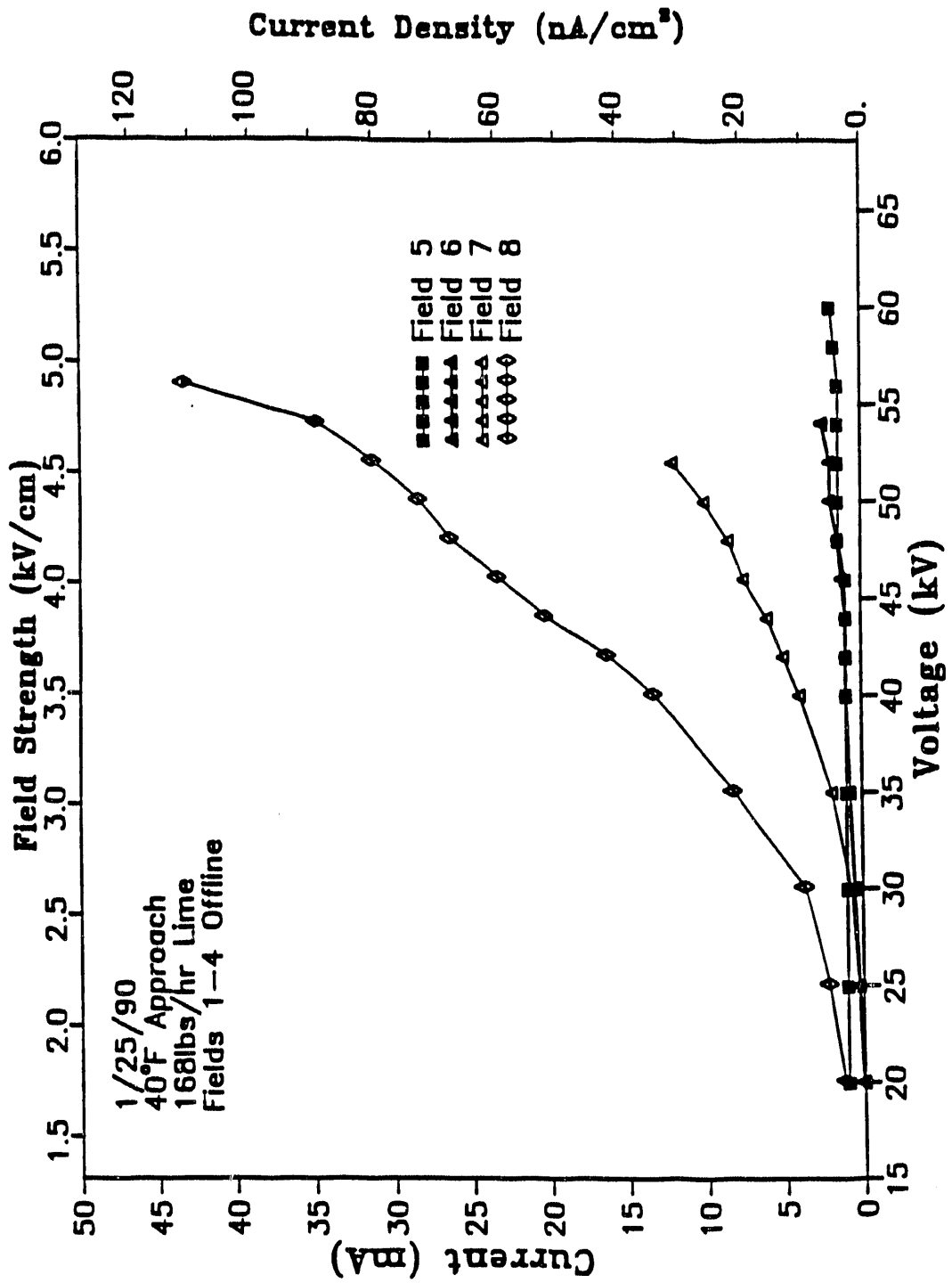

Figure 4-4. Typical Electrical Characteristics for Downstream Sorbent Injection

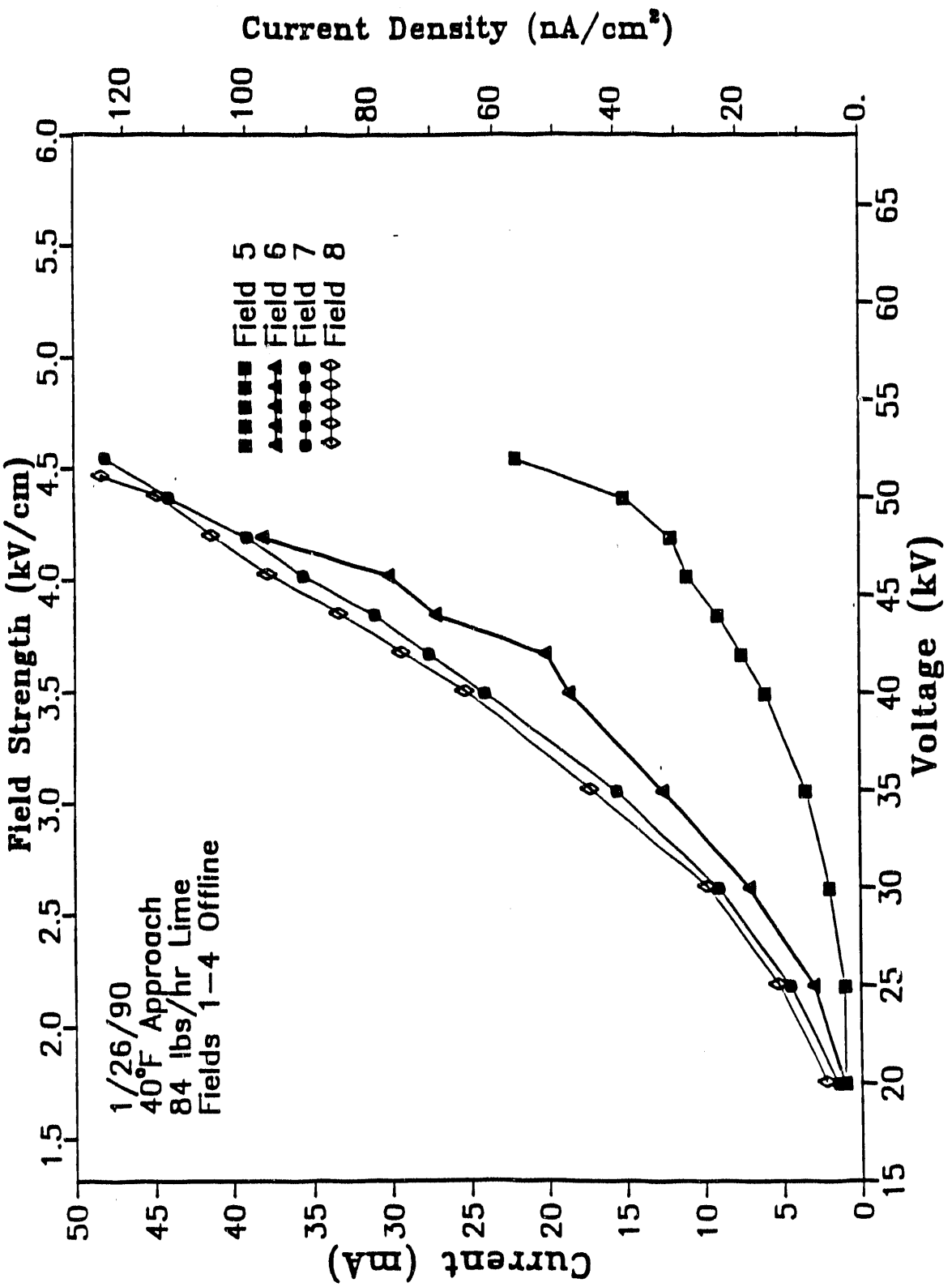

Figure 4-5. Typical Electrical Characteristics for Upstream Sorbent Injection

29.9 mg/dscm in the concentration of particles less than 0.4μm at duct injection conditions. Since this corresponds to the mass of the sulfate aerosol that is produced during humidification, it can be concluded that all of these fine particles are generated not from the injected sorbent but from the spray quenching of the flue gas.

These test demonstrated that during sorbent injection, the increase in particles less than 0.4 μm was due primarily to the condensation of an acid aerosol produced by quenching the flue gas in the humidification system. However, VI curves plotted in Figure 4-6 which were measured under humidification conditions with no sorbent injection, did not show the severe corona quenching in the first field. Therefore, the generation of the acid mist cannot fully account for all of the space charge effects that occur at sorbent injection conditions. It is probably the combination of the acid aerosol and the submicron sorbent particles that lead to severe quenching in the first field. When either of these two sources of particles are eliminated, the severe quenching does not occur.

4.5.2 Resistivity Measurements

Both laboratory and field extractive resistivity measurements indicate that the resistivity of the sorbent/flyash mixture was on the order of 10^{11} to 10^{12} ohm-cm. However, these resistivity levels were not consistent with the excellent electrical operating characteristics of the ESP at these conditions. With a resistivity of 10^{11} ohm-cm, sparking would be expected in the ESP. However, at these conditions the ESP was able to operate at voltages up to 60 kV and current densities greater than 100 nA/cm^2.

It is possible that the particles equilibrate with the moisture in the flue gas after the particles enter the ESP. There was only a one second residence time between the sorbent injection location and the port where the field extractive measurements were made. Since the particles reside on the collector plates from several minutes to hours, it is possible that the particle resistivity decreases as they begin to absorb water. However

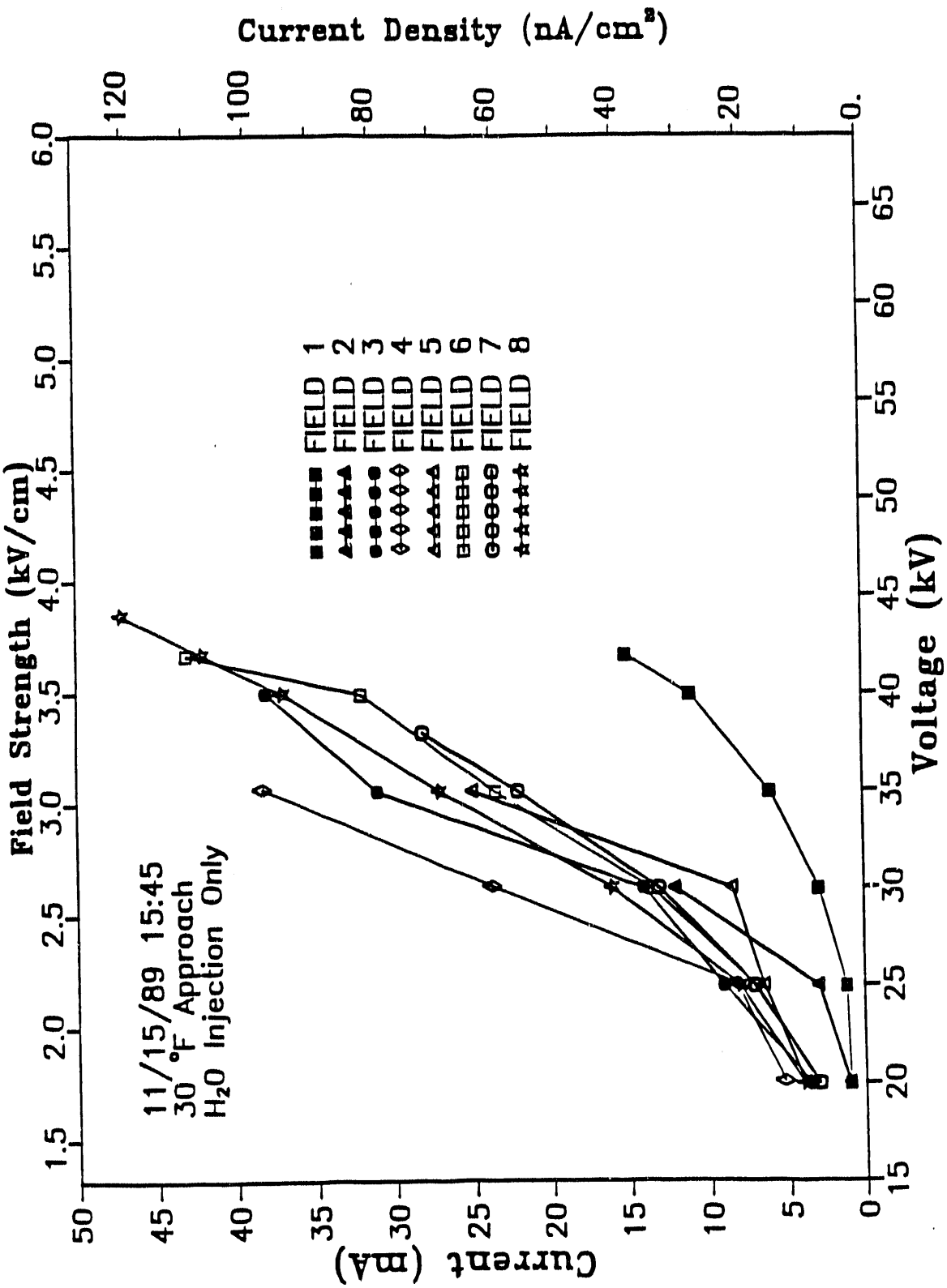

Figure 4-6. Effect of Water Injection on Electrical Characteristics

this effect should also occur in the laboratory resistivity cells where the samples are conditioned for several hours, but this effect was not seen in the laboratory tests.

4.5.3 ESP Performance

The efficiency of the ESP was measured at four different values of specific collection area. The results of the tests for lime only are presented in Table 4-3, and results with recycle are presented in Table 4-4. The most significant effect of duct sorbent injection was an increase in mass loading at the ESP inlet from 1.5 gr/dscf at baseline conditions to 7.3 gr/dscf for lime only injection and 11.3 gr/dscf for lime with recycle.

Based upon the resistivity measurements, it was expected that the ESP performance at duct injection conditions would be much better than at baseline conditions. However, although the efficiency increased for the two fields, the collection efficiencies measured after four, six, and eight fields were very similar to the baseline efficiencies. These collection efficiencies were significantly lower than would be expected from the resistivity measurements, electrical characteristics, particle size distribution, and flue gas conditions.

These data were modeled in a similar manner as the baseline results using 0.25 for the gas flow parameter and adjusting the reentrainment parameter until the predicted performance equaled the measured efficiency. The resulting value determined for reentrainment for the duct injection conditions was 0.44 which is identical to the value used for the baseline tests. This indicates that the material was very easy to reentrain.

Table 4-3

Duct Injection with Lime Only (No Recycle)

ESP Fields	SCA (ft^2/kacfm)	Face Velocity (ft/s)	Inlet Loading (gr/dscf)	Outlet Loading (gr/dscf)	Collection Efficiency (%)*	Emission Rate (lb/MBTU)
8	543	5.0	7.293	0.00507	99.93	0.0124
4	271	5.0	7.293	0.223	96.95	0.538
6	404	4.9	7.404	0.01757	99.76	0.0432
2	135	4.9	7.404	0.547	92.62	1.322

* Collection efficiency does not include final field rap.

Table 4-4

Duct Injection with Lime with Recycle

ESP Fields	SCA (ft^2/kacfm)	Face Velocity (ft/s)	Inlet Loading (gr/dscf)	Outlet Loading (gr/dscf)	Collection Efficiency (%)*	Emission Rate (lb/MBTU)
8	537	4.9	11.329	0.00605	99.95	0.0149
4	269	4.9	11.329	0.260	97.71	0.628

* Collection efficiency does not include final field rap.

4.5.4 Effect of Recycle

The addition of recycle produced a significant increase in the inlet mass loading to the ESP. However, because the mass was primarily associated with particles greater than 1μm, there was minimal effect on the corona suppression in the first three ESP fields. The recycle also had minimal effect on the resistivity measurements. Since the recycle did not affect the primary parameters that control ESP performance, no change in collection efficiency from the lime only test would be expected. The performance data measured during the recycle test confirmed that this was true.

Figure 4-7 shows a plot of collection efficiently versus SCA for the baseline and both duct injection conditions. The lime only and recycle injection tests produced essentially identical collection characteristics. For each value of SCA, higher collection efficiencies were measured at sorbent injection conditions than at baseline conditions. However, the magnitude of the increase in efficiency was not sufficient to overcome the increase mass loading of the sorbent as shown in Figure 4-8, which is a plot of outlet emissions in terms of lb/MBtu for the three cases. It should also be noted that this comparison is biased because the efficiencies are quite low for the baseline results and subsequently the emissions are much higher due to the low temperature operation of the pilot ESP. With more realistic baseline results, the impact of the sorbent injection would appear to be much more severe.

4.6 Testing of ESP Upgrades

The final phase of ESP testing was designed to evaluate the effectiveness of ESP upgrades to increase the collection efficiency at duct injection conditions. The first upgrade that was tested was the use of high current density electrodes in the first field of the ESP. However, the use of barbed wires as emitter electrodes in the first section of the ESP could not overcome the corona suppression caused by duct injection.

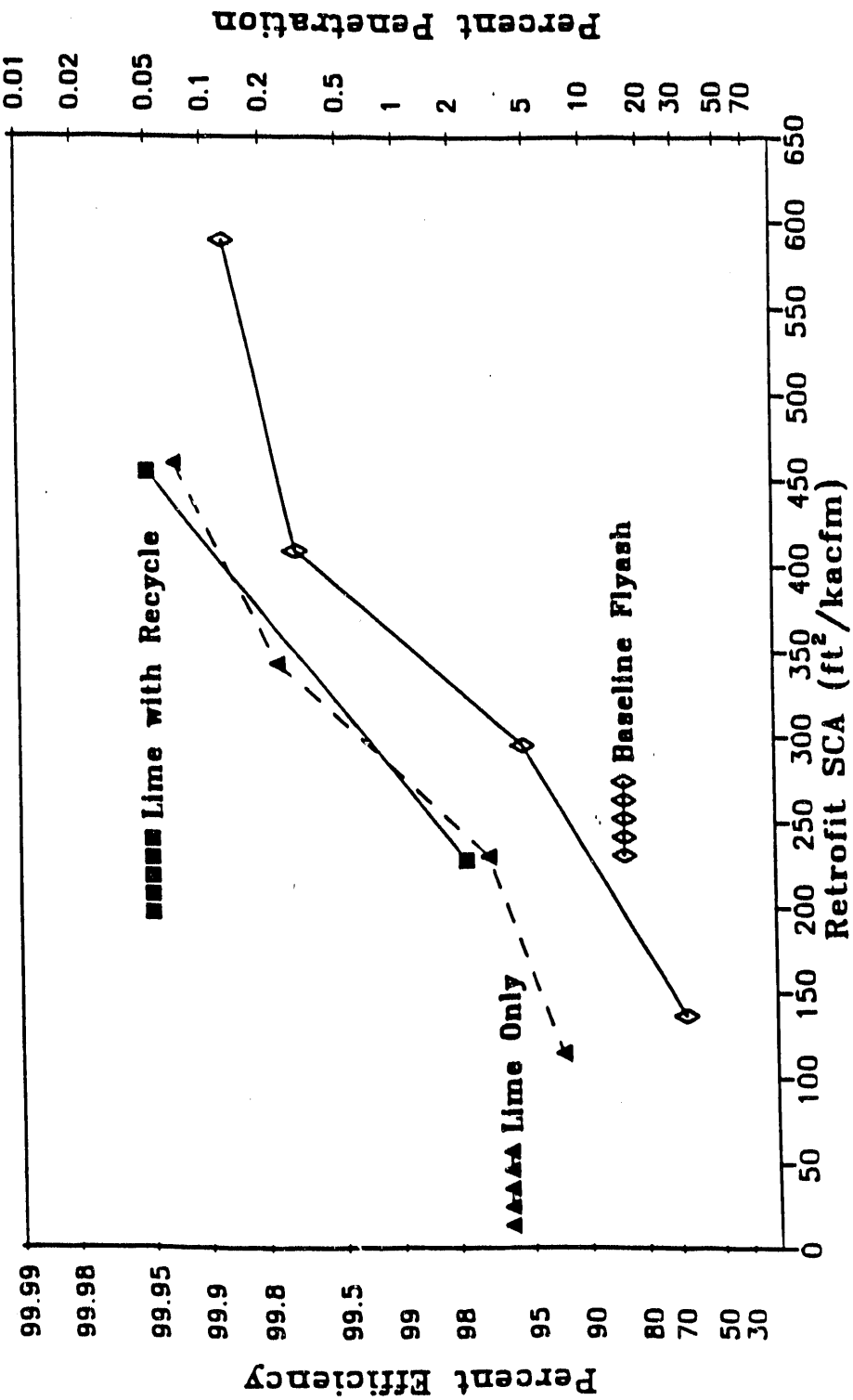

Figure 4-7. No Rap ESP Performance as a Function of SCA - Lime Only vs. Lime With Recycle vs. Baseline Conditions

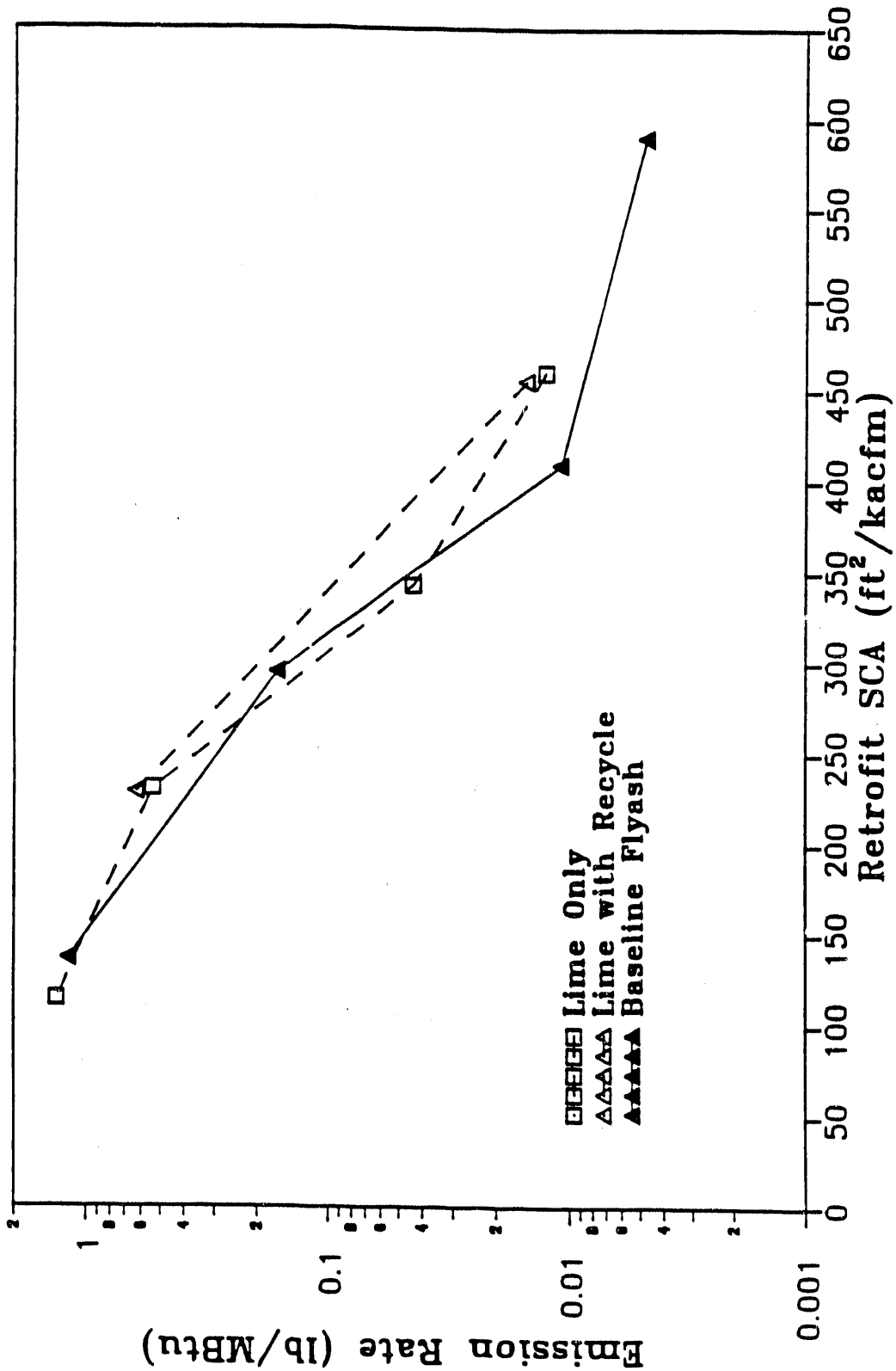

Figure 4-8. No Rap ESP Outlet Emissions for Baseline and Duct Injection Conditions

In all of the previous tests, the TR controllers were set to provide a maximum voltage of 50 kV in order to simulate the power supplies that would be used in existing ESPs. However, the low temperature operation produced by the duct injection conditions allowed for operation at much higher voltages. Therefore, a series of tests was conducted to determine if improved collection efficiency could be obtained if higher voltage power supplies were used to operate at increased voltages. The TR sets at the pilot plant were rated at 75 kV and 50 mA. Therefore, the tests were run with the controllers set up to operate in a spark rate mode.

Every section operated either at sparking conditions or at the 50 mA current limit of the supplies. The primary improvement in operating conditions occurred in the first three fields which operated at increased currents and voltage levels greater than 60 kV. At the increased voltage, the first section had an increase in current to above 5 mA which provided a current density on the order of 15 nA/cm^2. However, this did not improve the performance of the ESP. This is not surprising for a situation that appears to be dominated by low-resistivity reentrainment. The increased operating voltage would lead to higher electric fields for charging and collecting. However, for low-resistivity particles, the repulsion force on the collected particles is proportional to the electric field and therefore, the increase in operating voltage has both a positive and a negative effect on collection efficiency as it increases the collection force but it also increases the repulsion force. Increasing the capacity of the power supplies is, therefore, not an effective ESP upgrade to overcome the impact of duct sorbent injection on emissions.

One of the means to reduce reentrainment is to improve the cohesive characteristics of the dust. Tests performed at the TVA Spray Dryer Pilot Plant (1) have shown that the addition of calcium chloride has improved ESP performance. Therefore, calcium chloride was selected as an additive to test during this test program.

The use of chloride as an additive for sorbent injection brought about dramatic improvement in the removal of sulfur dioxide as efficiencies as high as 70% were obtained. Although the chloride addition also produced a large reduction in the resistivity of the particles, there appeared to be no significant effect on the performance of the ESP. However, this conclusion should be considered preliminary and may not be correct.

The chloride addition test were conducted at the very end of the pilot plant test program. This restricted the time that was available to complete the tests. The characteristics of the chloride also increased the potential for plugging the small ducting of the pilot plant leading to many operational problems. For all of these reasons, the chloride addition test represented only about 24 hours of operation. Therefore, these tests may not have been run for sufficient time for improvements due to a more cohesive dust to take place.

4.7 Full-Scale Test at Edgewater

The evaluation of the full-scale ESP operating at the demonstration of the Coolside process at the Ohio Edison Edgewater Station provided some data to compare with the pilot plant results. Data pertaining to mass concentrations, particle size distributions, particle resistivity, and ESP operating characteristics were successfully obtained during the test program. The data from this test program were analyzed using the SRI ESP computer model. It appears that the full-scale unit also suffered from low-resistivity reentrainment but not to as great an extent as the pilot ESP. The results indicated that the reentrainment in the ESP was 26%, which is much lower than the reentrainment at the pilot plants. The difference may be due to increased particle cohesion at a lower approach temperature at Edgewater, or due to differences in the coal, sorbent, and process conditions.

The particle size distributions show an increased loading of fine particles over the background levels during rapping. This increased loading of fine particles was much greater than the amount of fine particles shown in the EPRI rapping puff study which was determined for ESPs collecting flyash only (2).

4.8 References

1. Durham, M. D., D. B. Holstein, R. G. Rhudy, R. F. Altman, T. A. Burnett, J. DeGuzman, G. A. Hollinden, R. A. Barton, and C. W. Dawson. "Effects of Coal Chloride and Spray Dryer Operating Variables on Particle Cohesion and Resistivity in Downstream ESPs." EPA/EPRI 1990 SO_2 Control Symposium, New Orleans, LA, May 8-11, 1990.

2. Gooch, J. P., and G. H. Marchant. "Electrostatic Precipitator Rapping Reentrainment and Computer Model Studies." EPRI Report No. FP-792, Vol 3., EPRI Contract RP 413-1, June 1978.

5.0 NOZZLE PERFORMANCE CHARACTERIZATION

5.1 Introduction

The University of California at Irvine Combustion Laboratory (UCI) was subcontracted to provide water droplet size and velocity measurements for several humidification nozzles that potentially could be used at the Meredosia pilot plant. Such two-fluid nozzles characteristically produce dense sprays featuring very narrow dispersion angles and high droplet velocities. A schematic of the UCI spray test facility is provided in Figure 5-1. The objective of this work was to characterize sprays produced by nozzles to: 1) better understand the atomization process, 2) provide a data base for computational fluid dynamics (CFD) modeling of the process, and 3) provide data to support nozzle selection.

5.2 Results

Droplet size and velocity distribution data were obtained for the eight atomizers listed in Table 5-1. Data were generated from measurements of the water spray using an Aerometrics Phase Doppler Particle Analyzer (PDPA), at a distance of 3 feet from the tip of the nozzle. Results are presented graphically in Figures 5-2 through 5-9.

The PDPA measures droplet size and velocity within a small volume, essentially at a point within the spray pattern. A laser diffraction instrument, such as the Malvern, measures a line-of-sight. It is convenient to report a single number for an overall droplet size distribution as a composite Sauter mean diameter (SMD). A composite SMD is a mean diameter that represents the average size of the droplets across the entire diameter of the spray. Composite SMD values, calculated from PDPA data for various air pressures and water flow rates, are presented in Figures 5-10 and 5-11.

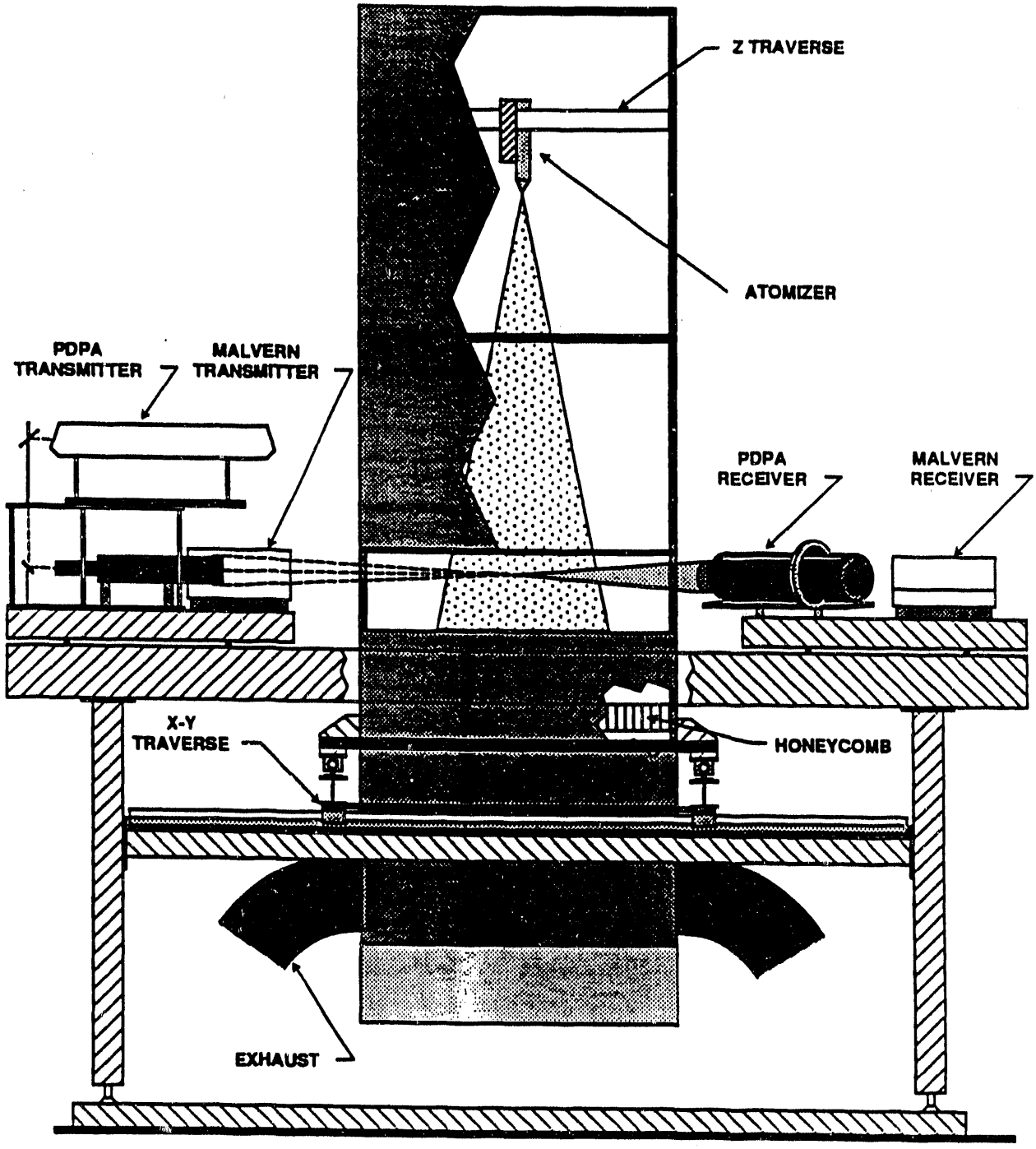

Figure 5-1. Spray Stand Side View

Table 5-1

Atomizers Characterized at UCI

Atomizer	Manufacturer	Style	Model No.	Date Tested
A	Bete	Fog	SA 12H-14N-.238	July 1989
B	Delavan	Bypass (large)	35051-8	June 1989
C	Delavan	Bypass (small)	38635-3	July 1989
D	Delavan	Airo (large)	30616-17	July 1989
E	Delavan	Airo (large)	30616-17	April 1990
F	Lechler	Supersonic (small)	170.641.17	March 1990
G	Lechler	Supersonic (large)	170.721.17	May 1990
J	Delavan	Airo (medium)	30616-11	June 1990
K	Delavan	Airo (small)	30615-46	June 1990

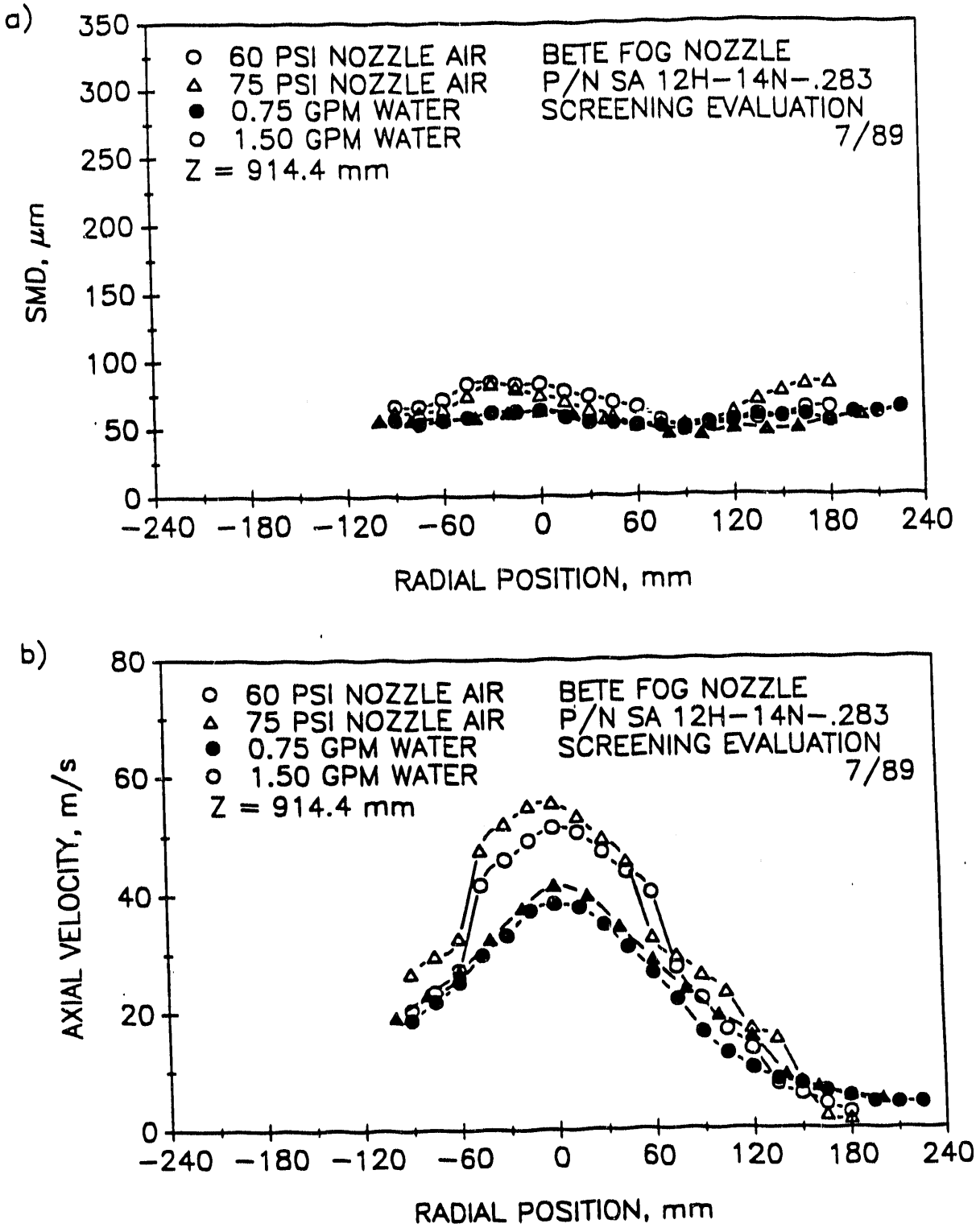

Figure 5-2. Bete Fog Nozzle (Atomizer A) - Spatially Resolved SMD and Axial Velocity Phase Doppler Data

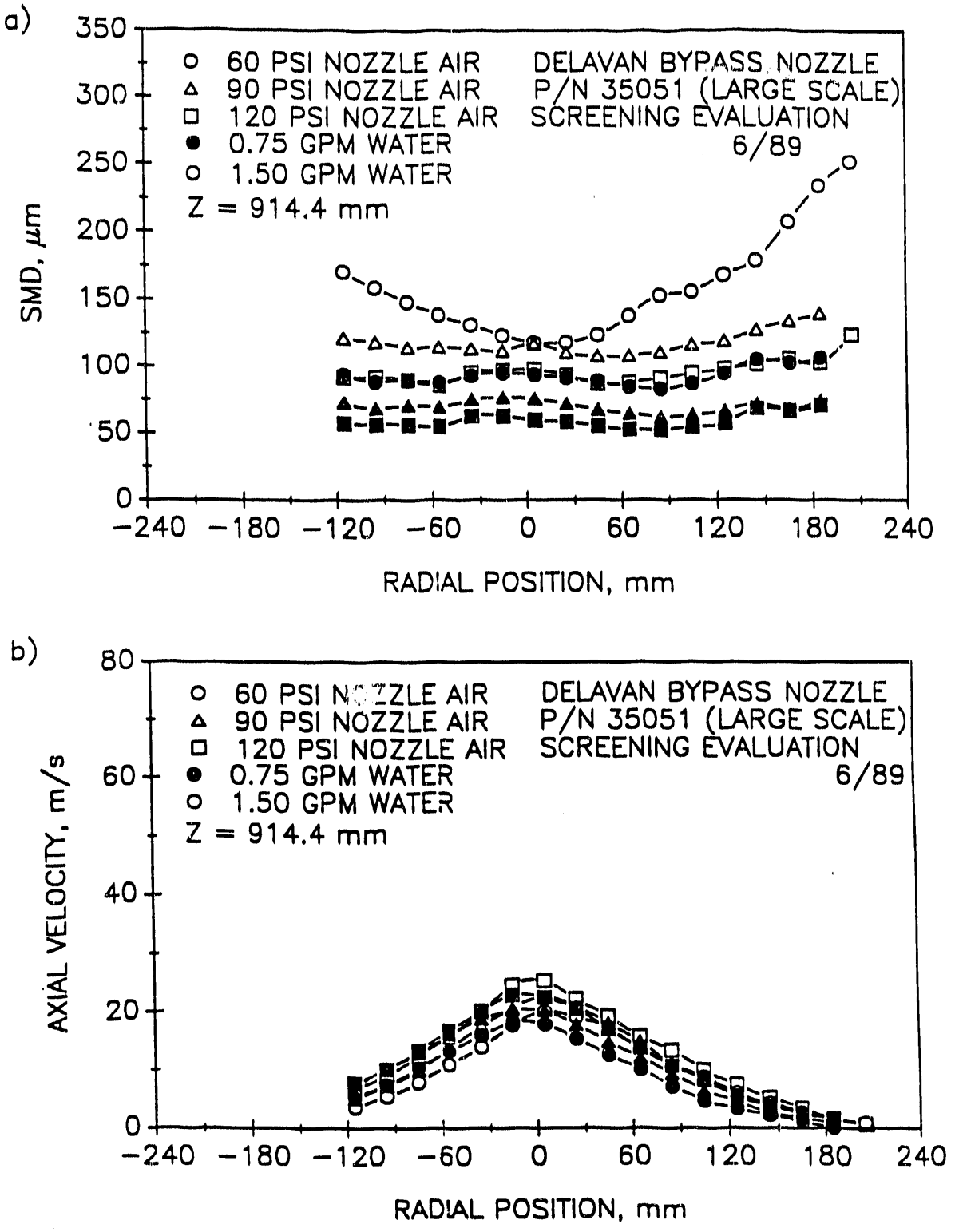

Figure 5-3. Large Scale Delavan Bypass Nozzle (Atomizer B) - Spatially Resolved SMD and Axial Velocity Phase Doppler Data

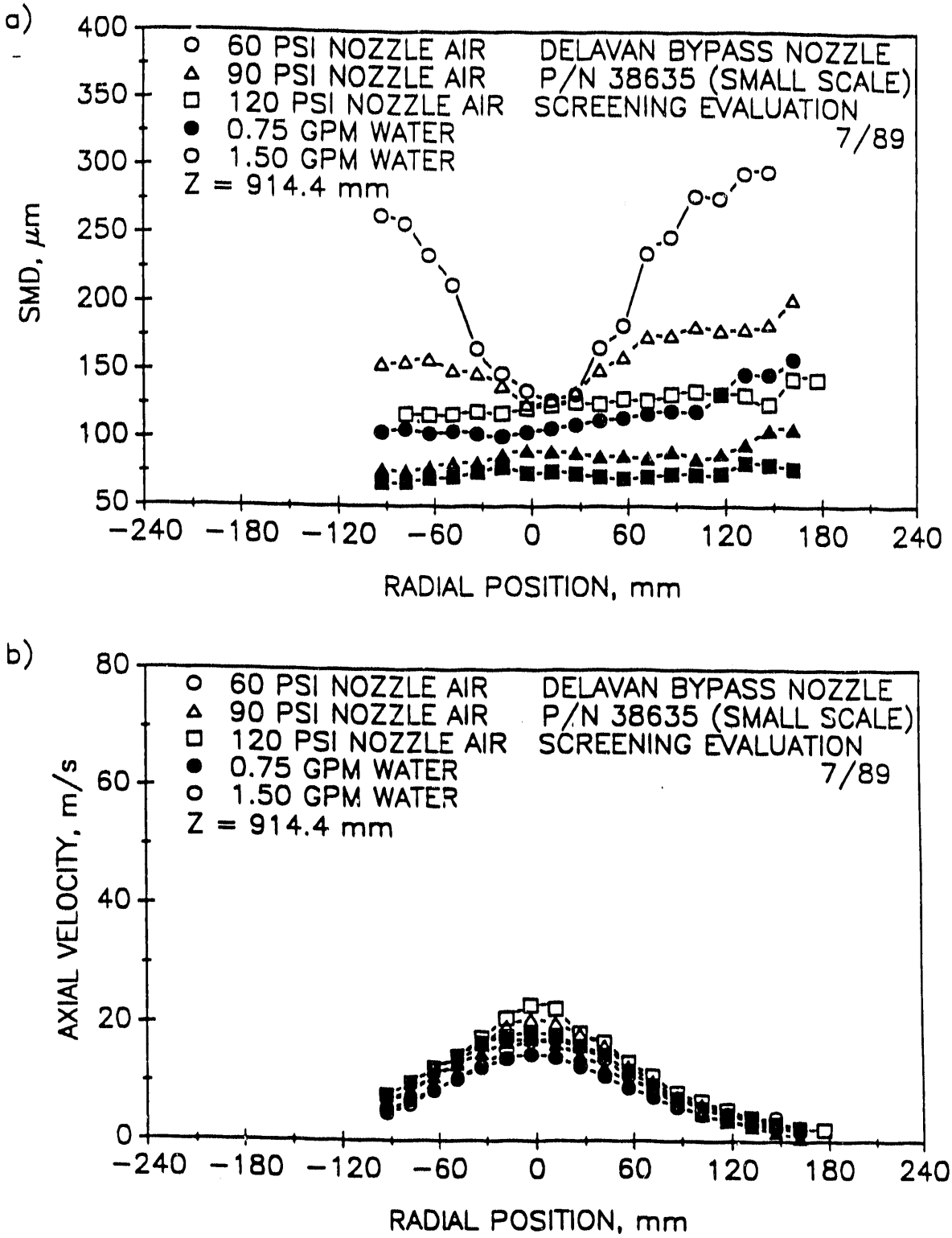

Figure 5-4. Small Scale Delavan Bypass Nozzle (Atomizer C) - Spatially Resolved SMD and Axial Velocity Phase Doppler Data

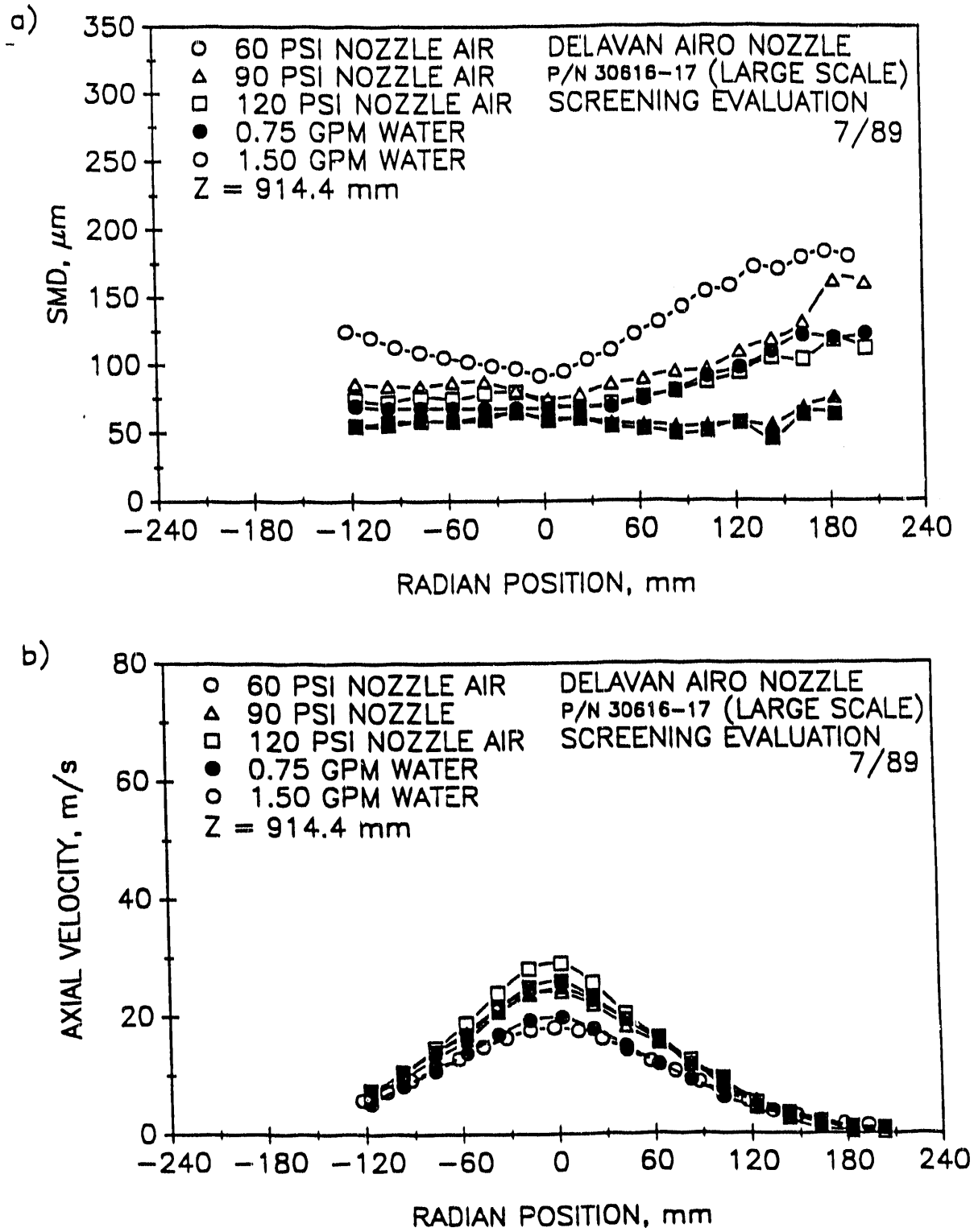

Figure 5-5. Large Scale Delavan Airo Nozzle (Atomizer D) - Spatially Resolved SMD and Axial Velocity Phase Doppler Data

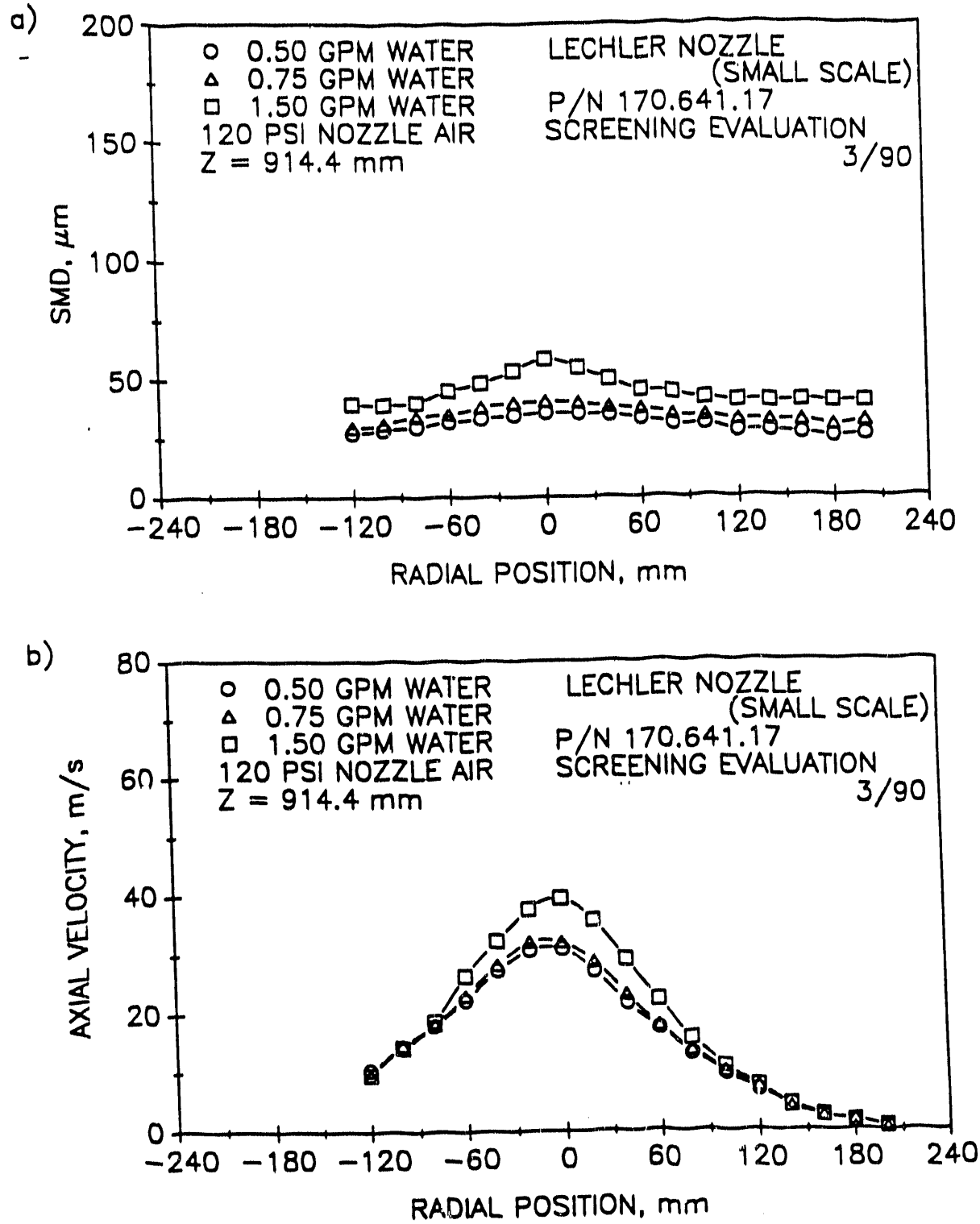

Figure 5-6. Small Scale Lechler Nozzle (Atomizer F) - Spatially Resolved SMD and Axial Velocity Phase Doppler Data

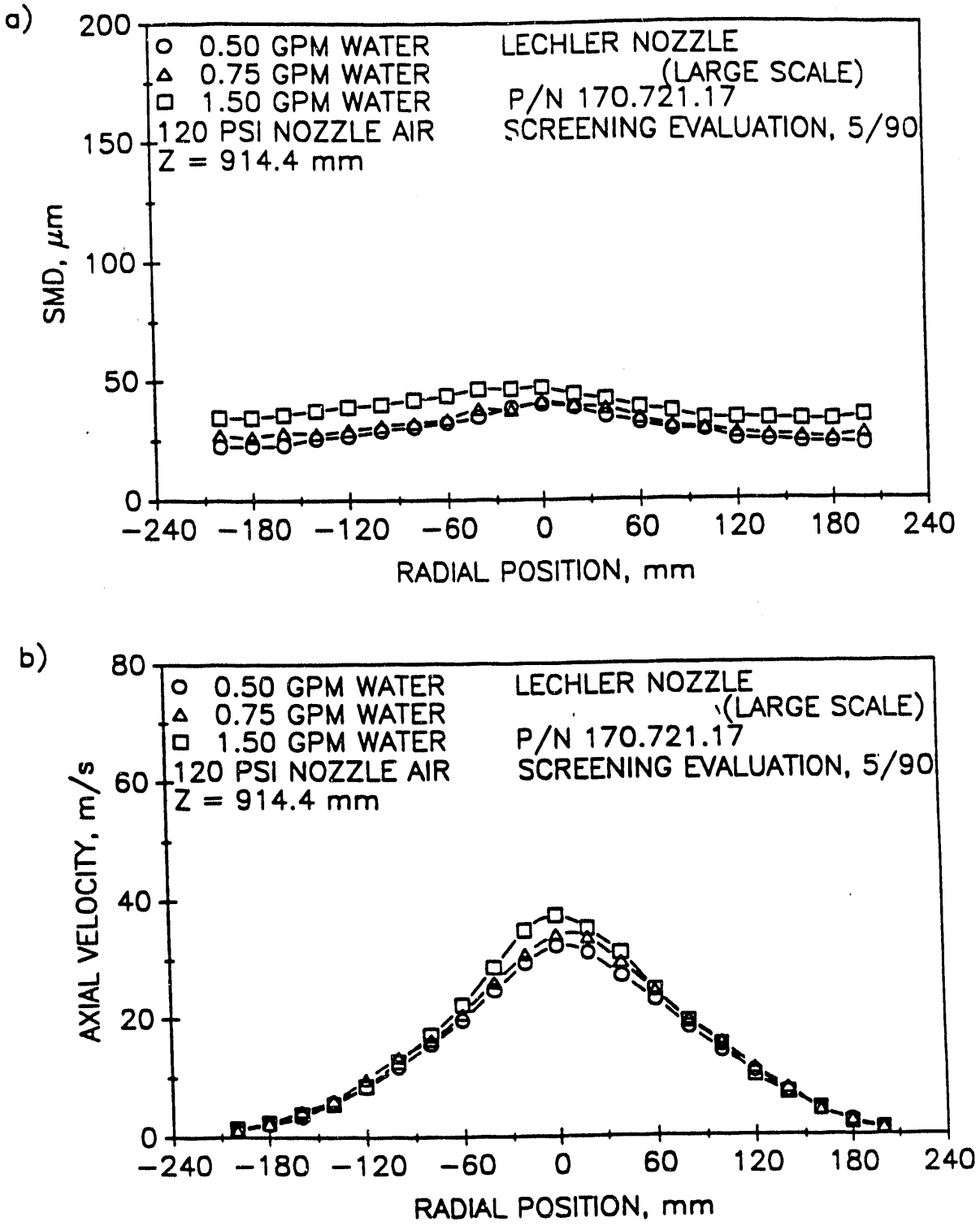

Figure 5-7. Large Scale Lechler Nozzle (Atomizer G) - Spatially Resolved SMD and Axial Velocity Phase Doppler Data

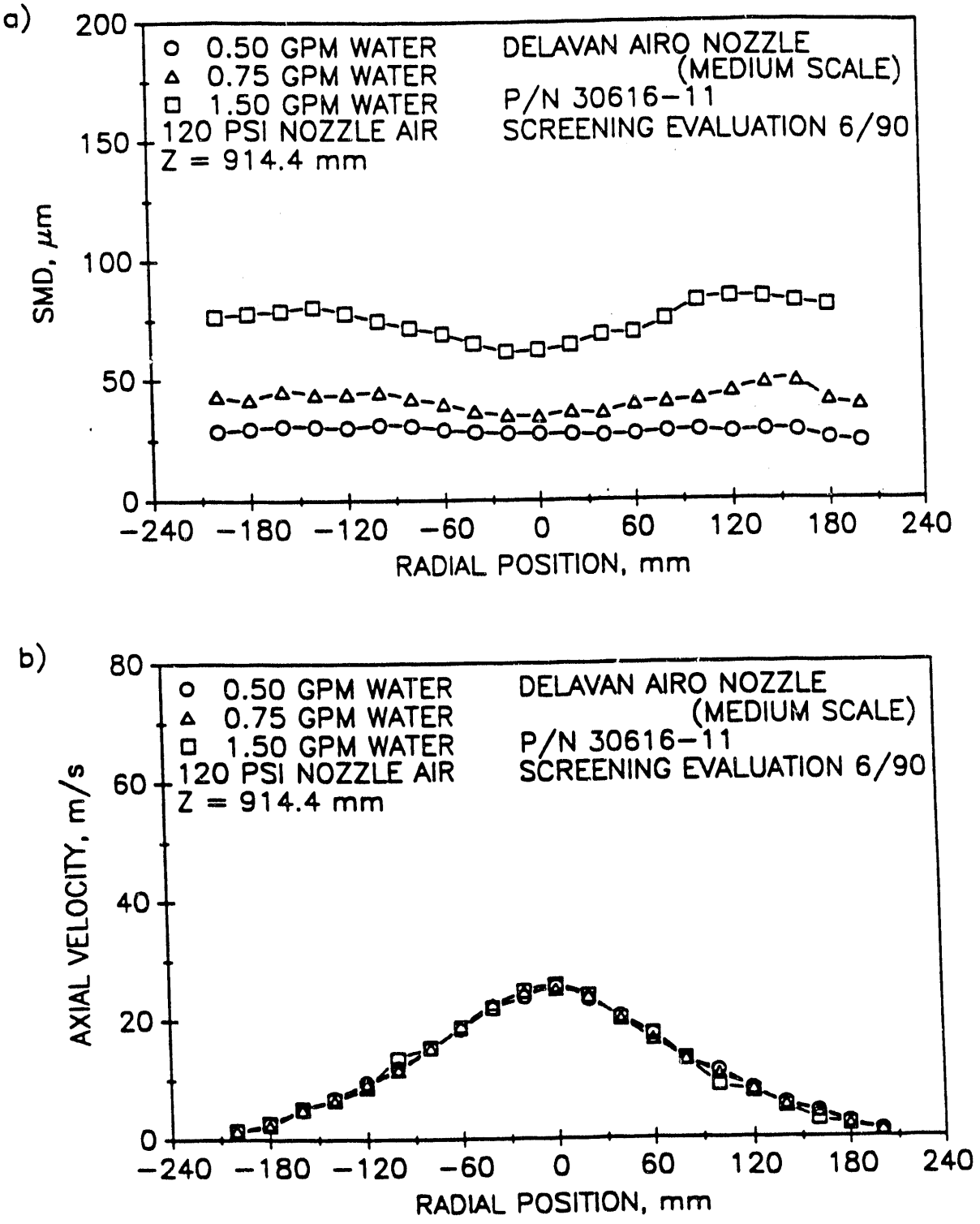

Figure 5-8. Medium Scale Delavan Airo Nozzle (Atomizer J) - Spatially Resolved SMD and Axial Velocity Phase Doppler Data

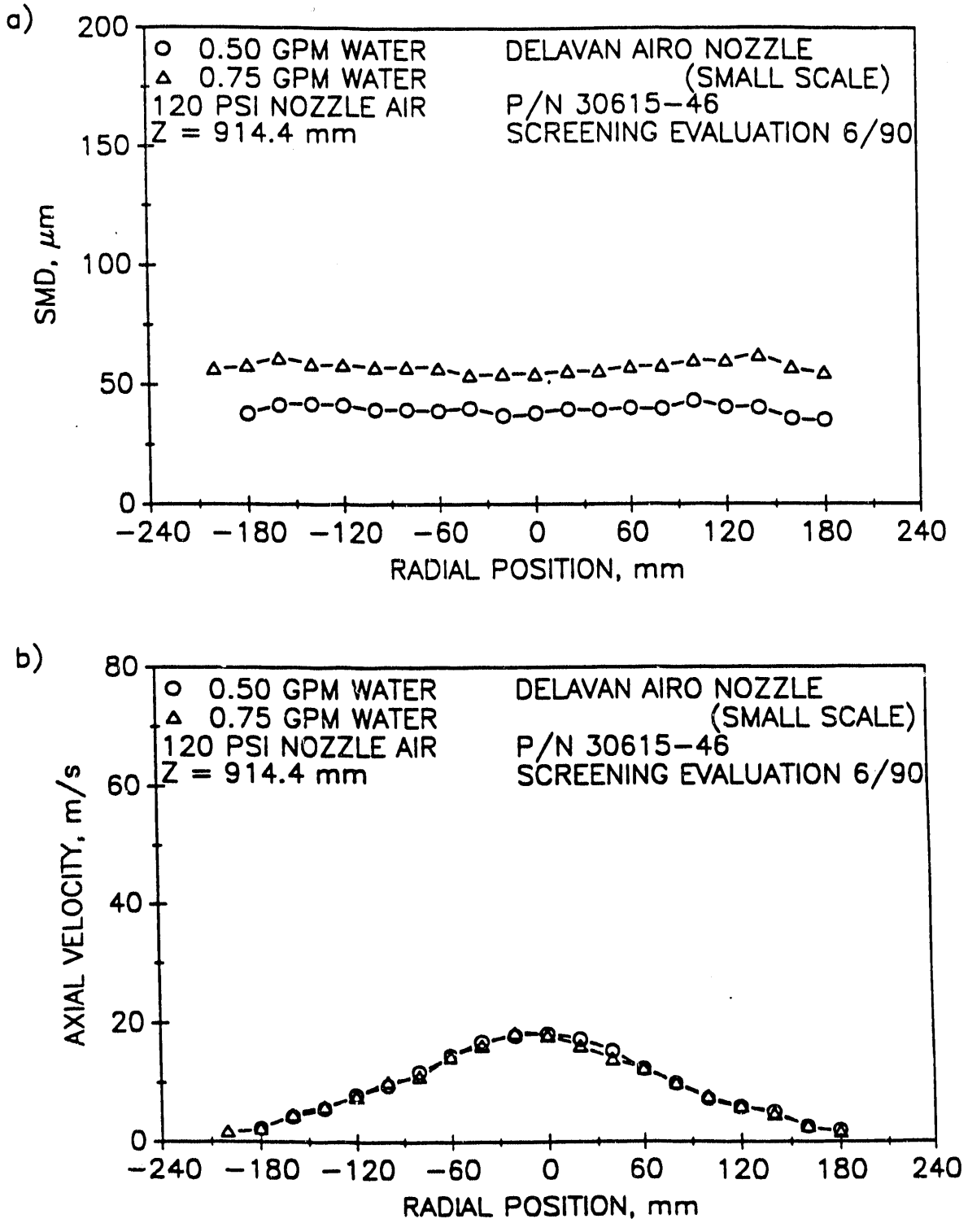

Figure 5-9. **Small Scale Delavan Airo Nozzle (Atomizer K) - Spatially Resolved SMD and Axial Velocity Phase Doppler Data**

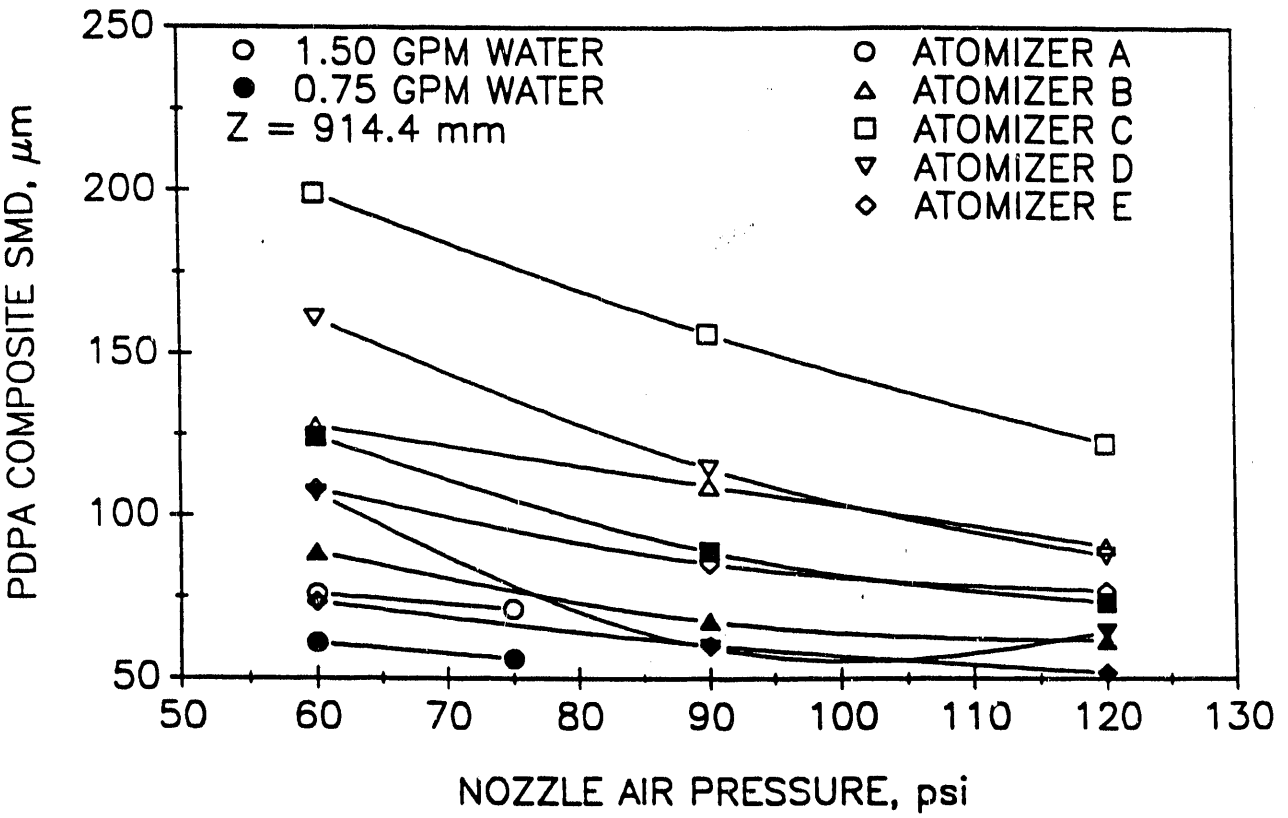

Figure 5-10. Phase Doppler Composite SMD Summary (Atomizers A, B, C, D, and E)

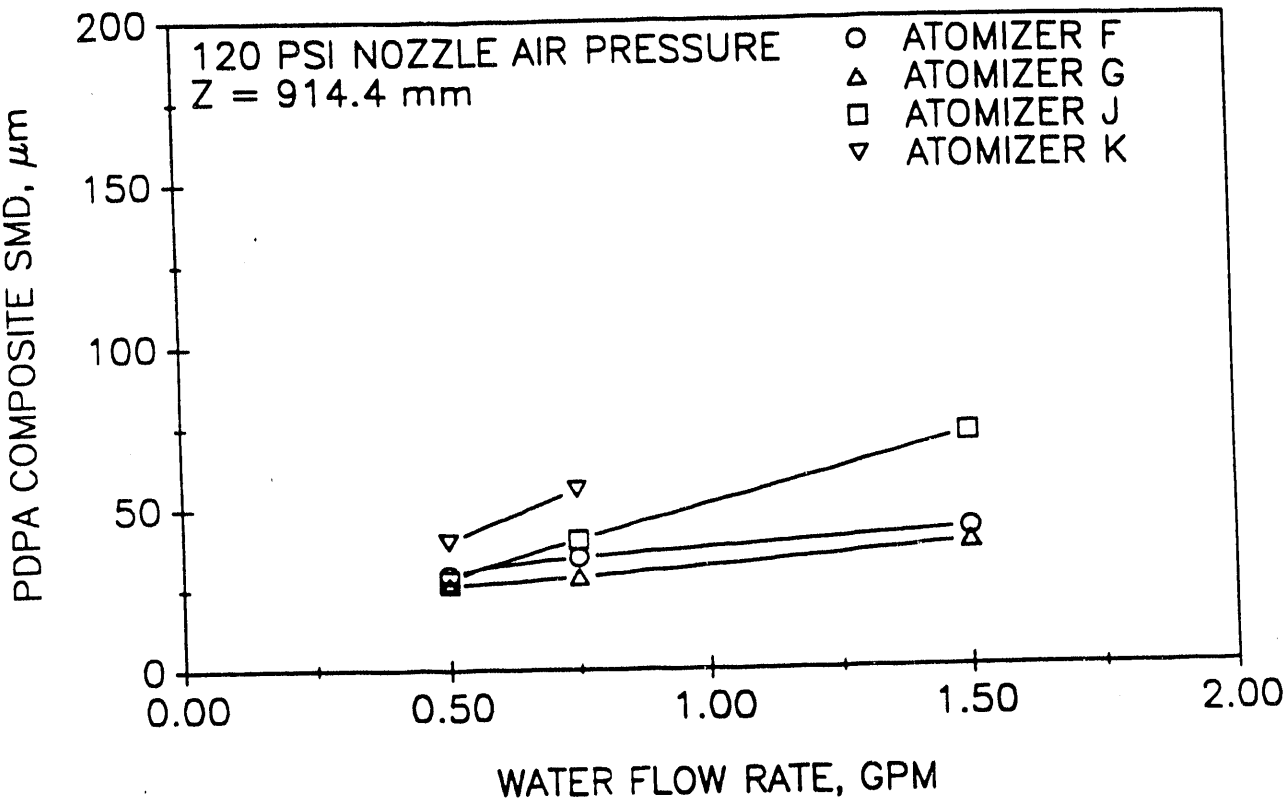

Figure 5-11. Phase Doppler Composite SMD Summary (Atomizers F, G, J, and K)

Atomizers A, B, C, and D were characterized in the summer of 1989. Prior to characterizing atomizers F, G, J, and K, the spray test stand was modified to increase the water flow capacity of the stand, including increasing the exhaust flow rate. Atomizer D was characterized again after the spray stand modifications, and the later results are reported as atomizer E. The composite SMD for atomizer E is lower than the composite SMD for atomizer D. The discrepancy may be attributable to one or more of the following reasons:

- Nozzle asymmetry, if the nozzle was not mounted in exactly the same position or if the nozzle was disassembled and reassembled;
- Corrosion, which was observed in a small amount;
- Increased exhaust flow improved control of recirculation; and
- PDPA probe volume corrections, which seemed qualitatively to be more consistent after the spray stand modifications.

General observations regarding the results include the following five points:

- Droplet size decreases when inlet air pressure increases for a given water flow rate;
- Droplet size decreases as the water flow rate decreases for a given air pressure;
- Spatially resolved profiles of SMD become relatively flatter when there is relatively more atomizer air and less water;
- Mean axial velocity increases as inlet nozzle air pressure increases; and
- Mean axial velocity is almost unaffected by variations of water flow rate for a given inlet water pressure (with the exception of the small Lechler nozzle 170.641.17).

5.3 Phase Doppler vs. Laser Diffraction Measurements

Laser diffraction instruments are commonly used to report droplet size distributions for atomizers. Phase Doppler and laser diffraction measurements are inherently different. The laser diffraction instrument produces a spatial measurement which is analogous to taking a sequence of snapshots with a camera. Such a spatial measurement is weighted toward droplets which are moving slower (1). However, the phase Doppler produces a temporal measurement which is equivalent to taking a moving picture with the camera aperture constantly open. As such, these temporal measurements are biased toward droplets which are moving faster (2).

To compare results obtained by the PDPA and a laser diffraction (Malvern) instrument, the spray from atomizer D was measured using both instruments. Figure 5-12 illustrates that the composite SMD from laser diffraction size measurements are about 30% lower than from the phase Doppler.

One factor that can affect laser diffraction measurements is obscuration, or the attenuation of the laser beam as the light travels from the transmitter to the receiver. For the flow conditions studied, the obscurations were on the order of 80 percent. Previous studies indicated that laser diffraction data must be corrected for possible biasing toward smalled sizes (3). Two common types of corrections for obscuration were applied to the laser diffraction results presented in Figure 5-12 (3, 4). It has since been shown that the phase Doppler and the laser diffraction instruments have the closest agreement when the laser diffraction model independent results are corrected for multiple scattering effects (5).

5.4 References

1. Dodge, L. G., D. J. Rhodes, and R. D. Reitz. "Drop-Size Measurement Techniques for Sprays: Comparison of Malvern Laser-Diffraction and Aerometrics Phase Doppler." Applied Optics. Vol. 26, pp. 2144-2154.

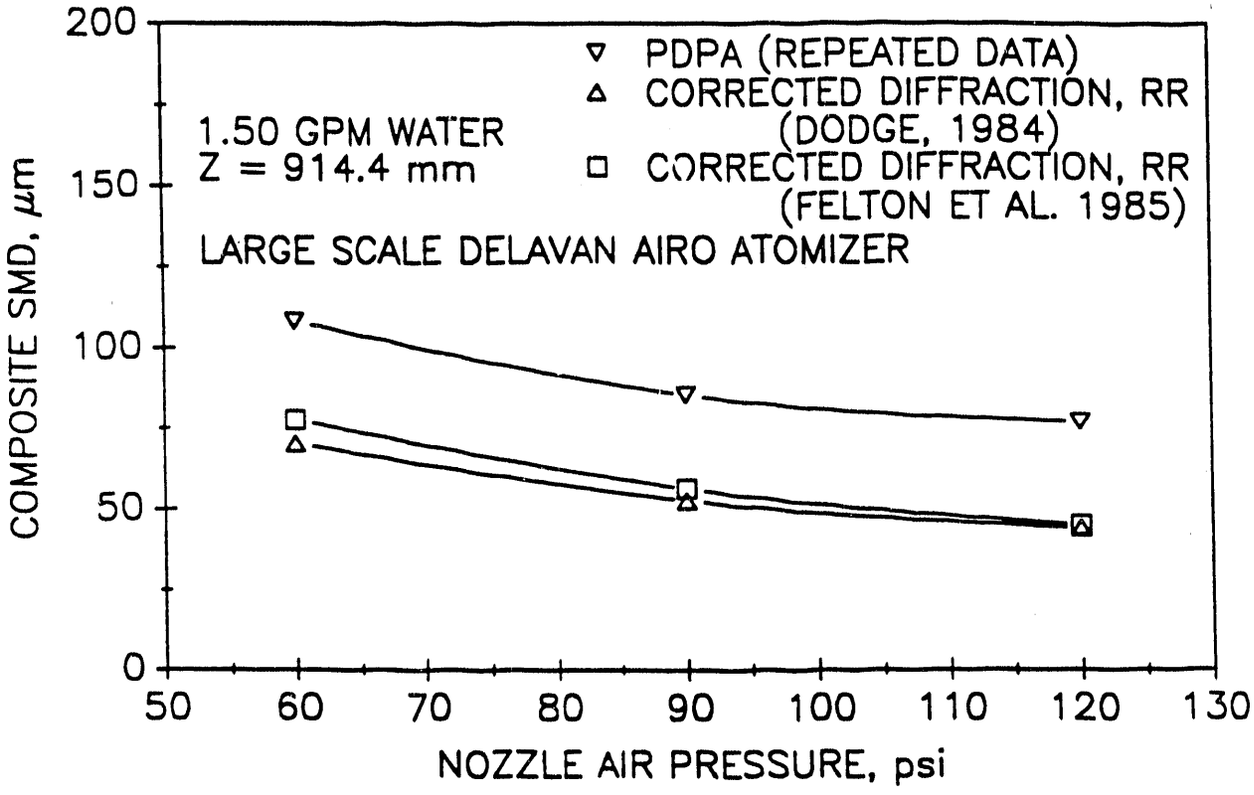

Figure 5-12. Comparative Composite SMD Measurements - Phase Doppler and Laser Diffraction

2. McLaughlin, D. K., and W. G. Tiederman. "Biasing Correction for Individual Realization of Laser Anemometer Measurements in Turbulent Flows." The Physics of Fluids. Vol. 16, No. 12, pp. 2082-2088.

3. Dodge, L. G. "Change in Calibration of Diffraction-Based Particle Sizers in Dense Sprays." Optical Engineering. Vol 23, No. 5, pp. 626-630.

4. Felton, P. G., A. A. Hamidi, and A. K. Aigai. "Measurement of Drop-Size Distribution in Dense Sprays by Laser Diffraction." Proceedings, ICLASS-85, Third International Conference on Liquid Atomization and Spray Systems. The Institute of Energy, London, P. IVA/4/1.

5. Brown, C. T., W. A. Sowa, and G. S. Samuelson. "Performance Characteristics of Twin Fluid Atomizers Applied to Duct Humidification." Draft to be submitted for publication, UCI Combustion Laboratory, 1991.

6.0 HOT-FLOW, GLASS DUCT PHYSICAL MODEL

6.1 Introduction

To facilitate observation of the humidification process in a 17.5 inch diameter duct, a full-scale glass model of the Meredosia pilot plant duct was constructed by Fossil Energy Research Corporation. Air was heated to 300° F, then sprayed with water using two-fluid atomizers. Thus, the pilot plant humidification process was simulated and visualized. Wetting of duct walls due to impingement of water droplets could be observed. Atomizers and atomizer configurations were screened in this facility prior to installation at the pilot plant.

The specific objectives of the glass duct flow visualization task were to:

- Design and fabricate a 1:1 scale physical model of the humidification region of the Meredosia pilot plant for flow visualization and screening of different atomizers under different operating conditions;
- Develop atomizer selection criteria for application to the Meredosia pilot plant in order to screen potential commercially available atomizers;
- Conduct dynamic atomizer characterizations under similar temperature, humidity, and relative velocity conditions as a function of atomizer operating conditions; and
- Evaluate results and make recommendations for selecting an atomizer(s) for achieving the desired approach temperature without wall deposition, noting that the focus is on viable approaches for the 18-inch diameter pilot scale duct, and not necessarily full scale applications.

The 17.5 inch diameter duct, used for the pilot scale fundamental evaluation of the duct injection process at Meredosia, imposes several constraints upon the selection of humidification nozzles that would not normally exist in full scale

applications. Nozzles selected for the pilot scale facility must generate drop size distributions and exhibit spray angle characteristics that are commensurate with available droplet evaporation times. In the near field region, the spray angle and droplet velocity determines the available residence time for droplet evaporation. The confined flow field also imposes added limitations by limiting the extent to which the air/liquid ratio can be practically increased. A jet within a confined flow establishes a recirculating flow near the duct wall, which not only limits available residence time for evaporation, but promotes wall deposition as well. In addition, nozzle alignment within the duct becomes a critical issue as minor deviations from centerline alignments significantly enhance the degree of wall deposition.

6.2 Glass Duct Facility Description

A schematic of the glass duct flow visualization facility is presented in Figure 6-1. The facility is operated under forced draft. Air is heated to 300° F by a natural gas burner. To provide the capability for adjusting the humidity to typical flue gas levels, two pressure atomizers are located just downstream of the duct burner. Following a 180° turn, test atomizers are mounted in a section of steel duct upstream of the glass duct section. The glass duct section is 6 feet long to allow observation of wall wetting in the crucial area just downstream of the atomizers. An end view of the spray pattern is provided by a view port on the downstream end of the elbow where the flow makes a 90-degree turn to the stack.

Unevaporated water which impinges on the walls or the end plate is collected through a drain and measured. To provide a quantitative comparison between the performance of different atomizers, water utilization was computed from the following equation:

$$\text{Utilization} = \frac{M_{inj} - M_{drain}}{M_{inj}} \times 100$$

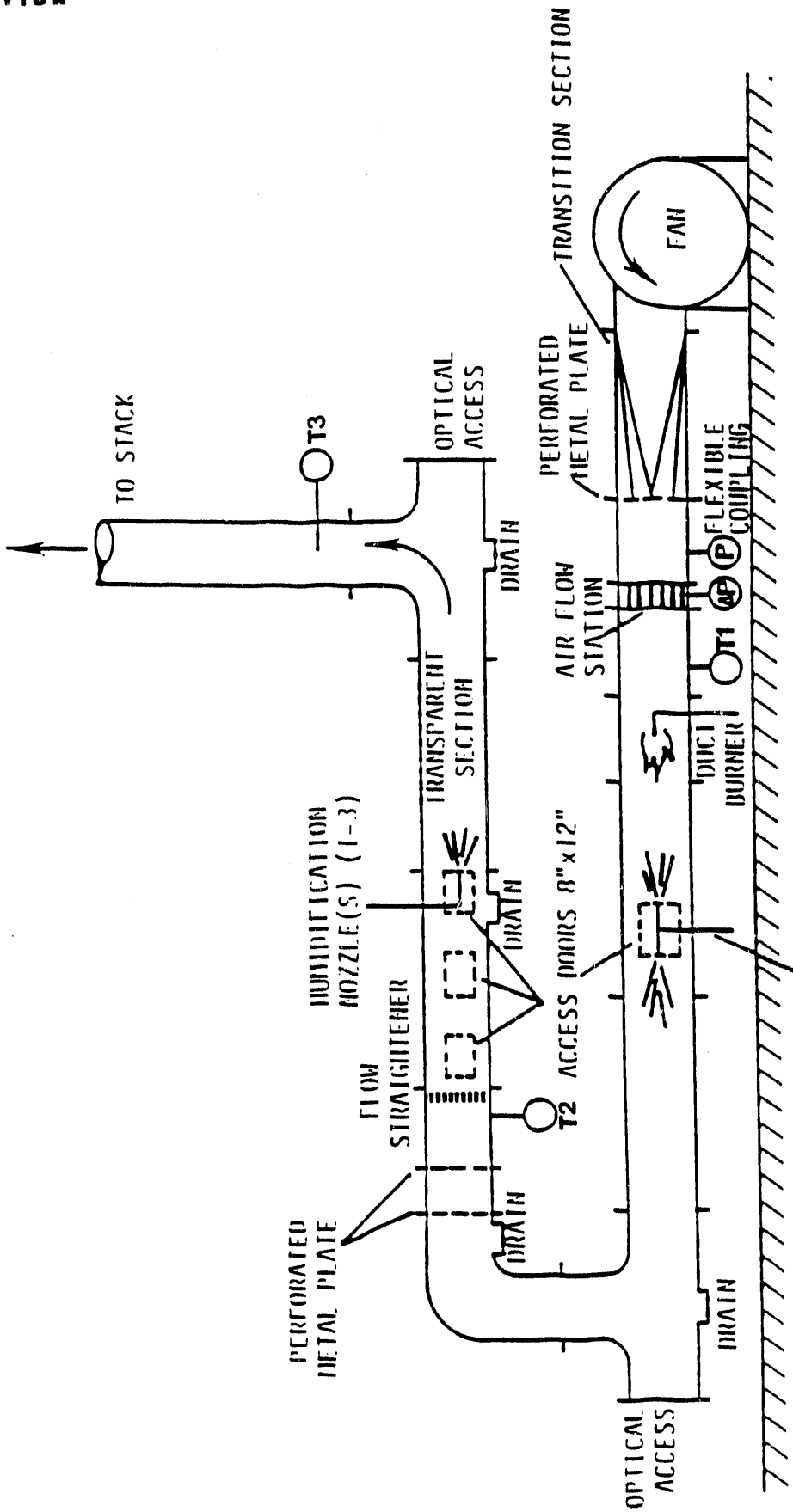

Figure 6-1. Schematic of Flow Visualization Facility

The drain collected both droplets deposited on the duct walls and droplets that did not make the 0-degree turn up toward the stack.

The atomizers were tested in one of five configurations:

- In the baseline, single nozzle configuration, the atomizer was positioned in the centerline of the duct. The inlet temperature was 300° F, and the water flow was 1.5 gpm.
- In the single nozzle configuration, atomizers were also tested with an inlet temperature of 300° F and the water flow set at 0.75 gpm. This configuration represented the first stage of two nozzles in series.
- Selected atomizers were subsequently tested in a simulated two-stage, series configuration. The second stage was simulated by reducing the inlet temperature to that measured at the exit of the first-stage tests (200° F) while holding the water flow to 0.75 gpm. Because the inlet humidity was not reduced, these conditions represented best-case conditions for a second stage atomizer. Thus, if complete evaporation could not be achieved under these conditions, it would not be achieved in a real two-stage configuration either.
- One set of two atomizers was tested with the atomizers in a two-stage, series configuration. The inlet temperature was 300° F, and the water flow was 1.5 gpm.
- Selected atomizers were tested in a parallel configuration with two atomizers mounted over variable side-by-side distances, with the inlet temperature controlled to 300° F and the total water flow controlled to 1.5 gpm.

6.3 Humidification Results

A summary of atomizers, operating conditions, and water utililization results is provided in Table 6-1. In the baseline, single-stage configuration, water utilizations varied from 73.1 to 92.0% and averaged 86.4 percent. In the simulated two-stage series configuration, higher water utilizations, averaging 92.3% (excluding an

Table 6-1

Summary of Operating Conditions and Water Utilization Results for Each of the Atomizers Tested

Manufacturer	Model	Configuration	Air		Water		Air/Water	T2	Drain (GPM)	Water Utilization
			(SCFM)	(PSIG)	(GPM)	(PSIG)				
INTERNALLY MIXED ATOMIZERS:										
B & W I-Jet	Mark 4	Centerline	58	90	1.50	90	0.35	300	0.159	89.4
			60	80	0.75	65	0.71	300	0.000	100.0
			57	75	0.75	60	0.69	200	0.070	90.7
			82	128	1.50	115	0.50	300	0.120	92.0
			88	120	0.75	90	1.05	300	0.000	100.0
			88	120	0.75	90	1.05	200	0.052	93.0
	Mark 12		24	145	1.50	158	0.14	300	0.234	84.4
			32	142	0.75	120	0.38	300	0.000	100.0
			32	140	0.75	120	0.39	200	0.055	92.7
BETE Fog Nozzle	SA 12-H14N-283	Centerline	63	88	1.50	90	0.38	300	0.200	86.7
			61	66	0.75	65	0.72	300	0.001	99.9
			60	66	0.75	65	0.72	200	0.070	90.7
Delevan Airo	30615-46	Centerline	5	120	0.75	120	0.06	300	0.037	95.1
	30616-11		20	120	0.75	120	0.24	300	0.000	100.0
			20	120	0.75	120	0.24	200	0.080	89.3
	30616-17		41	140	1.50	145	0.24	300	0.147	90.2
			48	130	0.75	130	0.58	300	0.000	100.0
			48	130	0.75	130	0.58	200	0.028	96.3
			55	145	0.75	140	0.66	200	0.044	94.2

Table 6-1 (Continued)

Manufacturer	Model	Configuration	Air		Water		Air/Water	T2	Drain (GPM)	Water Utilization
			(SCFM)	(PSIG)	(GPM)	(PSIG)				
			32	122	1.50	135	0.19	300	0.279	81.4
			42	117	0.75	118	0.50	300	0.000	100.0
			42	117	0.75	118	0.50	200	0.102	86.4
	30616-27		38	120	1.50	132	0.23	300	0.184	87.8
			48	115	0.75	116	0.57	300	0.000	100.0
			48	115	0.75	116	0.57	200	0.066	91.2
	30616-30		48	115	1.50	125	0.29	300	0.176	88.3
			57	110	0.75	110	0.68	300	0.000	100.0
			57	110	0.75	110	0.68	200	0.055	92.6
			47	108	0.75	108	0.56	200	0.050	93.4
Delevan Bypass	38635-3	Centerline	7	140	1.50	145	0.04	300	–	–
			7	135	0.75	130	0.09	300	0.033	95.6
			7	135	0.75	130	0.09	200	0.106	85.9
	35051-8		8	120	1.50	120	0.05	300	0.403	73.1
			12	120	0.75	110	0.15	300	0.031	95.9
Delevan Shirl Air	32740-4	Centerline	6	145	0.75	145	0.08	300	0.056	92.5
Lechler Supersonic	170.641.17	Centerline	64	140	1.50	180	0.38	300	0.163	89.1
			77	140	0.75	150	0.92	300	0.000	100.0
			77	140	0.75	140	0.91	200	0.039	94.8
			58	135	1.50	143	0.35	300	0.192	87.2
			70	130	0.75	130	0.84	300	0.000	100.0
			70	130	0.75	130	0.84	200	0.042	94.4
	170.721.17		98	125	1.50	130	0.59	300	0.132	91.2
			102	115	0.75	115	1.22	300	0.000	100.0
			105	117	0.75	115	1.26	200	0.028	96.3
Spraying Systems	SSU-J42	Centerline	9	145	0.75	133	0.11	300	0.139	81.5
			9	145	0.75	133	0.11	200	0.250	66.7

Table 6-1 (Continued)

Manufacturer	Model	Configuration	Air		Water		Air/Water	T2	Drain (GPM)	Water Utilization
			(SCFM)	(PSIG)	(GPM)	(PSIG)				
Turbotak	--	Centerline	64	60	0.75	45	0.76	300	0.000	100.0
			64	60	0.75	45	0.76	200	0.053	92.9
Delevan Airo	30616-11	Parallel	50	130	1.50	122	0.30	300	0.165	89.0
	30616-17		82	129	1.50	115	0.49	300	0.168	88.8
Lechler Supersonic	170.641.17	Parallel	99	120	1.50	100	0.59	300	0.183	87.8
Delevan Airo	30616-17	Series	80	128	1.50	112	0.48	300	0.104	93.1
EXTERNALLY MIXED ATOMIZERS:										
Parker Hannifin	6890764M1	Centerline	82	48	1.50	40	0.49	300	--	--
			82	48	0.75	15	0.98	300	0.000	100.0
	6890764M2		111	53	1.50	55	0.66	300	0.186	87.6
			111	53	0.75	25	1.33	200	0.062	91.8
PRESSURE ATOMIZERS:										
Delevan Spray Dryer	Orifice 902-58	Centerline	--	--	1.50	2500	0.00	300		<90.0
	Orifice 902-30		--	--	0.75	3750	0.00	300	0.011	98.5

exceptionally low data point at 66.7%), were acheived. The actual series configuration produced a water utilization of 93.1%, which is lower than produced by the same atomizer when configured in the simulated series configuration (96.3 percent). This difference may be attributable to the difference in the second stage inlet humidity between the simulated and actual series configurations. Water utilization resulting from atomizers in the parallel configuration was 88.5 percent, which is lower than achieved in the two-stage, series configuration.

Complete evaporation (100% water utilization) was obtained only in the single-stage configuration when the inlet temperature was 300° F and the water flow was reduced to 0.75 gpm, which does not represent desired conditions for a low approach-to-adiabatic-saturation temperature in the pilot plant.

Results indicate that, at a flow rate of 1.5 gpm, a tradeoff existed within the 18-inch duct geometry. In order to approach an acceptable drop size distribution, and minimize droplet evaporation times, the air/liquid ratio needed to be increased to maximum achievable levels. Increases in the air/liquid ratio within a confined flow, however, enhanced the recirculating flow out toward the duct wall, thereby reducing available time for droplet evaporation.

Reductions in spray angle also proved to be counter productive in that the drop size distribution generally increased with narrower spray angles. Once again, a tradeoff situation is presented. Narrower spray angles are desirable from the perspective of increasing the available residence time for droplet evaporation before the growth in the spray boundary from entrainment reaches the duct wall. The residence time required for droplet evaporation, however, also increases with narrower angle sprays. As the droplet evaporation time increases by the square of the droplet diameter, this approach is also counterproductive to the objective.

6.4 Strategies to Reduce Droplet Size Distribution

The use of heated water and surfactants were two options that were considered to reduce the droplet size distribution and evaporation time. The benefit of preheating the water to a nominal 200° F temperature is twofold. First the droplet evaporation time is reduced by eliminating the time required to heat the drop to its evaporation temperature. However, calculations of the time for a 50 micron drop to reach the boiling point demonstrate that this constitutes less than 10% of the overall droplet evaporation process. Second, and more importantly, the water viscosity is reduced. Increasing the water temperature from nominally 70° F to 200° F reduces the water viscosity from 0.0010 to 0.0003 kg/m-s. Benefits over this range of viscosity change, however, will only produce marginal reductions in the SMD.

Although surface tension also has an effect on droplet diameter, experiments with sodium lauryl sulfate indicated that only a 30% reduction could be achieved with a 0.1% solutions. As indicated by Lefebvre (1), however, the surface tension only exhibits a 0.2 power dependence on the mean drops size for low viscosity fluids. Thus, this approach would not appear fruitful in providing significant reductions in the drop size distribution.

6.5 References

1. Lefebrve, A. Atomization and Sprays. Hemisphere publishing Co., 1989.

7.0 FIRST GENERATION DUCT INJECTION MODEL

7.1 Introduction

This section describes the First Generation duct Injection Model developed for the analysis of the fundamental processes of flue gas desulfurization by sorbent injection. The model is a two- and three-dimensional, multiphase reacting flow analyzer using computational fluid dynamics methods. The gaseous phase is solved in an Eulerian frame of reference while the droplets of particles are traced in a Lagrangian frame. The model has an associated preprocessor which allows problem set up by the user without in-depth knowledge of computational fluid dynamics.

The aerodynamics of the First Generation Duct Injection Model were successfully validated with a number of test cases for which experimental data are available. Data from the Meredosia pilot plant humidification tests were used to validate the gas and droplet dynamics of the model with good agreement. Comparison of SO_2 removal results using the present model (with one injector) and the one-dimensional model previously developed by Energy and Environmental Research Corp. (1) indicates lower SO_2 capture rates for the present multi-dimensional flow model. The differences are mainly due to the more realistic nature of the multi-dimensional flows handled by the First Generation Duct Injection Model.

7.2 Conclusions

The following general conclusions may be drawn from the development of the First Generation Model:

- A multi-dimensional model (CFD code DIAN3D) has been developed which simulates the fundamental physicochemical processes of flue gas desulfurization by sorbent injection.

- The model which has been developed and delivered in source form uses an Eulerian frame for the gas phase calculations and Lagrangian frame for the particle or liquid droplet dynamics.

- The chemical reaction of SO_2 removal from the flue gases is handled by the SO_2 model developed by EERC. This model has been suitably extended to full 3D flows handled by DIAN3D.

- An in-built convergence control method allows use of the First Generation Model with minimal user adjustment of the solution control parameters.

- Simulations using the model without activation of sprays (i.e. without Lagrangian calculations) are very fast. Simulations with active sprays but without SO_2 removal reaction are much faster than with SO_2 removal active.

- To facilitate use of the model, a separate computer program has been developed (also in source form) which may be used as a preprocessor. The preprocessor allows easier setting up of a particular problem without in-depth knowledge of computational fluid or particle dynamics.

- The First Generation Model has been successfully validated for a number of single-phase flows such as laminar, turbulent and swirling pipe flows, and turbulent flow in a backward facing stope. Two-phase flow and heat/mass transfer simulations produced plausible results.

- Results of 3D simulations of the Meredosia humidification tests showed good agreement with observations at the pilot plant. These simulations indicated that a more even distribution of humidifying sprays and finer droplets will result in lower wall deposition rates. Droplets in excess of 100 μm may deposit on the duct walls. Buoyancy effects appear to be important for the flow rates used in the Meredosia pilot plant tests.

- Results of 2D simulations of the Meredosia pilot plant with SO_2 removal active showed lower sorbent utilization and SO_2 capture levels than those predicted by the 1D model developed by EERC. The differences are mainly due to the more realistic nature of the present multi-dimensional flow calculations. The slurry droplet injection produces the highest SO_2 capture levels and the dry sorbent injection the lowest.

- The SO_2 removal submodel is very sensitive to the prevailing ambient conditions in the duct and will often diverge during the calculation of the liquid calcium and sulfur profiles.

7.3 Recommendations

Based on the experience of the CHAM project team with the code DIAN3D and its SO_2 removal submodel, the First Generation Duct Injection Model could be improved by implementing the following recommendations:

- Perform further validation tests especially for SO_2 removal reaction calculations. A complete set of data from the Meredosia pilot plant (circular duct) and the Beverly test facility (rectangular duct) would be most helpful. This would allow for a wider acceptance of the First Generation Model not only as an analytical research model but also as a useful design tool for practical flue gas desulfurization systems.

- Extend the preprocessor and SO_2 model to allow other systems of units (e.g., GB) to be used. The main model of DIAN3D is not unit-dependant and can be used with any system of units.

- Enhance the SO_2 submodel by improving the accuracy of its geometric and physical property calculations and removing most ow its present limitations.

- Use a different solution approach in order to improve the accuracy and speed of convergence of SO_2 removal calculations. The SO_2 removal submodel usually diverges in the liquid calcium and sulfur profile calculations. This may be due to a combination of neglecting the transient terms in the governing equations and using an initial value (Runge-Kutta) solution algorithm. It is recommended that a boundary value (e.g. TDMA) solution algorithm be used instead of the present Runge-Kutta integration method.

- Introduce the time dependent terms of the governing equations in the SO_2 removal model. These terms are important during any change of boundary conditions between the droplets and the gases such as near the injectors (droplet acceleration/deceleration) or farther down the duct (gas temperature concentration gradients).

- Use a simpler SO_2 removal submodel to reduce the overall model execution times which may promote a wider use of the First Generation Model.

- Develop a simplified version of the DIAN3D model (d.g., a PC version) to be used for the analysis and design of basically two-dimensional (cartesian or axisymmetric) configurations of flue gas desulfurization systems.

- Introduce a knowledge-based system into the preprocessor to build a wide expert-system data base of various flue gas desulfurization designs. This would allow the user of the Duct Injection Model to perform parametric studies of give flue gas desulfurization systems and to identify areas of design improvement.

7.4 References

1. In-Duct Slurry Droplet Process Model. U.S. DOE Contract No. DE-AC22-88PC88873, Topical Report No. 3, November 1, 1989.

8.0 ESP PERFORMANCE MODEL

8.1 Introduction to the ESP Performance Model

This section describes the development of a personal computer based model to characterize the performance of electrostatic precipitators (ESPs) operating downstream of duct injection scrubbing systems. This work was performed by ADA Technologies, Inc. acting as a subcontractor to the Radian Corporation on a program entitled "Fundamental Investigation of Duct/ESP Phenomena".

The development of a mathematical model that accurately describes the performance of ESPs operating under duct injection conditions is essential to understanding any detrimental effects of duct injection on ESPs and developing strategies to improve ESP performance to overcome these problems. Existing models are not applicable for the high mass loadings and low resistivities experienced during duct injection due to one or more of the following limitations:

- Particle space charge is not taken into account when calculating the electric field at the plate;
- Particle space charge is not taken into account when calculating the average electric field for charge calculations;
- Non-rapping reentrainment is not incorporated in the model as an independent variable; or
- The empirically derived correction factors for rapping reentrainment are for ESPs handling only fly ash.

The approach taken to develop the model was to review the calculational techniques used in the existing models and build upon those techniques which are suitable for use in high mass loading situations. In addition to the non-ideal effects of sneakage, gas velocity distribution and rapping reentrainment, non-rapping reentrainment and particle charge limitations were also considered. Particle charge limitations are

caused by space charge induced corona quenching and the build-up of high potentials along the center lines of the ESP gas passages. Non-rapping reentrainment is experienced in all ESPs but has been found to be especially important in ESPs handling low resistivity materials. The model addresses the problem by the addition of a non-rapping reentrainment factor as a non-ideal effect. Model self-consistency was obtained by explicitly calculating the ion distribution, voltage distribution including particle space charge, particle charges, and current density using an iterative technique until mathematical convergence was achieved for each length increment within the ESP. In addition to improving the accuracy of the model calculations, making the model easier to use was also a prime objective. The model provides a full-screen, menu-driven interface that isolates the user from the complexity of the ESP model input formats, validates input data, and performs unit conversions.

The model is fully operational and has been extensively compared to the existing ESP models which are available to the public. Additional testing to enlarge the data base relating to particle charge, rapping reentrainment, and non-rapping reentrainment in duct sorbent injection ESPs needs to be conducted. This is necessary for further validation of the model, since data were available for only a limited number of pilot-scale duct sorbent injection cases and empirical data were gathered from a single full-scale source.

Execution of the ESP model requires an IBM compatible 386 computer with 640 kilobytes (KB) of random access memory (RAM), a math coprocessor chip, and a high density (1.2 MB) disk drive; a hard disk is preferred by not required. Model run times vary depending upon the number of sections in the ESP under consideration but average approximately five minutes for a five section ESP. Data, for graphing purposes, can be generated and saved in an ASCII file. The plot "masks" (x and y axis) included with the model are only applicable when used with the "GRAPHER" program from Golden Software, Inc.

END

DATE
FILMED
4/10/92